

MEASUREMENTS AND MODELS OF 802.11B SIGNAL STRENGTH VARIATION OVER SMALL DISTANCES

by

Hweechul Shin

A thesis submitted to the Faculty of the University of Delaware in partial fulfillment of the requirements for the degree of Master of Science in Electrical and Computer Engineering

Winter 2010

© 2010 Hweechul Shin
All Rights Reserved

MEASUREMENTS AND MODELS OF 802.11B SIGNAL STRENGTH VARIATION OVER SMALL DISTANCES

by

Hweechul Shin

Approved: _____
Stephan K. Bohacek, Ph.D.
Professor in charge of thesis on behalf of the Advisory Committee

Approved: _____
Kenneth E. Barner, Ph.D.
Chair of the Department of Electrical and Computer Engineering

Approved: _____
Michael J. Chajes, Ph.D.
Dean of the College of Engineering

Approved: _____
Debra Hess Noriss, M.S.
Vice Provost for Graduate and Professional Education

ACKNOWLEDGEMENTS

First of all, I am very grateful to my Advisor Prof. Stephan Bohacek. His guidance and encouragement during my visiting scholar years and graduate school for master science was supportive and powerful to me. Anytime and anywhere, he always left time for me to ask him questions about the research and the course works. I had few problems like my poor English skills, but he always gave me easy explanations and helped me to improve my English skills, which made my study and research possible. I will never be able to forget him from my life. I will always remember and have the attitude that he taught me to have towards a problem during my research. I feel that it was lucky for me that I met him during my life in U.S.A.

I had a good time with my research group friends, Vinay, Jonghyn, Peng, Andres and Carlos. I thank Vinay Sridhara, who was a good partner and a good tutor. Some problems like the weather, time, and place constraints made it harder for us to make concise measurements, but the experiments were enjoyable with him. I would also like to thank Jonghyun Kim, who was a good friend, roommate, and mentor for my life in U.S.A. As a good helper, he allowed me to use his time to solve many problem in my research. I also thanks to other roommate, Deokwon Kang,. He was the best friend during last two years.

I would like to thank my parents, Hyunbok Shin and Soonja Choi, and my older sisters and my brothers in law. My family encouraged me with their unconditional love, and immeasurable support, so that I could finish my degree. I dedicate my thesis to my family.

TABLE OF CONTENTS

LIST OF FIGURES	vi
ABSTRACT	xi
Chapter	
1 INTRODUCTION	1
1.1 Introduction	1
1.2 Motivation	1
1.3 Main Results	2
1.4 Thesis Outline	5
1.5 Abbreviations	6
2 EXPERIMENT DESCRIPTION	7
2.1 Experimental Setup	7
2.1.1 Measurement Equipment	7
2.1.2 Setting Measurement	9
2.1.2.1 Experiment Parameters	9
2.1.2.2 Transmitter Cisco1240 a/b/g setting	10
2.1.3 Experimental Process	11
2.2 Experiment Environment	13
2.2.1 Indoor Environment	13
2.2.1.1 Office Indoor	13
2.2.1.2 Apartment	13

2.2.1.3	House	16
2.2.2	Outdoor Environment	16
2.2.2.1	Green Field	16
2.2.2.2	Small Parking Lot	17
2.2.2.3	Building Canyon	19
3	EXPERIMENT RESULT	20
3.1	Received signal Strength	20
3.1.1	Measurement Environment Control	20
3.1.2	Indoor Result	23
3.1.3	Outdoor Result	24
3.2	CCDF Result Plot	27
4	MODELING SIGNAL STRENGTH VARIATION	32
4.1	Model Description	32
4.2	Fast-Fading: Impact of Delay Spread	34
4.3	Modeling Results	38
5	CONCLUSION	70
6	APPENDIX	72
6.1	Experiment Program	72
6.1.1	Receiver Controller	72
6.1.2	Transmitter Controller	80
6.1.3	Cisco AP Channel Control	93
	BIBLIOGRAPHY	95

LIST OF FIGURES

1.1	The probability of experiencing a change in signal strength of 3 dB or greater	4
2.1	The figure shows the experimental setup for measuring the varying signal strength over small distances with Linear Actuator. Red arrow indicates the moving direction of linear actuator and black thick line indicates the UTP Ethernet cable connection used for controlling the transmitter by sending packet from transmitter computer to Cisco1240 router. Yellow line is 20feet 400 series assemble cable with rp(reverse polarity)-tnc jack and rp-tnc plug from cisco1240 to 3dB antenna which is used in Cisco 1240 router. Blue arrow indicates USB to RS-422 communication converter cable used for controlling linear actuator. The receivers are on the stand in 1.5m.	8
2.2	This shows the Cisco 1240 a/b/g router transmits very stable power signal.	9
2.3	Left plot shows that the linear actuator is not repeatable when it is under low temperature. Right plot shows it is repeatable even though temperature is low because of the small movements. Both measurements were took at outside at night.	12
2.4	The layout for the Indoor office environment measurement. The top figure shows the 3rd floor structure and the bottom figure shows the 2nd floor structure. The 1st floor and basement was not explored in this measurement. Each rectangular box represents office rooms. Long rectangle in the middle is the hallway. The actuator was moving through this hallway from right side to left side on 3rd floor. This measurement was taken on the entire hallway. Each measurement was repeated 11 times (11 channels) on different linear places with fixed positions of receivers.	14

2.5	Layout for the Indoor Apartment measurement.	15
2.6	Layout for the Indoor House measurement	16
2.7	Layout for the Outdoor measurement on Green Field in University of Delaware.	17
2.8	Layout for the Outdoor measurement on Small Parking Lot between Evans Hall and Dupont Hall in University of Delaware.	18
2.9	Layout for the Outdoor Building Canyon measurement on near Dupont Building in University of Delaware.	19
3.1	This plot shows 3 other routers. Even 3 routers are stable, router 3 is the most stable in this plot. So, router 3 was used in measurement to get more stable and reasonable data set.	21
3.2	This plot shows that there is jumping power of signal even it is same receiver and same channel in empty office.	22
3.3	This plot is the result of receiver 1 and channel 3 measurement in office building.	23
3.4	This plot is the result of receiver 4 and channel 3 measurement in office building.	24
3.5	This plot is the result of receiver 5 and channel 5 measurement in Apartment.	25
3.6	This plot is the result of receiver 3 and channel 3 measurement in House.	25
3.7	This plot is the result of receiver 3 and channel 3 measurement on Green Field.	26
3.8	This plot is the result of receiver 3 and channel 1 measurement on small parking lot near Evans Hall.	26
3.9	This plot is the result of receiver 1 and channel 1 measurement on building canyon near Dupont Hall.	27

3.10	This plot shows several gamma distribution CCDF graph. Our data plot is better fitted normal distribution (Gamma distribution with large k).	28
3.11	CCDF plot for Indoor (Office) Receiver 2 Distance 3cm. This is well-fitted with normal distribution CCDF which has zero mean and σ 0.974.	29
3.12	CCDF plot for Outdoor (Green Field) Receiver 3 Distance 12cm. This is well-fitted with normal distribution CCDF which has zero mean and σ 1.438.	30
4.1	Translation of the receiver	33
4.2	The probability that the change in signal strength exceeds 3dB as a function of the delay spread and the number of rays for the narrow bandwidth case ($h = 1.5$ cm to $h = 24$ cm)	35
4.3	The probability that the change in signal strength exceeds 3dB as a function of the delay spread and the number of rays for the narrow bandwidth case ($h = 48$ cm to $h = 198$ cm)	35
4.4	The probability that the change in signal strength exceeds 3dB as a function of the delay spread and the number of rays for the wide bandwidth case ($h = 1.5$ cm to $h = 24$ cm)	36
4.5	The probability that the change in signal strength exceeds 3dB as a function of the delay spread and the number of rays for the wide bandwidth case ($h = 48$ cm to $h = 198$ cm)	36
4.6	The probability that the signal strength changes by more than 3 dB as a function of the displacement of the transmitter and the delay spread, when there are four rays in Wide band.	37
4.7	The probability that the signal strength changes by more than 3 dB as a function of the displacement of the transmitter and the delay spread, when there are four rays in Narrow band	38
4.8	The quality of fit for the model Office Receiver 1	40
4.9	The quality of fit for the model Office Receiver 2	41

4.10	The quality of fit for the model Office Receiver 3	42
4.11	The quality of fit for the model Office Receiver 4	43
4.12	The quality of fit for the model Apartment Receiver 1	44
4.13	The quality of fit for the model Apartment Receiver 2	45
4.14	The quality of fit for the model Apartment Receiver 3	46
4.15	The quality of fit for the model Apartment Receiver 4	47
4.16	The quality of fit for the model Apartment Receiver 5	48
4.17	The quality of fit for the model House Receiver 1	49
4.18	The quality of fit for the model House Receiver 2	50
4.19	The quality of fit for the model House Receiver 3	51
4.20	The quality of fit for the model House Receiver 4	52
4.21	The quality of fit for the model House Receiver 5	53
4.22	The quality of fit for the model Green Receiver 1	54
4.23	The quality of fit for the model Green Receiver 2	55
4.24	The quality of fit for the model Green Receiver 3	56
4.25	The quality of fit for the model Green Receiver 4	57
4.26	The quality of fit for the model Evans Receiver 1	58
4.27	The quality of fit for the model Evans Receiver 2	59
4.28	The quality of fit for the model Evans Receiver 3	60
4.29	The quality of fit for the model Evans Receiver 4	61
4.30	The quality of fit for the model Dupont Receiver 1	62

4.31	The quality of fit for the model Dupont Receiver 2	63
4.32	The quality of fit for the model Dupont Receiver 3	64
4.33	The median and 75th percentile of the modeling error for the complete model with the modeled standard deviation and the complete model with optimizes standard deviation.	67
4.34	The Values of the Delay Spread, R	67
4.35	The Maximum Standard Deviation of the Lognormal Fading, σ . .	68
4.36	The Distance where the Cross-correlation Changes from Zero to Non-zero, d_o	68
4.37	The Polynomial Exponent for the Decay of the Cross-correlation, α	69

ABSTRACT

This thesis presents results from a comprehensive channel measurement study. The 802.11 b/g channel was studied in 25 locations, including 14 indoor channels and 11 outdoor channels, where each measured used 11 wide bandwidths channels. For each location, measurements were taken along a 3 meter strip with 1.5 cm between each measurement, where the location of each measurement was controlled by a robotic linear actuator. Several hundred measurements were taken at each location, ensuring precise estimate of the signal strength. In all, 77 million signal strength measurements were made. However, in order to develop and verify the quality of the measurement, far more measurements were made. The collected data was used to estimate the change in signal strength as a function of the displacement. The observed change in signal strength was modeled with a standard channel model that contains a fast fading component and a lognormal shadowing component. While this standard model provided a good fit, we found that the lognormal shadowing component has much less spatially correlated than previous studies had found. Thus, this thesis developed a new model for the correlation of lognormal shadowing. Considering that the 802.11 b/g channel is a wide bandwidth channel (which reduce channel variations caused by fast fading), this study finds more significant variations in signal strength than has been previously known.

Chapter 1

INTRODUCTION

1.1 Introduction

Wireless networks have a dramatic impact people's lives. Using wired networks, one can access the Internet in fixed and restricted places. However, with the proper infrastructure, wireless networks allow mobile access anywhere that the infrastructure signal reaches. Consequently, wireless network is one area that has seen a tremendous amount of growth. Recently, wireless networks has been developed in infrastructureless Mobile Ad-Hoc networks, Sensor Networks and Mesh networks, which have infrastructure allow wireless connection to the Internet. Mesh networks have been deployed in several cities such as San Francisco[1], Philadelphia[2], and Taipei[3]..

1.2 Motivation

Simulation is one of the main methods for evaluating research in this field. Other than a few research papers, e.g. [4], most of the research utilize very simple models for conducting the simulations. This kind of research could be useful for testing the correctness of the protocols, but not for the performance evaluation. Experimental evaluations using test beds yield similar kinds of problems faced by the simplistic simulation models, that is, test-bed are useful for evaluating the correctness of a given protocol but not the performance. One of the reasons why the laboratory test beds are not suitable for the performance evaluation is that wireless

communication is evidently influenced by the environment in which it operates. Because of the complexities of the environment, it is difficult to replicate of the impact of the environment in the laboratory settings.

Experimentation is one of the main aides to the simulation in the sense that accurate models can be developed using the experimental data and incorporated into the simulation tools. This thesis focuses on measuring and modeling the change in signal strength due to small movements of the transmitter¹. Specifically, this thesis studies movements below 2 meters. The measurements were performed in several environments and utilized robotic linear actuator to move the transmitter in a controlled fashion. This thesis also focuses on modeling the variation in the signal strength.

1.3 Main Results

The models used in this thesis to model the changes in received signal strength are standard channel models [5]. They include small-scale fading (or fast fading) and slow fading modeled by lognormal shadow fading. One difference between the models developed here and models develop under other studies is that the correlation of the lognormal is modeled with a polynomial as oppose to an exponential as was done in [6, 7]. The polynomial model was selected because it achieves a better fit to the observations while the exponential model did not achieve a reasonable fit.

Another distinguishing aspect of this thesis is that this thesis also focuses on 802.11 g radios. Previous studies have focused on narrow bandwidth or narrower bandwidths used in mobile phones (see [5] and references therein). Note that while 802.11 b/g radios have been previously studied, there has been much confusion as to whether these channels follow the behavior described by the standard channel models. For example, it is widely believed that 802.11 g is subject to fast fading.

¹ Note, since propagation is symmetric, the impact of moving the transmitter is the same as the moving the receiver.

On the other hand, 802.11 g utilizes a wide bandwidth and hence should have some immunity to fast fading, which are mostly impacts narrow bandwidth radios. This study sheds considerable light on the impact of fast fading on 802.11 g.

Specifically, Figure 1.1 shows the probability of experiencing a change in signal strength of 3 dB or greater. Figure 1.1 shows the same probability but when a narrow bandwidth radio is used. In order to estimate this probability, we employ the model that models the observed signal, but only consider narrow bandwidth. Specifically, the channel modeled has two components, namely fast-fading and lognormal fading. The fast-fading part depends on the bandwidth. Thus, as described below, we determine parameters so that the model closely approximates the observations. Figure 1.1 includes the modeled probability that the signal changing by more than 3 dB. As can be observed, the model closely approximates the observations. Later, more details on the quality of fit are given.

Given the model and parameters, we can estimate the narrow bandwidth behavior by using the same model parameters for the fast-fading, but with a narrow bandwidth and use the same lognormal shadowing parameters. Figure 1.1 shows the results of this model. In order to understand the impact of the lognormal shadowing, Figure 1.1 also shows the model of the narrow bandwidth channel but without the lognormal shadowing component, and Figure 1.1 shows the results from the model of the wide bandwidth channel, but without the lognormal shadowing.

By comparing the narrow bandwidth without lognormal shadowing to the wide bandwidth without lognormal shadowing, we see that the wide bandwidth does indeed reduce the changes in the signal strength. However, it would not be correct to say that the wide bandwidth removes the impact of fast fading. Note that the impact of the fast fading increases with as the distance increases and the impact essentially is constant after the distance is about 10 cm, which is close to the wave length, which is 12.5 cm. This behavior is exactly as expected.

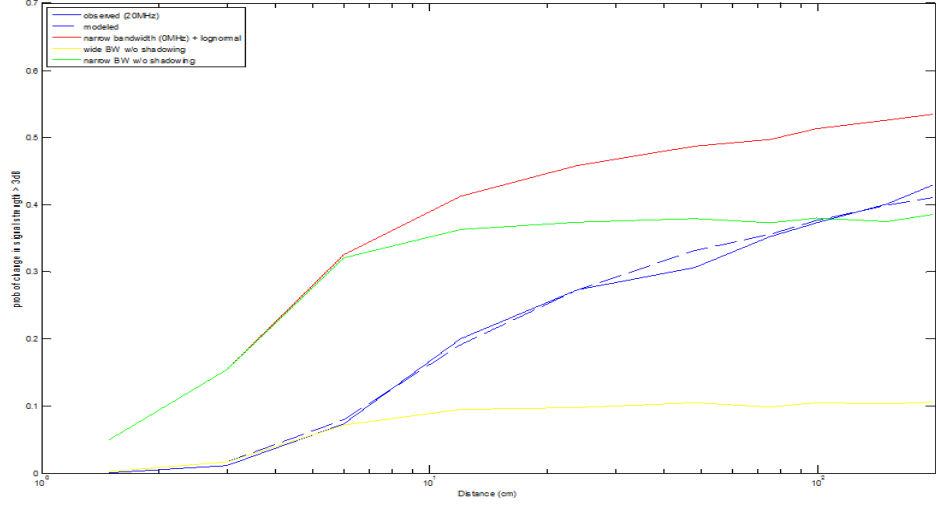


Figure 1.1: The probability of experiencing a change in signal strength of 3 dB or greater

As can be observed in Figure 1.1, the lognormal fading has little impact at short distances, i.e., distances below 6 cm. Beyond 6 cm, the impact is significant. In fact, after displacement of 1 m, the signal strength changes as much as it would if the channel was narrow bandwidth but without shadowing. Moreover, the difference between the wide bandwidth with lognormal shadowing and narrow bandwidth channel with lognormal shadowing is not very large. The small impact of shadow fading at small displacements is exactly as predicted. However, the significant impact at distances as small as one meter is considerably different from what was reported in [6, 7]. Specifically, [6, 7] found that correlation in the signal strength can be modeled as $\exp(-\rho d)$, where d is the distance and ρ is a parameter (note, our data did not support this model). A typical parameter value is $\rho = 1/10$. In this case, $\exp(-\rho 1) = 0.9$, implying that the lognormal shadowing has little impact when the transmitter is moved one meter. Therefore, we conclude that the model

presented in [6, 7] does not accurately model our observations.

These results explain some of the confusion between the common observation that 802.11g signal strength experiences significant changes in signal strength over relatively small distances and the theory, which says that impact of fast fading should be reduced by using wide bandwidth. One is tempted to blame the observed large changes in signal strength over short distances as a result of fast fading. However, since 802.11 b/g has a wide bandwidth, such a claim is clearly incorrect². On the other hand, based on the theory, it is common to assume that the signal strength changes little when the displacement is less than two meters. This belief is partly from the assumption that the 802.11 b/g channel is wide enough to average out any variations in signal strength. However, a more careful examination of the theory indicates that the variation of the signal strength is only reduced when wide bandwidth channels are employed. Moreover, it appears that the findings of [6, 7] are specific to mobile phone channels, and hence shadow fading has a significant impact even at small distances.

1.4 Thesis Outline

In Chapter2, I will explain experiment setup, the programs used are included in the appendix. In Chapter3, measurement result will be demonstrated. The model used to approximate the variation in signal strength is presented in Chapter4, while the modeling results are in Chapter 5. The Conclusion is discussed in the Chapter 6.

² It is interesting to note that mobile phones use in approximately the same frequency as 802.11 (specifically, W-CDMA uses 2.1-2.2 GHz, while 802.11 b/g use 2.3 GHz). It is widely assumed that 1 MHz is a wide bandwidth for W-CDMA. However, the 802.11 channels and W-CDMA channels should not be compared. The most significant difference is the transmit power of the base stations is far higher than 802.11 b/g, and hence the receive signals may propagate much further.

1.5 Abbreviations

SNR	Signal to Noise Ratio
BS	Base Station
AP	Access Point
LOS	Line of Sight
CCDF	Complementary Cumulative Distribution Function

Chapter 2

EXPERIMENT DESCRIPTION

2.1 Experimental Setup

2.1.1 Measurement Equipment

Measuring the varying signal strength with accurate result in repeatable fashion is key requirement for this experiment. All of the measurements need to be automatically controlled and the movement between measuring points should be accurate and repeatable. The Nook Industries Modular Linear actuator EG40 with 3 meter (Linear Actuator)[8], and Mdrive23plus motion control (Mdrive23)[9] meet these requirements. The Mdrive23 can be fully programmed and control actuator to move exact 1.5cm for each step, which is the difference between the positions of each measurements.

As shown in Figure 2.1, the transmitter and receiver were at the height of 1.5m. We assumed that handsets or wireless devices would be at this height when people use them while they are standing up or walking on. The Linear Actuator was carrying 3dB antenna which was connected with Cisco 1240 a/b/g (Cisco AP) with Broadcom chipsets[10]. Unlike some PCMCIA-based transmitters, the Cisco ap provides power stability of the transmitter in the Figure 2.2. The receivers were equipped with Proxim Orinoco b/g Gold Cards[11] with Atheros AR5212 chipset[12] and a modified MADWifi driver[13] was used to record all frames received. The sender was connected with transmitter via Ethernet cable. Also, Intelligent Motion Systems, Inc. (IMS) MD-CC400-000[14], which is a USB to RS-422 Communications Converter Cable, was used to communicate between sender and linear

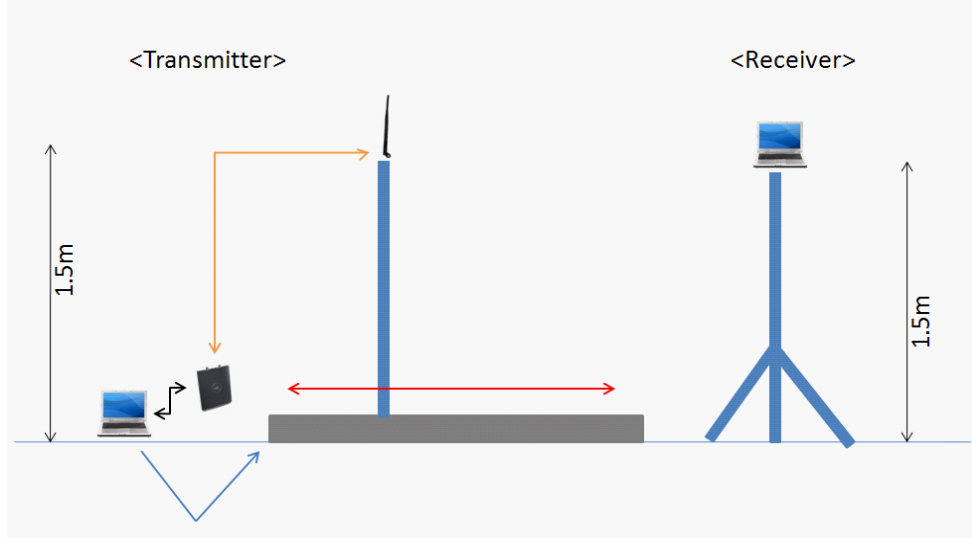


Figure 2.1: The figure shows the experimental setup for measuring the varying signal strength over small distances with Linear Actuator. Red arrow indicates the moving direction of linear actuator and black thick line indicates the UTP Ethernet cable connection used for controlling the transmitter by sending packet from transmitter computer to Cisco1240 router. Yellow line is 20feet 400 series assemble cable with rp(reverse polarity)-tnc jack and rp-tnc plug from cisco1240 to 3dB antenna which is used in Cisco 1240 router. Blue arrow indicates USB to RS-422 communication converter cable used for controlling linear actuator. The receivers are on the stand in 1.5m.

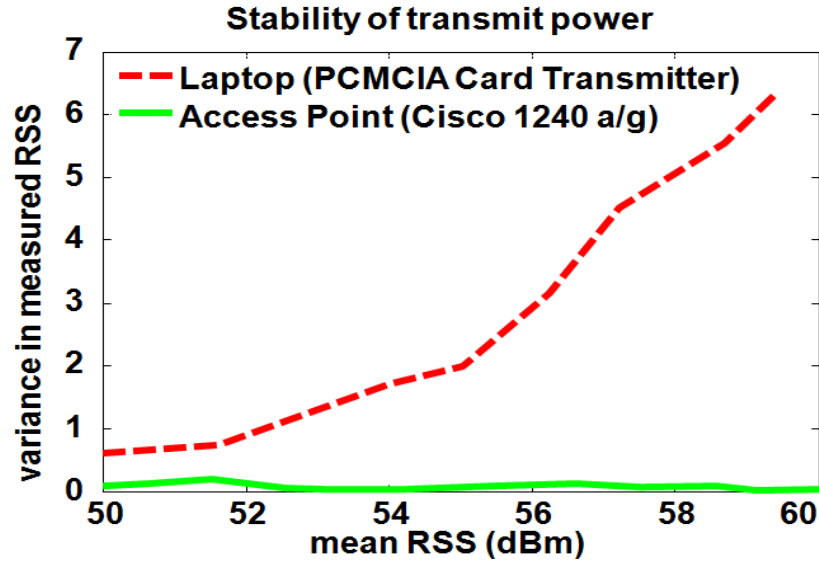


Figure 2.2: This shows the Cisco 1240 a/b/g router transmits very stable power signal.

actuator and Microsoft Visual Studio 2008 C++ software, and ActivePerl were used to control transmitter and linear actuator on the sender laptop. The transmitter is working on windows XP machine and other receivers are working on Linux Fedora 6 machines.

2.1.2 Setting Measurement

2.1.2.1 Experiment Parameters

This file has to be in Sender's laptop. The sender program should read these parameters for transmitting wireless signal.

<CtrlParams.conf>

- DEST_IP : 192.168.4.255 ; Broadcasting to be allowed all receivers to hear transmitted packet from transmitter and Disable RTS/CTS
- DEST_PORT : 7777 ; The port number was chosen randomly.

- NUM_PACKETS : 700 ; 700 packets were sent by transmitter on each position for indoor environment measurement. But 1400 packets were for outdoor environment measurement.
- TIME_INTERVAL : 10 ; There was 10 milliseconds interval between sending packets
- PACKET_SIZE : 40 bytes ; Pure data size was 40 bytes. In transmitting progress, it became 64 bytes because of added headers through NETWORK LAYERS
- COM_PORT: COM4 : To communicate with Linear Actuator, COM4 port was reserved.

2.1.2.2 Transmitter Cisco1240 a/b/g setting

<http://192.168.4.100/ap_network-if_802-11_c.shtml>

The Cisco ap had 192.168.4.100 ip address and the transmitter laptop had 192.168.4.101 ip address.

- Data Rates : 1, 2, and 11 Mbps was used for 802.11b experiment.
- Transmitter Power : 17dBm (50mW)
- Radio Channel : 11 channels from Channel 1 (2412 MHz) to Channel 11 (2462 MHz)
- Radio Preamble : Long Preamble
- Receive Antenna : Right (Disabled Diversity for using only one antenna)
- Transmit Antenna : Right (Disabled Diversity for using only one antenna)
- Beacon Period : 20 Kusec

2.1.3 Experimental Process

All of receivers have to be in monitor mode and be ready to record kernel messages. The Madwifi driver was modified to record kernel messages when packets were received. The receiver program ReadKernalMessage read the `/proc/kmsg` file and record it in output file. To record all packets, command `/etc/init.d/syslog stop` should be executed before than ReadKernelMessage. ReadKernelMessage code is shown in 6.1.1.

Next, ActuatorCtrl was executed in the transmitter laptop (sender). This program controlled the entire measurement process. First, the sender read CtrlParams.conf file (2.1.2.1) to get experiment parameters and it communicates with Cisco ap and Mdrive23 via the console application. Next, it sets up 802.11 wireless radio to channel 1, and moves Linear Actuator as specified length. The sender sent data frames to Cisco AP with a fixed interval of approximately 10 milliseconds between the transmissions. The sender is connected to the AP via an Ethernet cable. Hence, at each position, the AP add a 64bytes packet header and broadcasted the packets 700 or 1400 times at 1, 2 or 11 Mbps with RTS/CTS disabled through 20 feet of 400 series assemble cable with RP (reverse polarity)-TNC jack and RP-TNC plug 8 and 3dB antenna. After transmitting the packets, Linear Actuator was moved to next position, 1.5cm away. The sender waited for 8 seconds to differentiate the packets in different positions and to guarantee that Linear Actuator was moved. This process was repeated on 200 positions on one channel, which took about 61 minutes in indoor case. After finishing one process, the sender executed the terminal console program to change the wireless channel with SetCiscoChannel.pl (6.1.3). One reason that the Cisco AP was used was because it could be fully controlled by terminal application. Sender needed waiting time of 1 minute because the receivers had to know that the channel was changed with beacon of transmitter. After one channel measurement, Linear Actuator went back to its original position to repeat

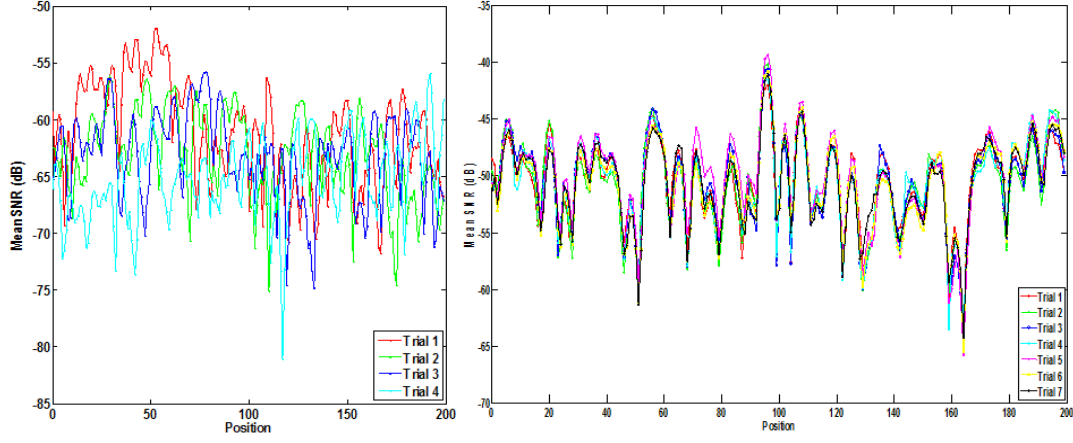


Figure 2.3: Left plot shows that the linear actuator is not repeatable when it is under low temperature. Right plot shows it is repeatable even though temperature is low because of the small movements. Both measurements were taken at outside at night.

the same process. Total 11 channels were explored with automatic setup that was mentioned above. Total time of making measurements of each scenario was about 11 hours.

The measurement should be taken at night time for repeatable because pedestrians who are walking near the measurement field could affect the received signal strength. But the Linear Actuator did not move at exactly same distance when the temperature was low. To solve this problem, the Linear Actuator had to be moved 4 times with 0.075cm moving for moving 0.3cm when we took outdoor environment measurements. The smaller it movements, the more accurate Linear Actuator shifts even in low temperature. So it was taken on 1000 positions through 3m as it moves 4 times with 0.075cm during outdoor measurement, even though 200 positions through 3m when it moves 4 times with 0.375cm during indoor measurements. The Figure 2.3 shows us the Linear Actuator is repeatable when it moves 4 times with 0.075cm in contrast to 4 times with 0.375cm in outdoor environment under low temperature.

For each scenario, 3, 4 or 5 receivers were deployed in different places based on different environments with different measurement scenarios. The information of receiver's locations and scenarios are shown in 2.2.

2.2 Experiment Environment

2.2.1 Indoor Environment

2.2.1.1 Office Indoor

Indoor measurements were made in Evans Hall, Electrical and Computer Engineering building in the University of Delaware. Because people near the measuring instruments could affect the received signal strength, indoor measurements were made during the winter break to eliminate this error.

As shown in Figure 2.4, the Linear Actuator moved through the hallway. In this measurement, Receiver 1 was on line of sight. Receiver 2 was near the Linear Actuator, but it was in office and the door was closed, which did not allow receiver 2 to see the Linear Actuator. Receiver 3 and 4 were on the 2nd floor. These two receivers were not in sight with Actuator. To continue measuring the entire hallway, the measurement was repeated 11 times with Actuator being shifted 3m for each time.

2.2.1.2 Apartment

For another case of indoor measurement, another measurement was taken in Fairfield Apartment, Stamford Dr. Newark Delaware. In the figure 2.5, the Linear Actuator was on the 2nd hallway, 2 receivers were on same floor inside the house, 1 receiver was in the laundry room on the 1st floor and 2nd floor, and others were at the same place and 3rd floor, except for the one on 1st floor. There are no receivers that could see the Linear Actuator directly.

Layout for office measurement

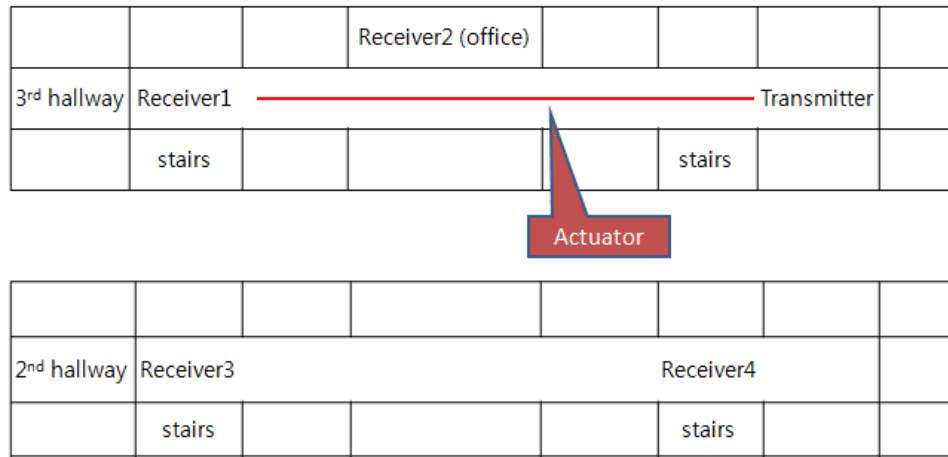


Figure 2.4: The layout for the Indoor office environment measurement. The top figure shows the 3rd floor structure and the bottom figure shows the 2nd floor structure. The 1st floor and basement was not explored in this measurement. Each rectangular box represents office rooms. Long rectangle in the middle is the hallway. The actuator was moving through this hallway from right side to left side on 3rd floor. This measurement was taken on the entire hallway. Each measurement was repeated 11 times (11 channels) on different linear places with fixed positions of receivers.

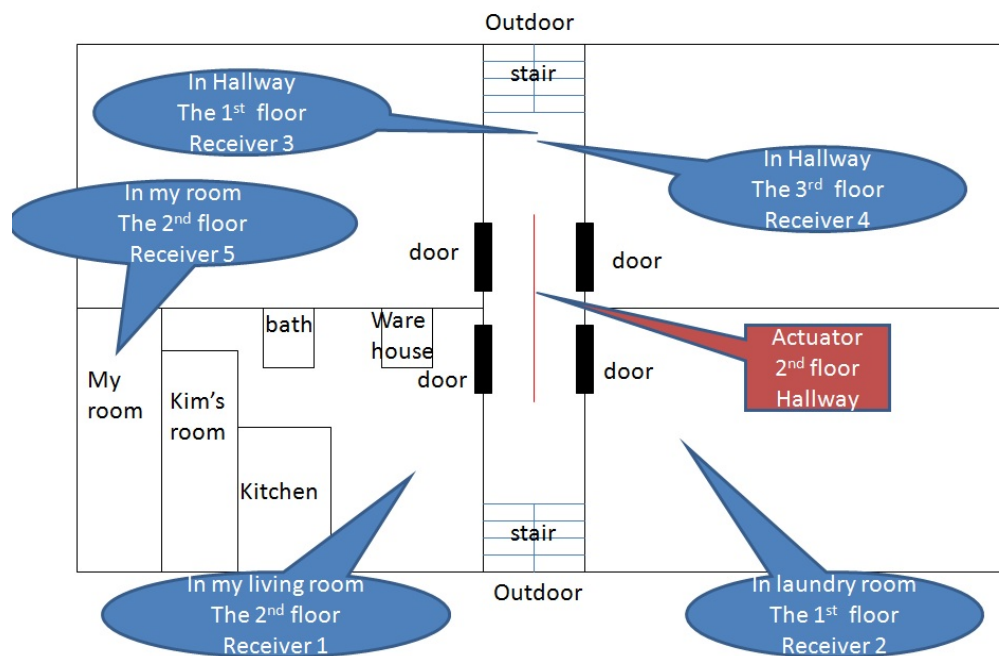


Figure 2.5: Layout for the Indoor Apartment measurement.

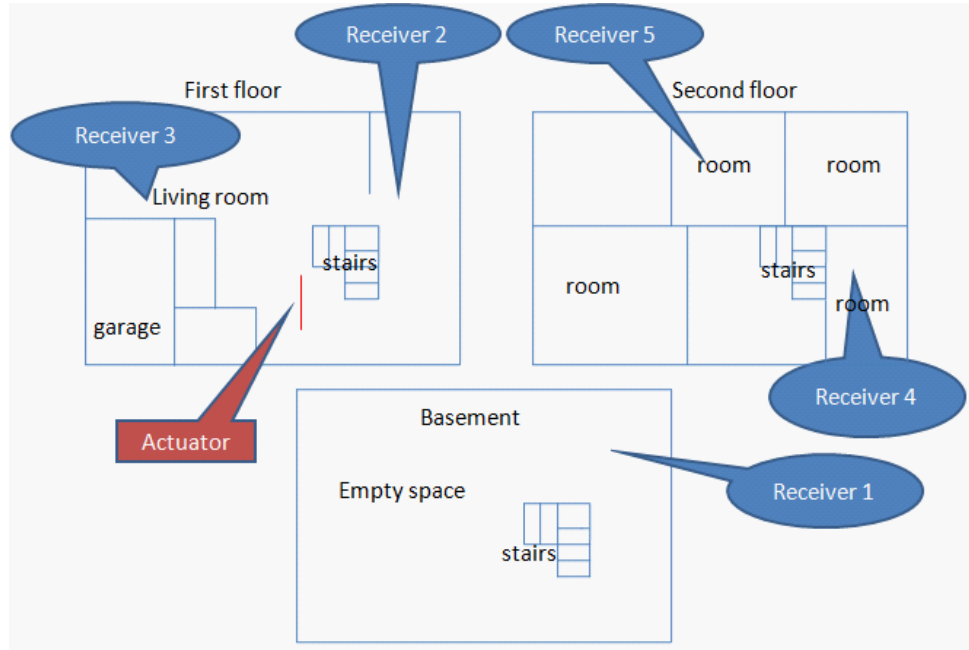


Figure 2.6: Layout for the Indoor House measurement

2.2.1.3 House

For another indoor case, the house was measured with 5 receivers. As shown in the figure 2.6, this house has 2 floors and 1 basement. Receiver 1 was on the basement, Receiver 2 and 3 were on the 1st floor, and Receiver 4 and 5 were on the 2nd floor. There were not line of sight receivers in this case.

2.2.2 Outdoor Environment

2.2.2.1 Green Field

Outdoor measurement was taken on the green field in University of Delaware. As shown in the figure 2.7, the Actuator was on the middle of the field and Receiver 1 was in our office. Because of the big tree between the Actuator and Receiver 1, this route from Transmitter to Receiver 1 was not in the line of sight. Receiver 2 was

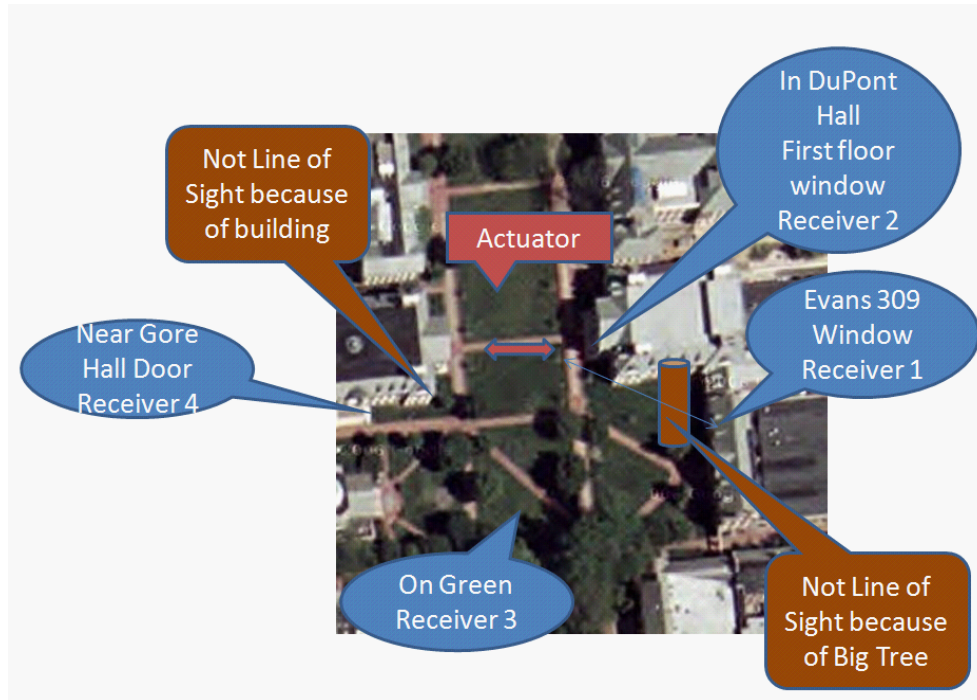


Figure 2.7: Layout for the Outdoor measurement on Green Field in University of Delaware.

beside window inside Dupont Hall. Receiver 3 was on Green field with line of sight. Receiver 4 was near Gore Hall, which did not allow receiver 4 to see the actuator.

2.2.2.2 Small Parking Lot

Backside of Evans Hall in University of Delaware was chosen to make the measurement of another outside scenario. As shown in the figure 2.8, the Linear Actuator was at the small parking lot near Evans Hall and Receiver 1 was at the side doorway of Evans Hall. This receiver was able to see the linear actuator directly during half time and it was not able to see it for another half of time. Receiver 2 was put on at the line of sight. Receiver 3 at backside of Evans Hall could not see Transmitter directly because of Evans Hall building. Receiver 4 was also not line of sight but far in distance than receiver 3.

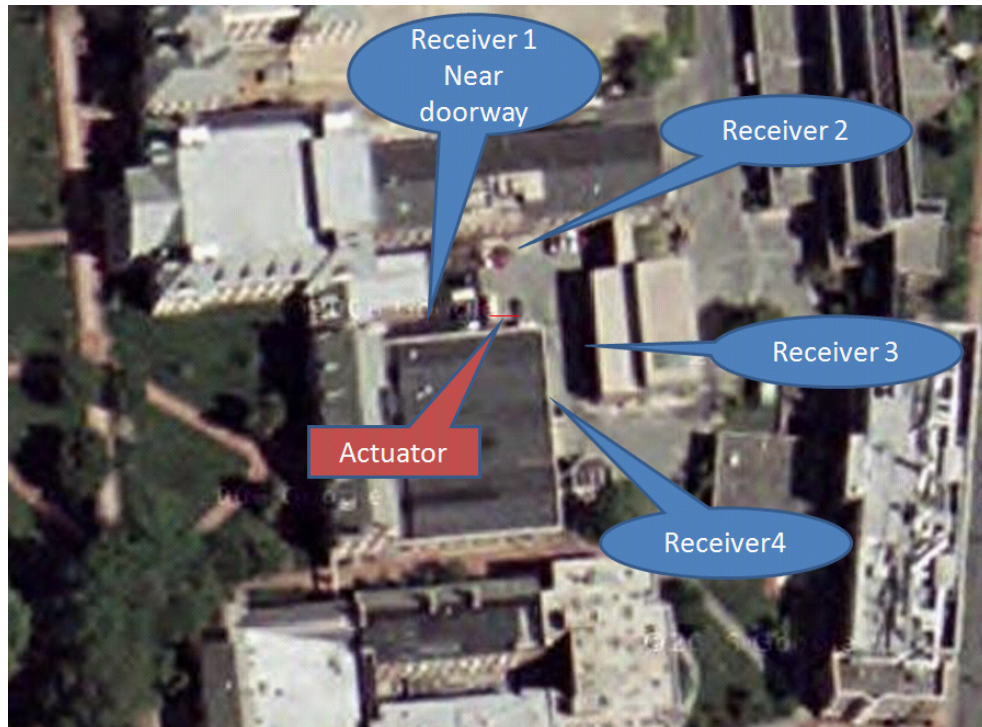


Figure 2.8: Layout for the Outdoor measurement on Small Parking Lot between Evans Hall and Dupont Hall in University of Delaware.

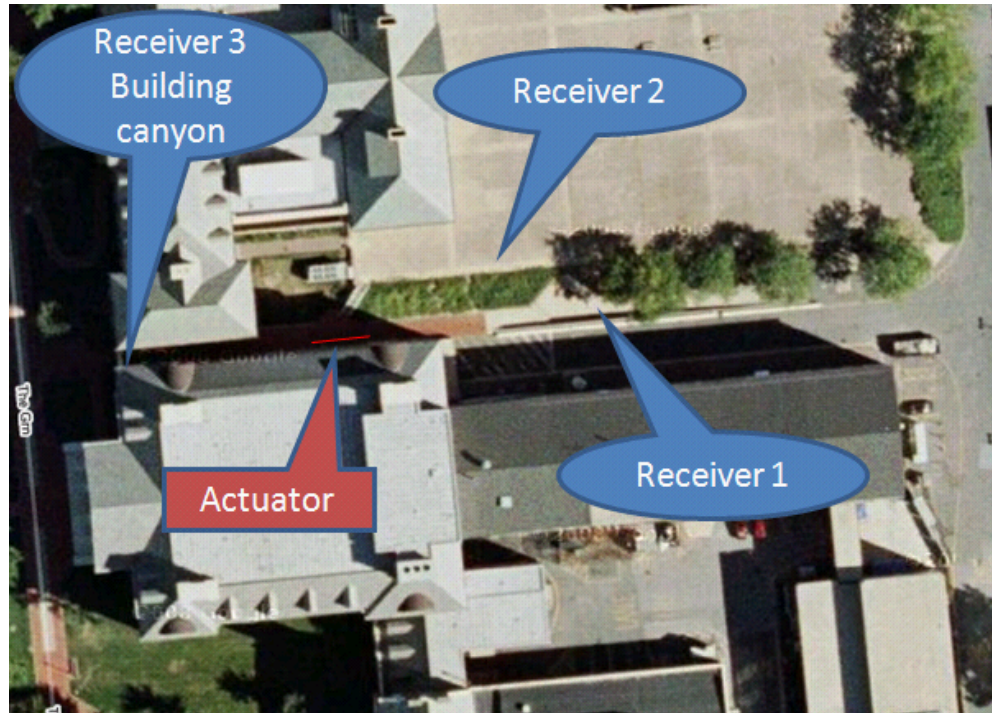


Figure 2.9: Layout for the Outdoor Building Canyon measurement on near Dupont Building in University of Delaware.

2.2.2.3 Building Canyon

Between Dupont Hall and Wolf Hall, there is Building canyon area. So this place was chosen for other outdoor measurement. As shown in the figure 2.9, the Linear Actuator was at Building canyon and receiver3 was opposite site of transmitter. The place of receiver 1 and receiver 2 is layer. So receiver 1 was lower than transmitter as 1 meter and receiver 2 was higher than transmitter as 2 meters. Both of receiver 1 and receiver 2 are not line of sight because of the layer.

Chapter 3

EXPERIMENT RESULT

3.1 Received signal Strength

3.1.1 Measurement Environment Control

During measurement, we experienced much difficulty to recorded uncorrupted data. Each measurement was performed several times because of other factors which are not expected in measurement. Passing people near measurement transmitter or receiver affected result. This could corrupt the measurements. There was no way to control people who passed around. For removing impact of pedestrians, measurements were taken at night and holiday and it was taken again if there are too many people during measurement. That's why these measurements campaign took very long time. And during outside measurement, the weather was the big problem. The rain and the snow but also low temperature caused errors. In the Nook Industries website, it claims that the Linear Actuator works from 15°F to 350°F [15]. However, we found significant errors well above the 15°F limit. Because this is made by aluminum, it was contracted in cold temperature. In the wind, the antenna would shake, causing errors. Once these problems were detected, we performed experiments on warm nights without wind. Of course, on warm nights it is more likely that people will linger on campus.

To make more stable and reasonable measurement, we tested transmitting AP. We found that some had a small variance in transmitted power, like the one shown in figure 2.2. But some had significant jumps in transmitted power, like that shown in Figure 3.1, 1 and 2 AP are big variance.

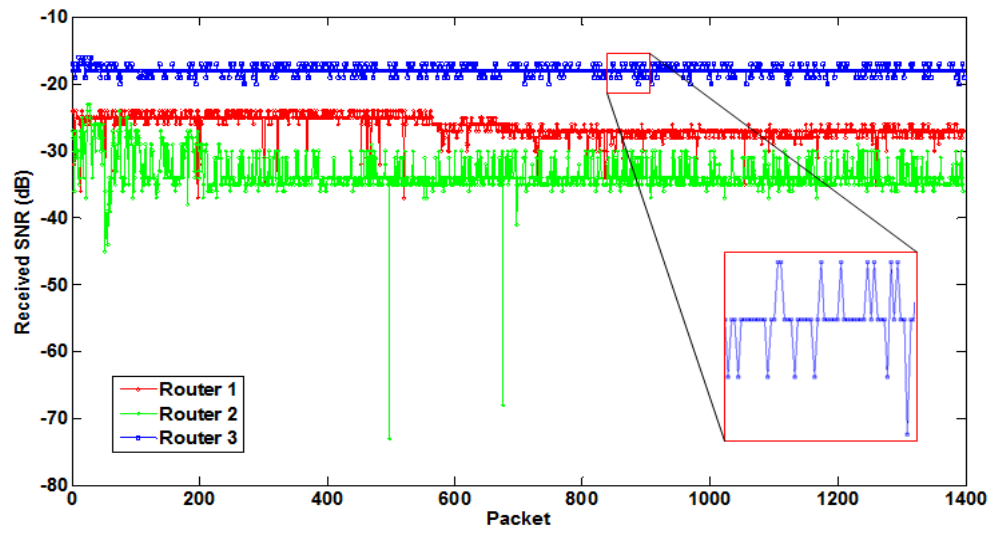


Figure 3.1: This plot shows 3 other routers. Even 3 routers are stable, router 3 is the most stable in this plot. So, router 3 was used in measurement to get more stable and reasonable data set.

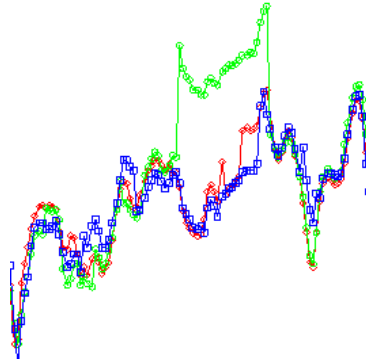


Figure 3.2: This plot shows that there is jumping power of signal even it is same receiver and same channel in empty office.

Determining that the transmitter was the source of the variation in received signal power required extensive testing and thought. Detecting this problem was made especially difficult since it was only a problem with some APs. Thus, sometimes the problem would occur and sometimes it would not occur. For example, in empty office, the same measurements repeated with same channel. In the figure 3.2, green line had jumped during 26 positions with similar pattern with others. In raw data plot, all received signals were up about 10dB than others. We tried to figure out what happened during 9 mins in that receiver. We assumed and tested that if there was some other program running that was hardware like cd-rom and caused the power supply to vary. But, by recording the processes, we determine that this was not the case. We tested more cases but we could not determine the source of this problem. Eventually, we determined that the problem was due to the AP and it was only a problem on some APs. Needless to say, precise channel measurements with low-cost equipment is very challenging and time consuming. These challenges calls into question the quality of other 802.11-based measurement campaigns, especially those that report unusual results, such as [16] which reported that Maxwell's equations to not hold.

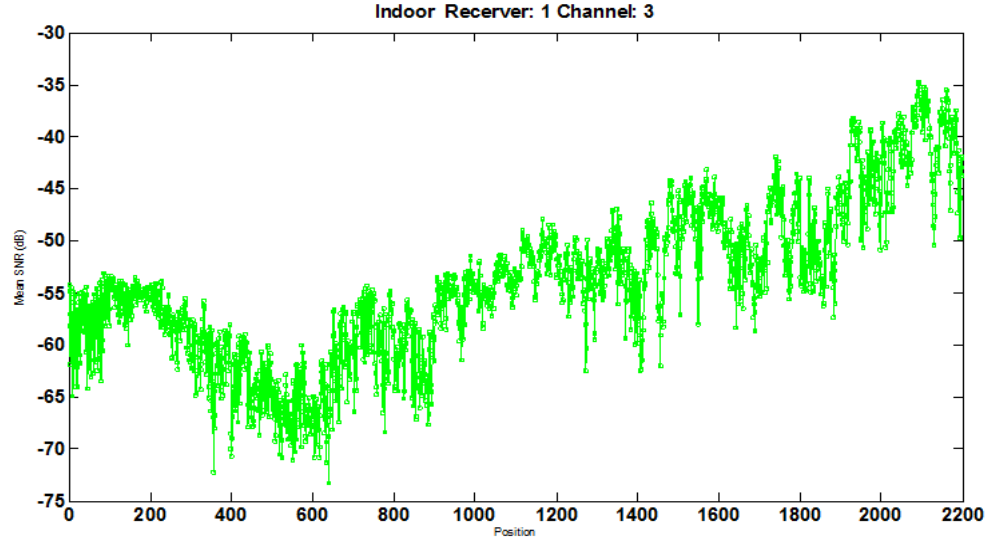


Figure 3.3: This plot is the result of receiver 1 and channel 3 measurement in office building.

3.1.2 Indoor Result

As we mentioned in the figure 2.4, indoor measurement was taken 11 times at linear positions. i.e., 2200 positions data was collected in linear positions. In the figure 3.3, the received signal strength is increasing because the linear actuator was coming to close receiver3. But it is decreasing until 600 positions. We thought that it would be from reflection in inside building environment. The receiver 4 was in 2nd floor and the transmitter was going far from receiver 4. So the received signal is decreasing as we expected in the figure 3.4.

As we normally expect the variance of received signal strength would be more varying with penetration in different floor, the receiver 4 has bigger variance than receiver 1 in figure 3.3 and figure 3.4.

The figure 3.5 and 3.6 are showing other indoor measurement i.e., apartment

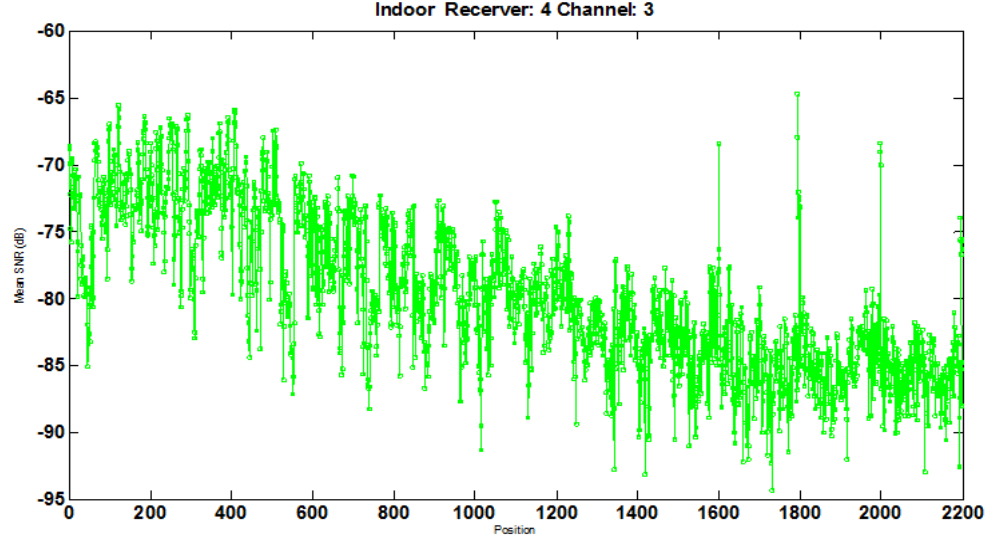


Figure 3.4: This plot is the result of receiver 4 and channel 3 measurement in office building.

measurement and house measurement, respectively. Unlike office indoor measurement, it was taken in 200 positions with obstruction of building layout. In these two plots, we can see variances are bigger than 10dB. Indoor environment, the received signal strength could be affected by more reflection rays because of building layout and ceiling and bottom dimensions.

3.1.3 Outdoor Result

On cases of outdoor measurement, we had measurements on Green Field, small parking lot near Evans Hall and building canyon near Dupont Hall. In outside measurement, their variances were under 7dB and smaller than Indoor. This is why there is less reflection than Indoor environment. In the figure 3.9, it was taken on 1000 points unlike others. It moved 0.3cm on each step to view changing power of received signal. The red line is 0.3cm moving data and the green line is 1.5cm moving data.

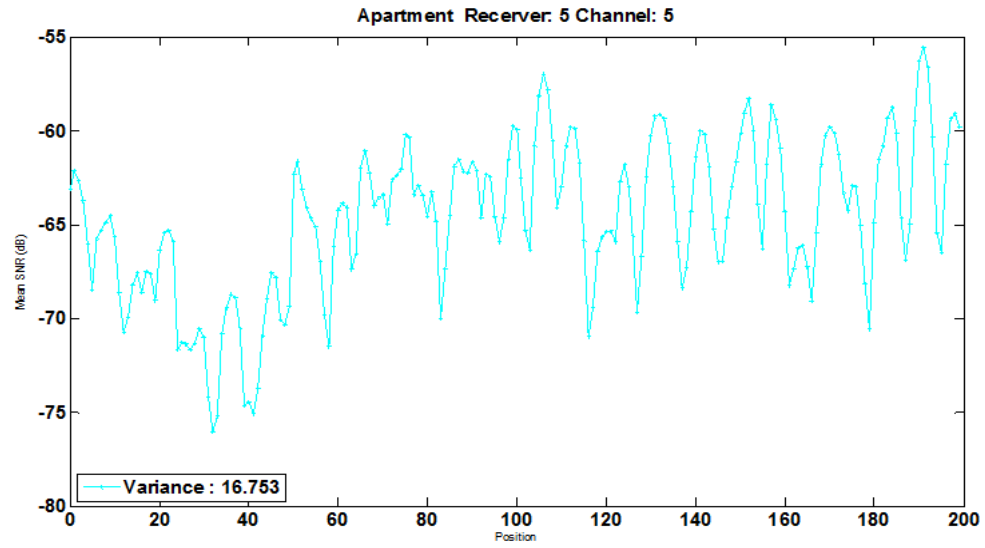


Figure 3.5: This plot is the result of receiver 5 and channel 5 measurement in Apartment.

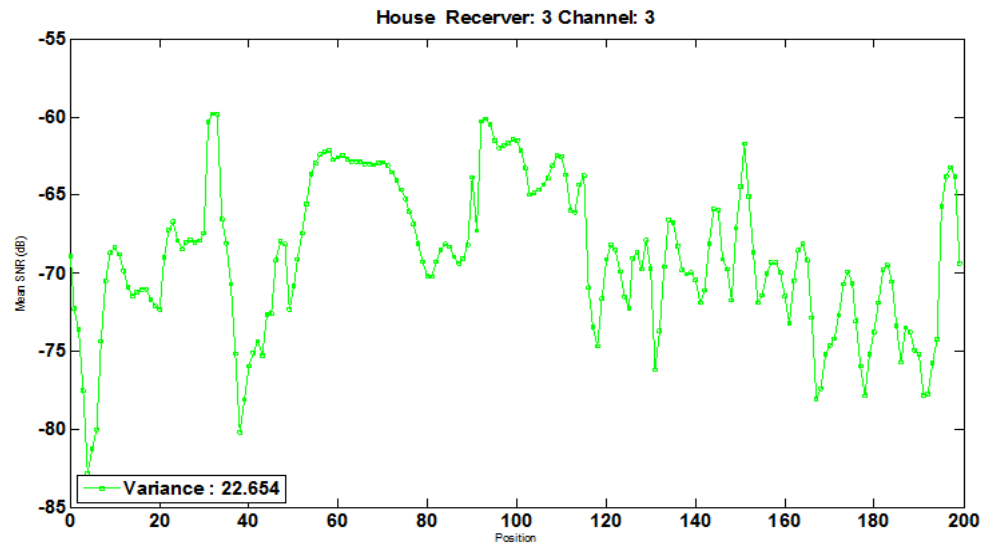


Figure 3.6: This plot is the result of receiver 3 and channel 3 measurement in House.

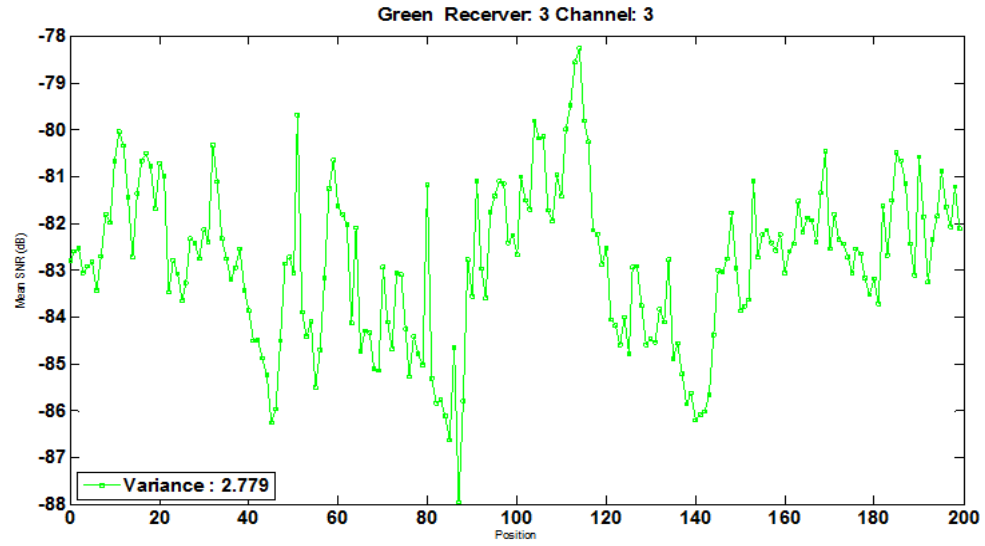


Figure 3.7: This plot is the result of receiver 3 and channel 3 measurement on Green Field.

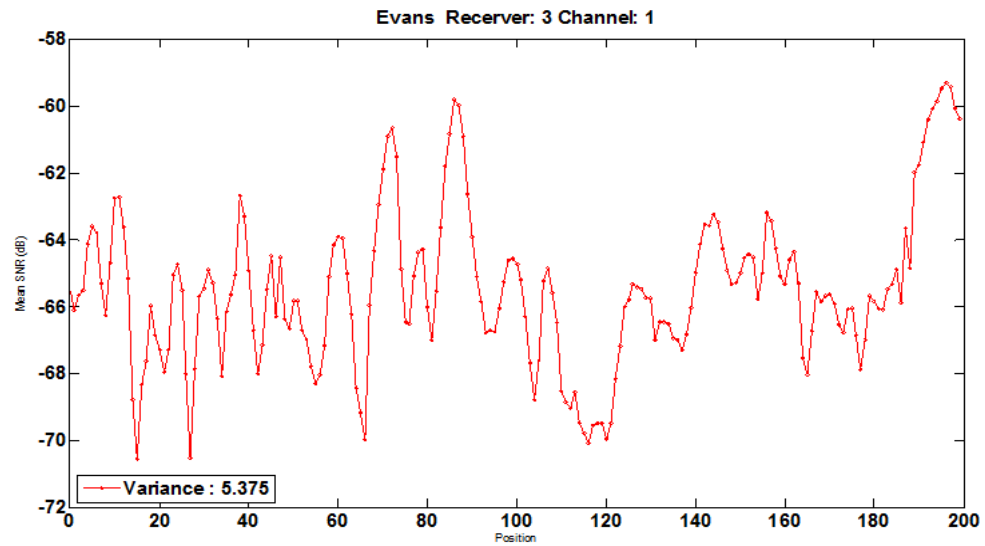


Figure 3.8: This plot is the result of receiver 3 and channel 1 measurement on small parking lot near Evans Hall.

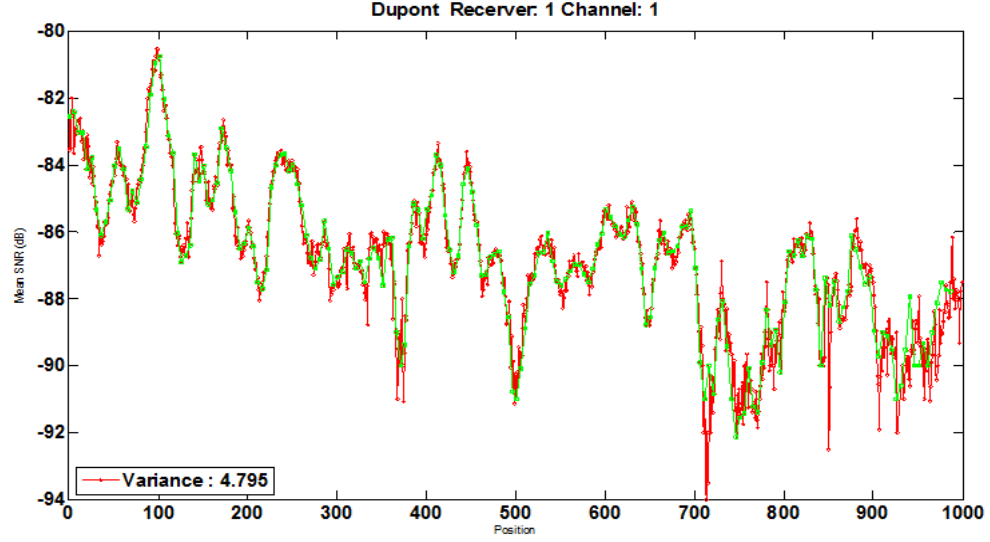


Figure 3.9: This plot is the result of receiver 1 and channel 1 measurement on building canyon near Dupont Hall.

3.2 CCDF Result Plot

In this section, we will show varying received signal strength CCDF graph when receiver moves. Because each step was 1.5 cm during measurement, we can get the varying signal if we compare two points (previous point and now point). In this way, CCDFs were computed for distances 3cm, 6cm, 12cm, 24cm, 48cm and 99cm. Each channel, 1-11, had a similar behavior, so the data from all channels were used to found a single set of measurements. In this way, a three meter linear strip results in 3×11 strips.

In fitting these CCDFs to simple models, we found that exponential distribution provided a much worst fit and the normal distribution. In the Figure 3.10, there are several gamma distribution CCDF graphs. Gamma distribution has 2 parameters (κ, θ). The first parameter is shape part and if κ is 1, the gamma distribution

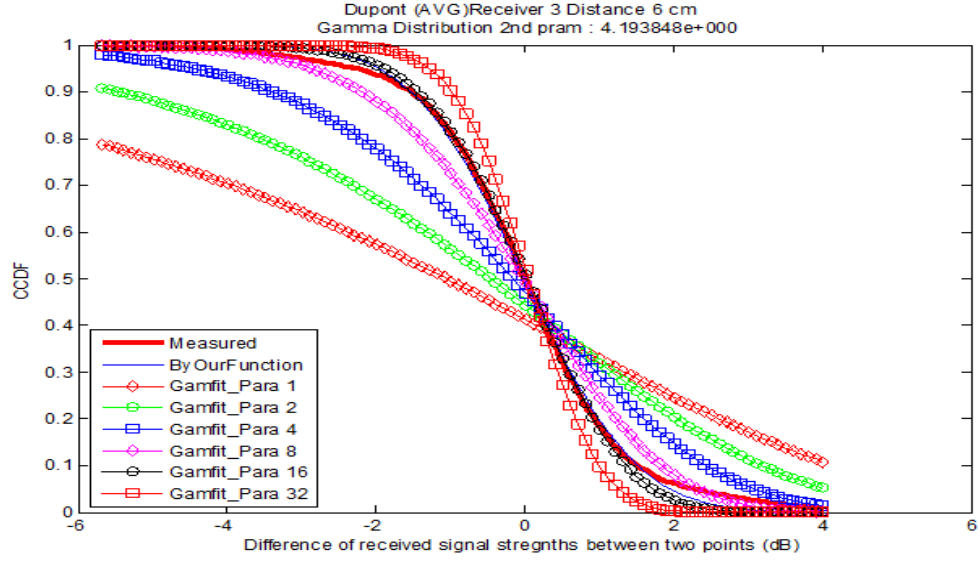


Figure 3.10: This plot shows several gamma distribution CCDF graph. Our data plot is better fitted normal distribution (Gamma distribution with large k).

is the exponential distribution [17] and if κ is large, the gamma distribution is approximately the same as the normal distribution [18]. Gamma distribution CCDF $\kappa = 16$ resulted in a better fit than $\kappa = 1$. i.e., the normal distribution is better fitted than the exponential distribution.

The figures 3.11 and 3.12 are showing our real measured data is well-fitted to normal distribution function. Because other plots can be regenerated by normal distribution function parameters, we omit others.

This table is for Indoor Office CCDF σ value. Because we know already zero mean, we just need σ value to determine normal distribution CCDF plot with

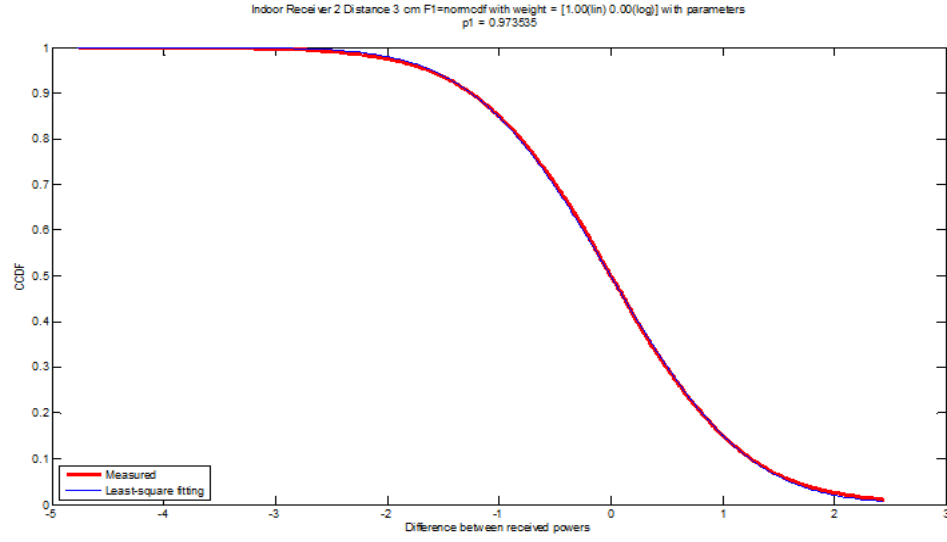


Figure 3.11: CCDF plot for Indoor (Office) Receiver 2 Distance 3cm. This is well-fitted with normal distribution CCDF which has zero mean and σ 0.974.

variance σ^2 . All values are rounded off the numbers to three decimal places.

σ	1.5 cm	3 cm	6 cm	12 cm	24 cm	48 cm	99 cm
Receiver 1	0.403	0.749	1.247	2.041	2.731	3.201	3.722
Receiver 2	0.515	0.974	1.688	2.698	3.302	3.548	3.872
Receiver 3	0.459	0.865	1.485	2.41	3.131	3.535	3.73
Receiver 4	0.474	0.881	1.501	2.402	3.055	3.414	3.541

Below table is for Indoor Apartment CCDF σ value.

σ	1.5 cm	3 cm	6 cm	12 cm	24 cm	48 cm	99 cm
Receiver 1	0.553	1.057	1.863	2.942	3.356	2.842	3.251
Receiver 2	0.586	1.1	1.845	2.958	3.722	4.101	5.471
Receiver 3	0.515	0.965	1.615	2.487	2.656	2.545	2.862
Receiver 4	0.577	1.115	2.02	3.319	4.239	4.282	4.52
Receiver 5	0.496	0.933	1.565	2.394	2.929	2.983	3.481

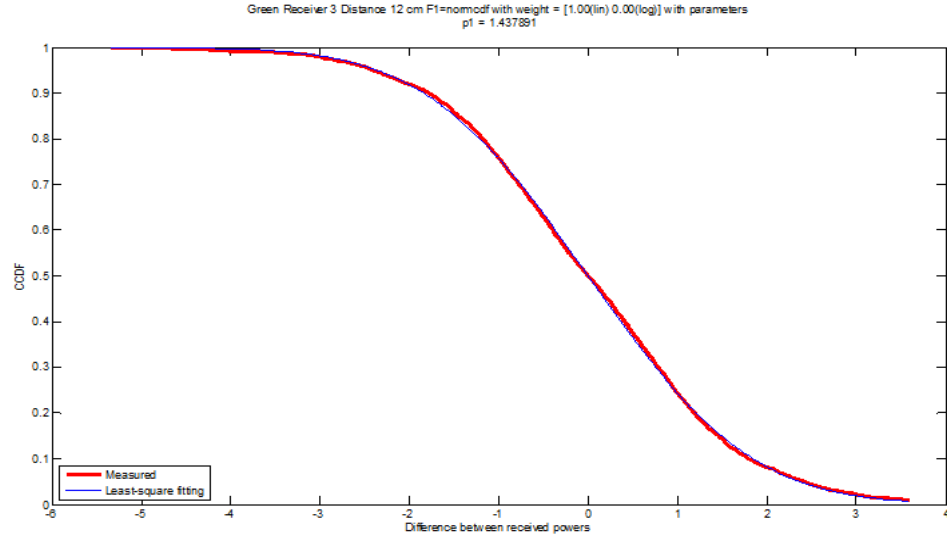


Figure 3.12: CCDF plot for Outdoor (Green Field) Receiver 3 Distance 12cm. This is well-fitted with normal distribution CCDF which has zero mean and σ 1.438.

Below table is for Indoor House CCDF σ value.

σ	1.5 cm	3 cm	6 cm	12 cm	24 cm	48 cm	99 cm
Receiver 1	0.564	1.08	1.915	3.136	3.718	3.682	3.983
Receiver 2	0.583	1.116	1.946	3.096	3.609	3.338	3.252
Receiver 3	0.533	1.017	1.793	2.878	3.827	4.069	4.946
Receiver 4	0.469	0.915	1.675	2.701	3.313	3.415	3.244
Receiver 5	0.578	1.112	1.983	3.239	4.073	4.387	4.639

Below table is for Outdoor Green Field CCDF σ value.

σ	1.5 cm	3 cm	6 cm	12 cm	24 cm	48 cm	99 cm
Receiver 1	0.431	0.792	1.235	1.716	2.329	3.41	4.954
Receiver 2	0.085	0.162	0.309	0.568	0.894	1.229	1.48
Receiver 3	0.24	0.458	0.852	1.438	1.966	1.968	2.042
Receiver 4	0.13	0.241	0.449	0.823	1.384	2.215	3.453

Below table is for Outdoor Small Parking Lot CCDF σ value.

σ	1.5 cm	3 cm	6 cm	12 cm	24 cm	48 cm	99 cm
Receiver 1	0.607	0.995	0.942	1.17	1.234	1.304	1.926
Receiver 2	1.021	1.912	3.059	4.049	2.993	3.839	3.883
Receiver 3	0.351	0.688	1.26	2.005	2.4	3.055	3.558
Receiver 4	0.29	0.576	1.1	1.899	2.651	3.058	4.015

Below table is for Outdoor Building Canyon CCDF σ value.

σ	1.5 cm	3 cm	6 cm	12 cm	24 cm	48 cm	99 cm
Receiver 1	0.749	1.344	1.918	2.265	2.217	2.196	3.008
Receiver 2	1.001	1.812	2.585	2.504	2.73	2.736	3.339
Receiver 3	0.396	0.685	0.993	1.621	2.585	3.662	2.99

Chapter 4

MODELING SIGNAL STRENGTH VARIATION

4.1 Model Description

In order to model the variation in signal strength, we use a fast fading model along with a lognormal shadowing model. The fast fading model is as follows. We assume that the channel allows N rays to pass from transmitter to receiver. Each ray has the same strength. However, each ray arrives at a different angle θ that is uniformly distributed between 0 and 2π (distributing the angle over a small set had little impact). Moreover, each ray has a length that is uniformly distributed from 0 to R wave lengths. The signal strength is the absolute value of the sum of these signals.

Consider the scenario in Figure 4.1. The initial signal along the ray of length d is

$$\exp\left(i\frac{2\pi}{\lambda}d\right).$$

After the receiver moves a distance h , the signal is

$$\exp\left(i\frac{2\pi}{\lambda}d'\right)$$

where $d' = \sqrt{d^2 + h^2 - 2dh \cos(\theta)}$. Taking the first order Taylor series, $d' \approx d + \frac{1}{2}(d^{-1})(2h - 2d \cos(\theta))h = d(1 - \cos(\theta)) + \frac{h}{d} \approx d(1 - h \cos(\theta))$, where the second approximation is valid when $d \gg h$, which is the case here. Thus, the signal strength before displacement of the receiver is

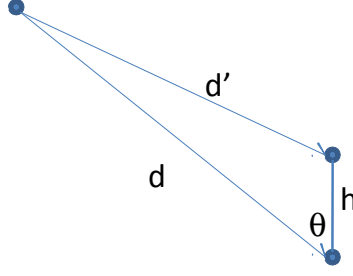


Figure 4.1: Translation of the receiver

$$H_{FF}(0) = \left| \sum_{k=1}^N \exp \left(i \frac{2\pi}{\lambda} d_k \right) \right|^2$$

and after displacement by a distance h ,

$$H_{FF}(h) = \left| \sum_{k=1}^N \exp \left(i \frac{2\pi}{\lambda} d_k (1 - h \cos(\theta_k)) \right) \right|^2.$$

Shadow fading also impacts the channel. Specifically, the channel gain at locate h is $H(h)$ where

$$H(d) = H_{FF}(h) Z(h).$$

Here $Z(h)$ accounts for the lognormal shadowing. Letting $\Delta H_M(d)$ denote the modeled change in signal strength in dB, we have

$$\Delta H_M(h) = \frac{\log_{10} \left(\left| \sum_{k=1}^N \exp \left(i \frac{2\pi}{\lambda} d_k \right) \right|^2 \right)}{\log_{10} \left(\left| \sum_{k=1}^N \exp \left(i \frac{2\pi}{\lambda} d_k (1 - \cos(\theta_k)) \right) \right|^2 \right)} + X - Y$$

where X and Y are Gaussian random variables that account for the lognormal shadowing where, due to spatial correlation, Y is correlated to X . Thus, the change in signal strength is

$$\Delta H_M(h) = \frac{\log_{10} \left(\left| \sum_{k=1}^N \exp \left(i \frac{2\pi}{\lambda} d_k \right) \right|^2 \right)}{\log_{10} \left(\left| \sum_{k=1}^N \exp \left(i \frac{2\pi}{\lambda} d_k (1 - \cos(\theta_k)) \right) \right|^2 \right)} + W$$

where W is the Gaussian random variable with standard deviation $\sigma(1 - \rho(h))$ where $\rho(h)$ is the correlation coefficient between X and Y .

Thus, we can model the lognormal shadowing component of the change in signal strength as a result of displacement of the receiver as Gaussian random variable with standard deviation s , where s depends on the displacement h . Alternatively, we can model the standard deviation as a specific function of displacement. Specifically, we found the following works well.

$$\sigma \begin{cases} \left(1 - \frac{h_o^\alpha}{h^\alpha}\right) & \text{if } h > h_o \\ 0 & \text{if } h \leq h_o. \end{cases} \quad (4.1)$$

Note that according to this model, the cross correlation decrease polynomially. This is different from the exponential model developed in [6, 7].

The lognormal shadowing adds three parameters, σ , α , and h_o to the parameters N and R , the number of rays in the fast fading model and then delay spread, or spread between the lengths of the rays.

4.2 Fast-Fading: Impact of Delay Spread

Before examining the quality of fit provided by this model, we will examine the impact of the parameters N , the number of rays, R , the delay spread, and the bandwidth. We begin by examining the impact of the number of rays. Consider Figures 4.2, 4.3, 4.4 and 4.5 which show the probability that the change in signal strength exceeds 3dB as a function of the delay spread and the number of rays for the narrow bandwidth case and for the wide bandwidth case. Note that in all cases, as long as the number of rays is four or larger, then the number of rays does not have any impact on the channel. Thus, we will only consider two rays and four rays.

Figures 4.6 and 4.7 show the probability that the signal strength changes by more than 3 dB as a function of the displacement of the transmitter and the delay spread, when there are four rays. Figure 4.6 shows the wide bandwidth case (i.e., the

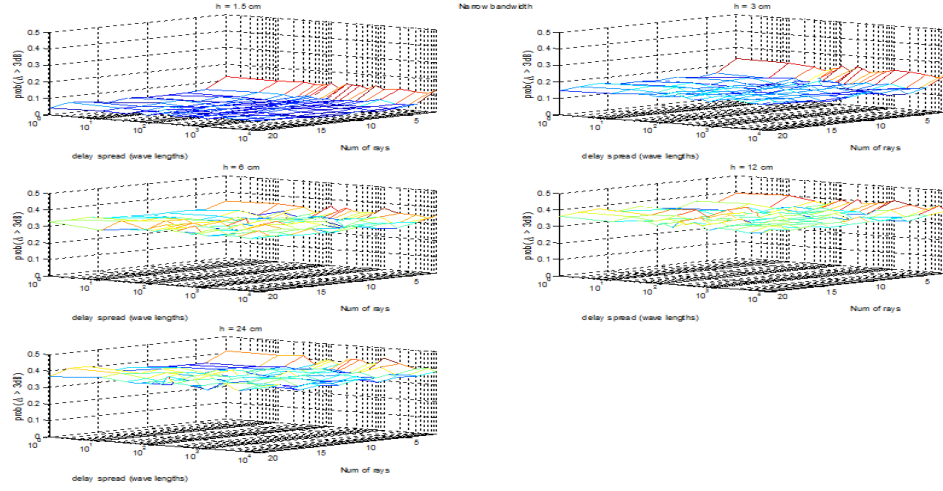


Figure 4.2: The probability that the change in signal strength exceeds 3dB as a function of the delay spread and the number of rays for the narrow bandwidth case ($h = 1.5$ cm to $h = 24$ cm)

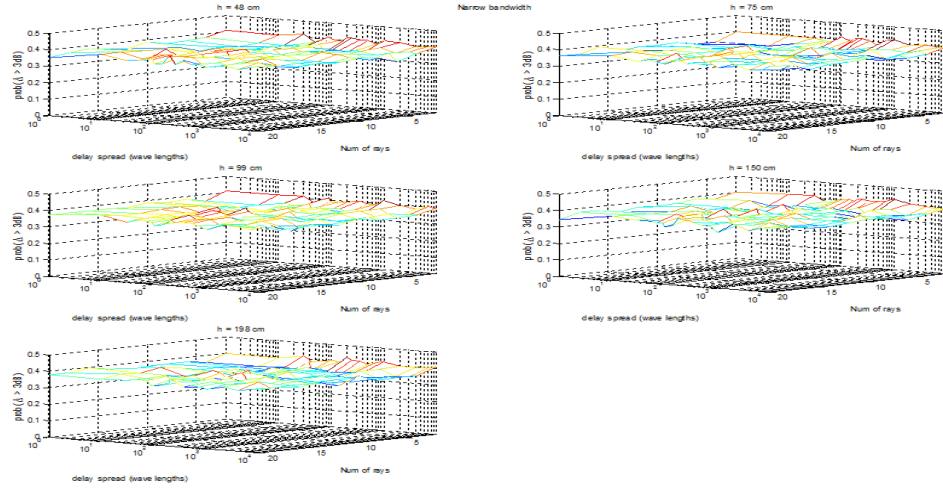


Figure 4.3: The probability that the change in signal strength exceeds 3dB as a function of the delay spread and the number of rays for the narrow bandwidth case ($h = 48$ cm to $h = 198$ cm)

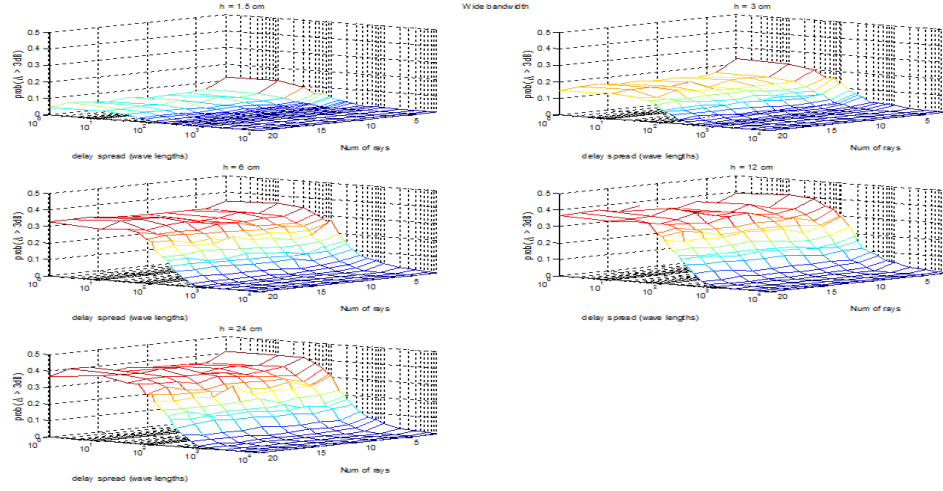


Figure 4.4: The probability that the change in signal strength exceeds 3dB as a function of the delay spread and the number of rays for the wide bandwidth case ($h = 1.5$ cm to $h = 24$ cm)

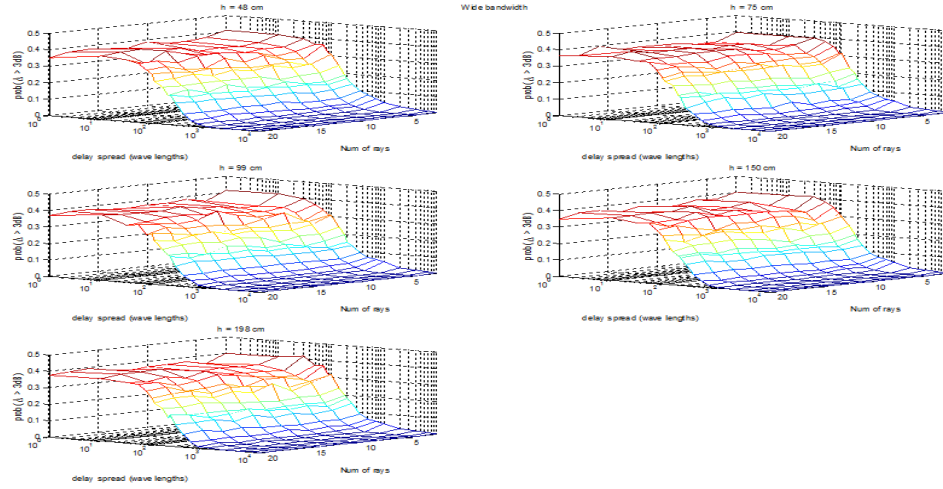


Figure 4.5: The probability that the change in signal strength exceeds 3dB as a function of the delay spread and the number of rays for the wide bandwidth case ($h = 48$ cm to $h = 198$ cm)

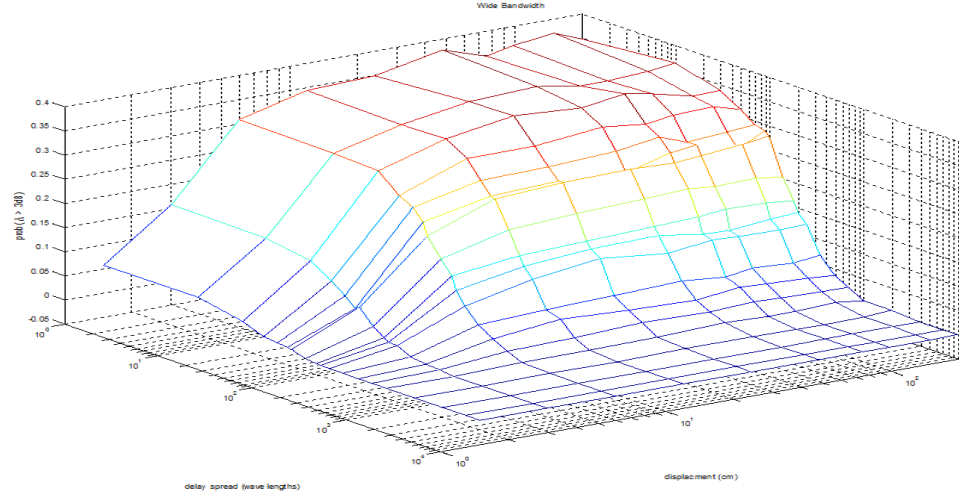


Figure 4.6: The probability that the signal strength changes by more than 3 dB as a function of the displacement of the transmitter and the delay spread, when there are four rays in Wide band.

bandwidth used by 802.11 b/g) while figure 4.7 shows the narrow bandwidth case. As can be observed, the impact of the displacement of the transmitter increases as the distance the transmitter is moved increases. However, after the transmitter moves more than a wave length (12.5 cm), the impact no longer increases. Furthermore, the wide bandwidth reduces the impact of the fast fading. However, the degree to which the impact is reduced depends on the delay spread. For values of delay spread less than 30 wave lengths (3.75 m), 802.11 b/g's wide bandwidth does not reduce the impact of fast fading. When the delay spread is larger than 1000 wave lengths (125 m), the impact of fast fading is completely eliminated. Thus, if different rays travel very different distances, then the wide bandwidth channel will experience much less variation in signal strength than the narrow bandwidth channel. On the other hand, if the rays travel approximately the same distances, the wide bandwidth channel will experience the same variations in signal strength as a narrow bandwidth channel.

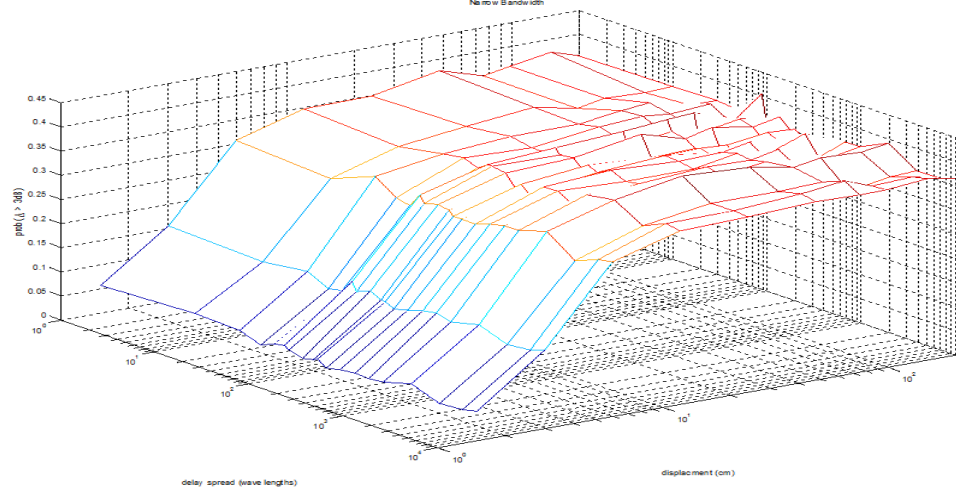


Figure 4.7: The probability that the signal strength changes by more than 3 dB as a function of the displacement of the transmitter and the delay spread, when there are four rays in Narrow band

Typically, the delay spread is smaller indoors than outdoors. The reason for this is that, indoors, the rays might experience a larger number of reflections off of walls and transmissions through walls before reaching the receiver. Each reflection and transmission greatly reduces the signal strength. Thus, indoors, the signal strength decreases rapidly with the distance the rays travel. And therefore, rays that travel different distances will have significantly different strengths. Thus, the set of rays that have the most significant signal strength are those that took paths of approximately the same length. Outdoors, the signal strength might decay rather slowly with distance traveled by the ray. Therefore, we expect low delay spread indoors.

4.3 Modeling Results

As mentioned above, the complete model has parameters σ , the maximum standard deviation of the lognormal fading, α , the polynomial exponent for the decay

of the cross-correlation, d_o , the distance where the cross-correlation changes from zero to non-zero, and R , the delay spread. For comparison purposes, we consider a model with parameters R and $s(h)$, the standard deviation at displacement h . For this second model, we use the same R used in the first model. Thus, this second model is useful to compare the model of the cross-correlation with a cross-correlation that is selected to optimally fit the data, given R .

In this study, the quality of fit metric was

$$\sum_{h \in \mathcal{D}} \max_c |P(\Delta H(h) < c) - P(\Delta H_M(h) < c)|, \quad (4.2)$$

where D is the set of displacements considered. In this case, $\mathcal{D} = \{1.5, 3, 6, 12, 24, 48, 75, 96, 148, 196\}$, in centimeters. When only a single displacement h is considered (i.e., when computing s in the second model), we use the metric

$$\max_c |P(\Delta H(h) < c) - P(\Delta H_M(h) < c)|. \quad (4.3)$$

In order to determine the parameters that minimize the metric, an exhaustive search of the parameter space was performed.

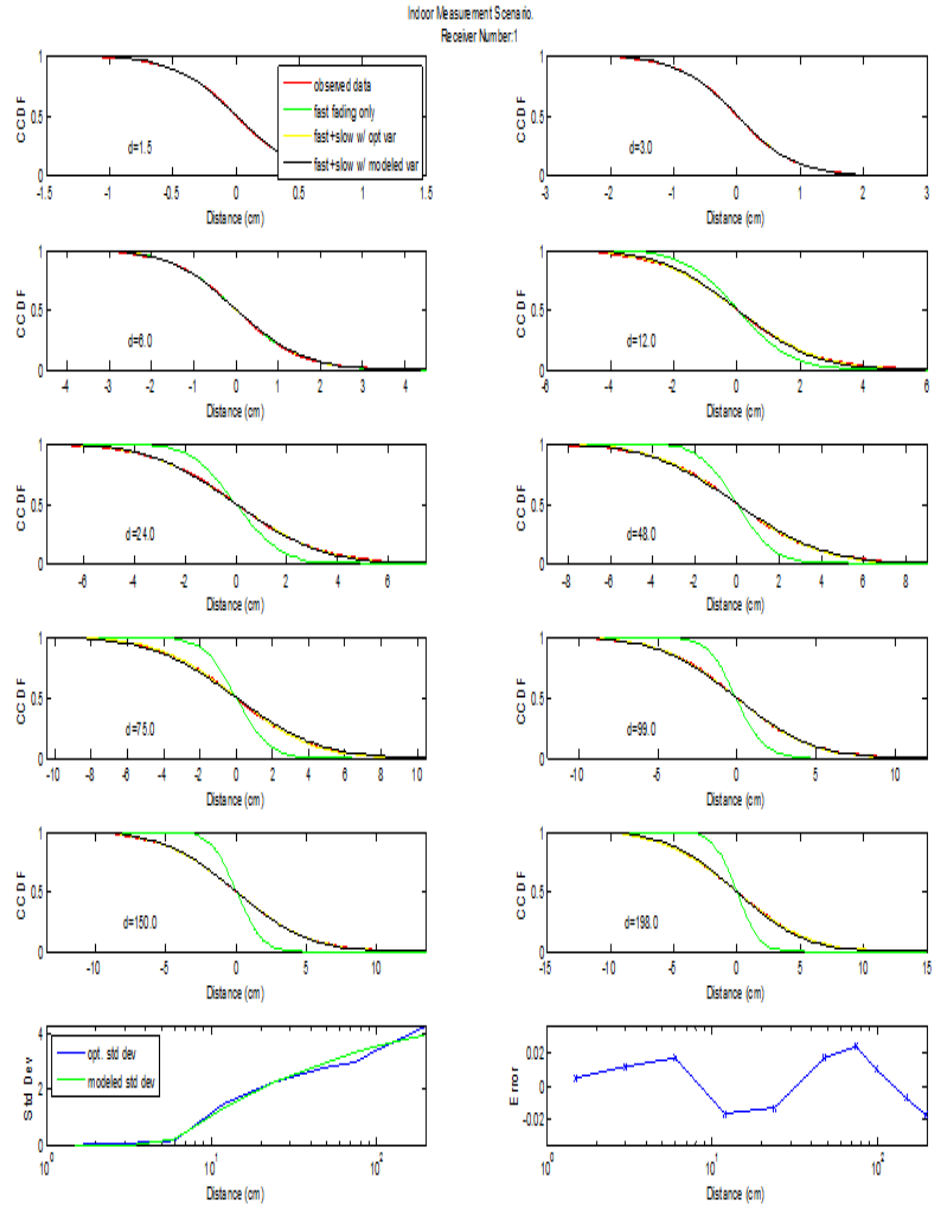


Figure 4.8: The quality of fit for the model Office Receiver 1

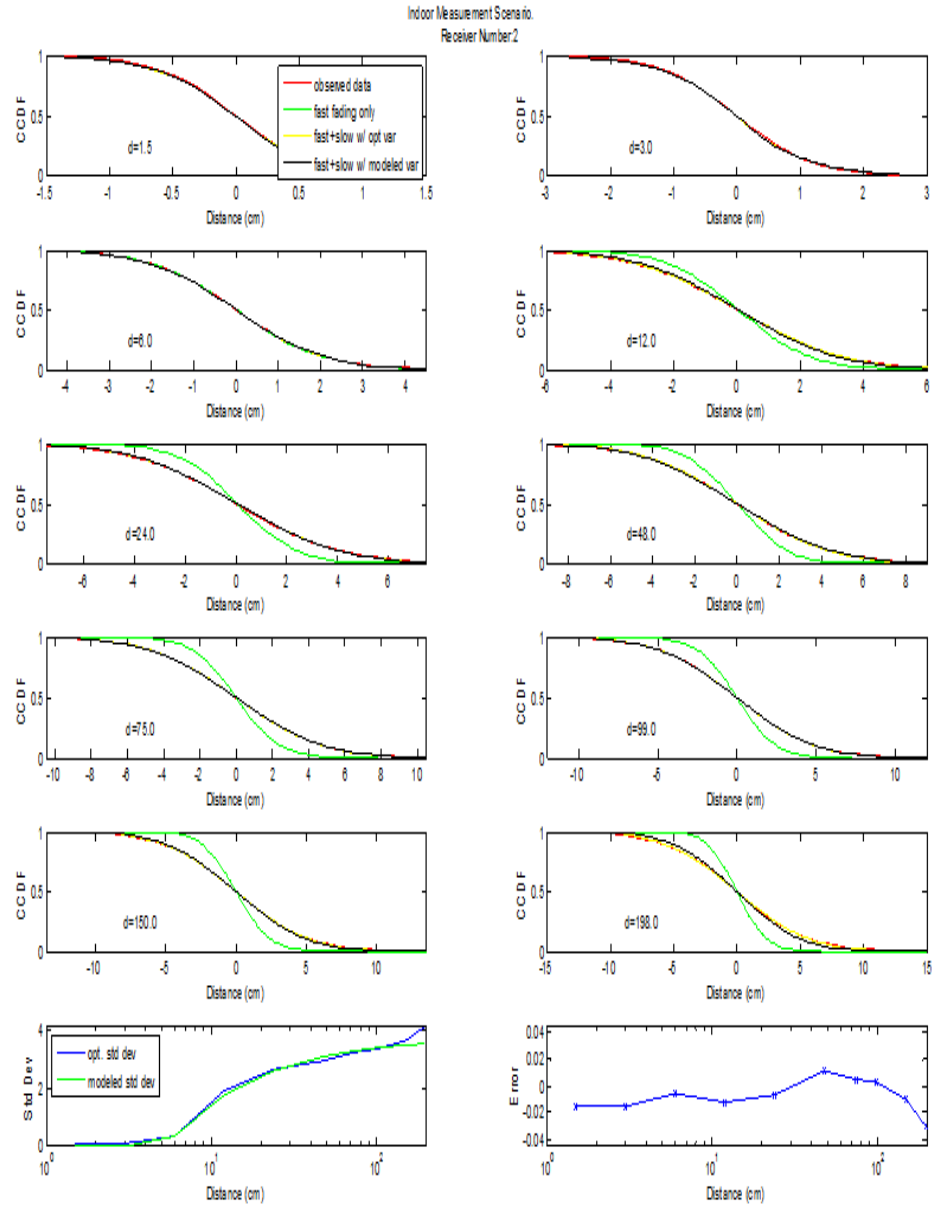


Figure 4.9: The quality of fit for the model Office Receiver 2

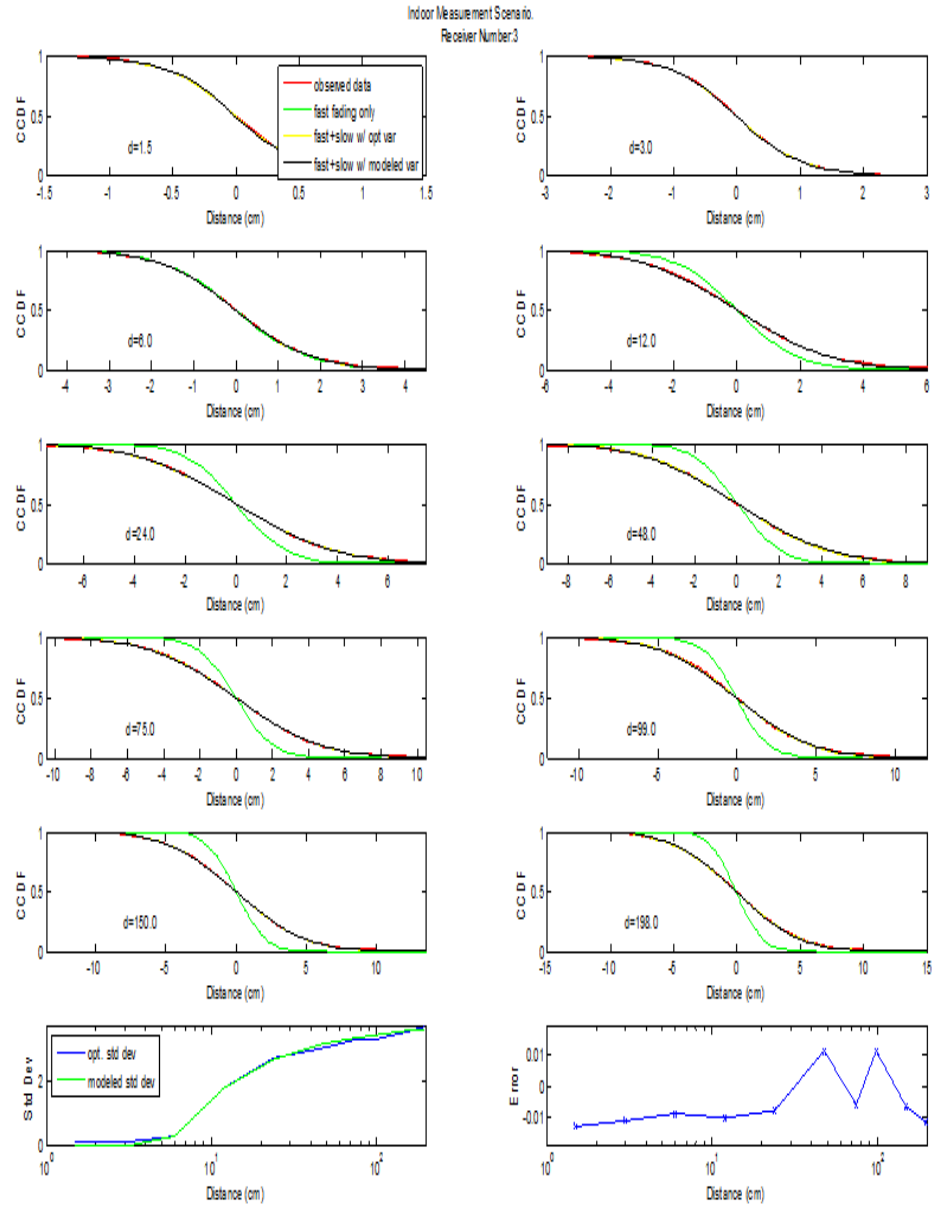


Figure 4.10: The quality of fit for the model Office Receiver 3

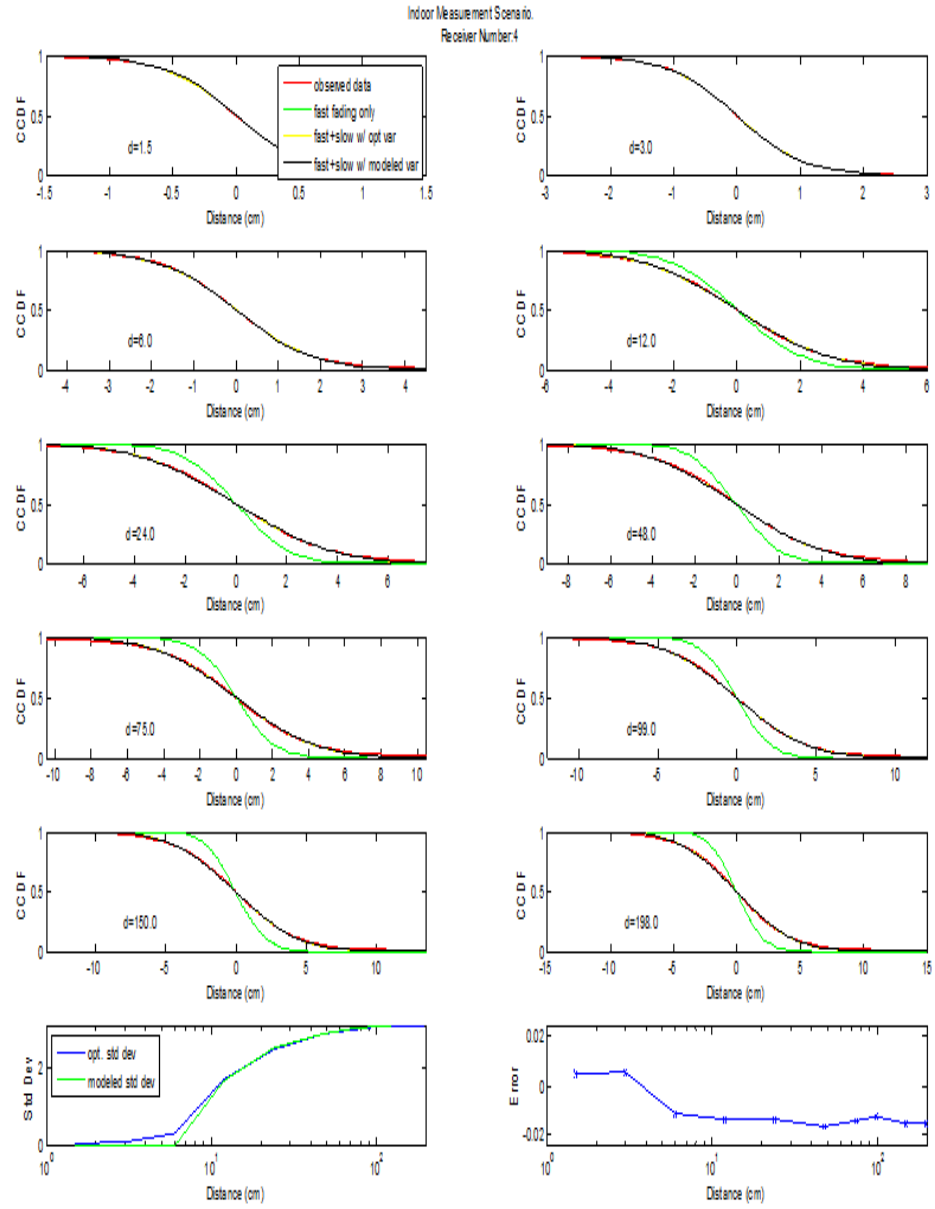


Figure 4.11: The quality of fit for the model Office Receiver 4

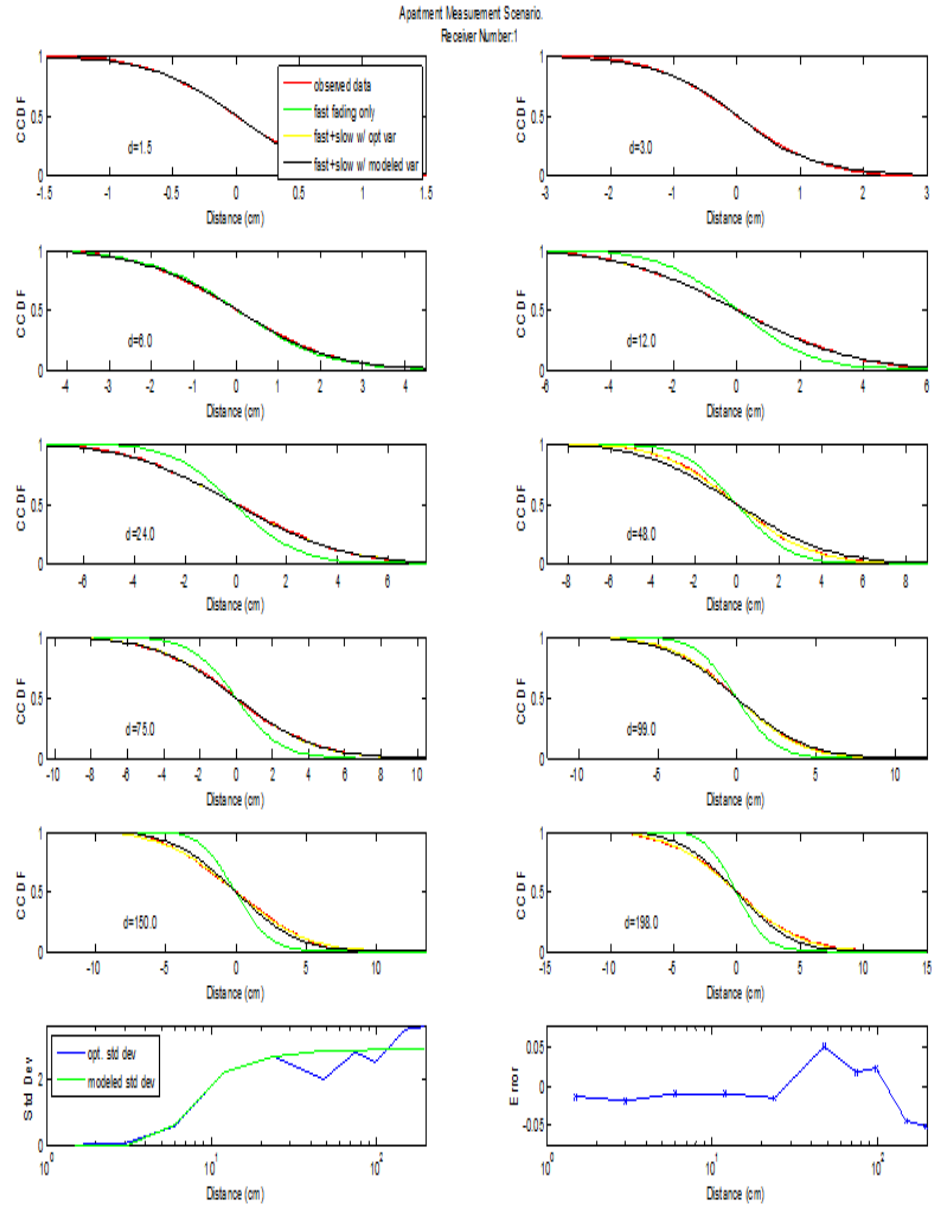


Figure 4.12: The quality of fit for the model Apartment Receiver 1

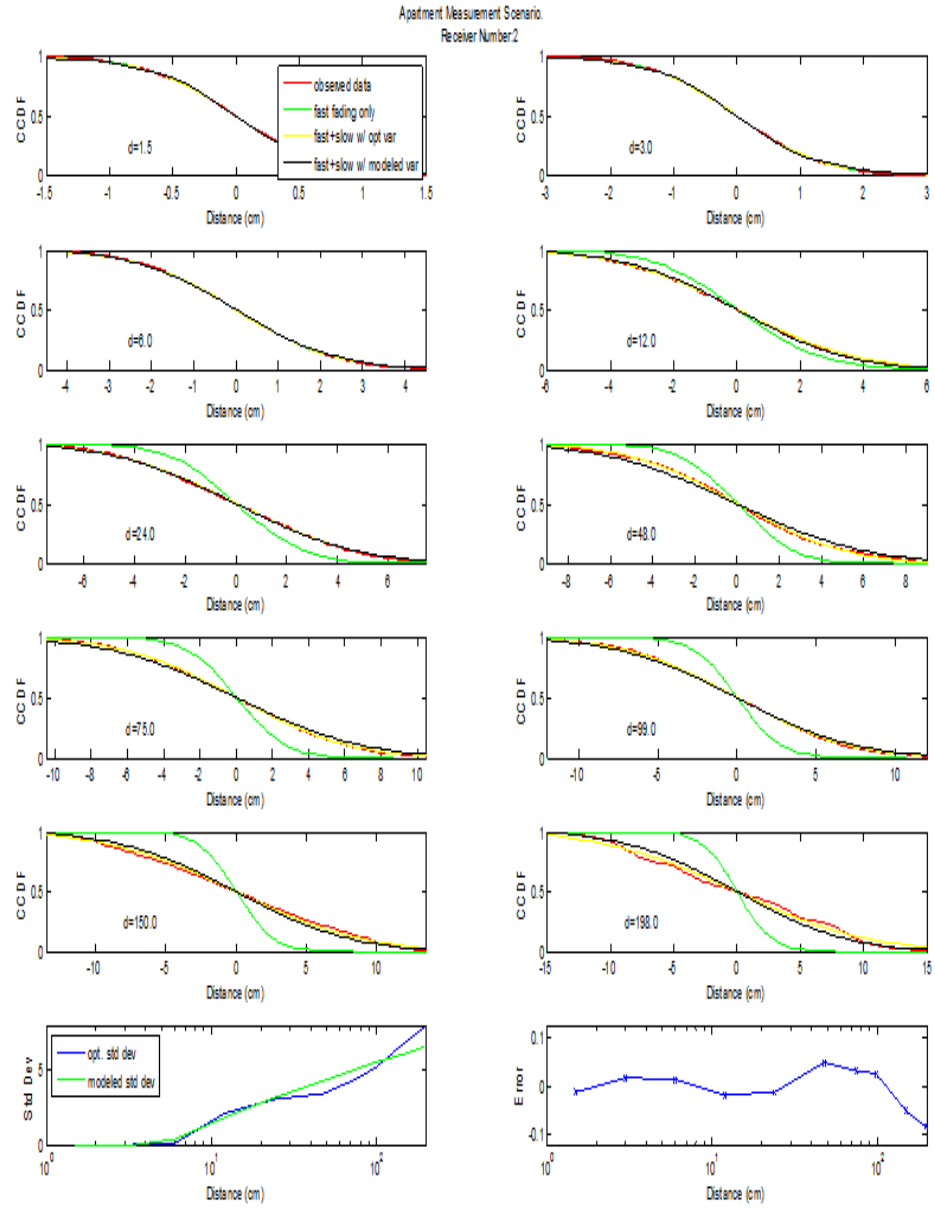


Figure 4.13: The quality of fit for the model Apartment Receiver 2

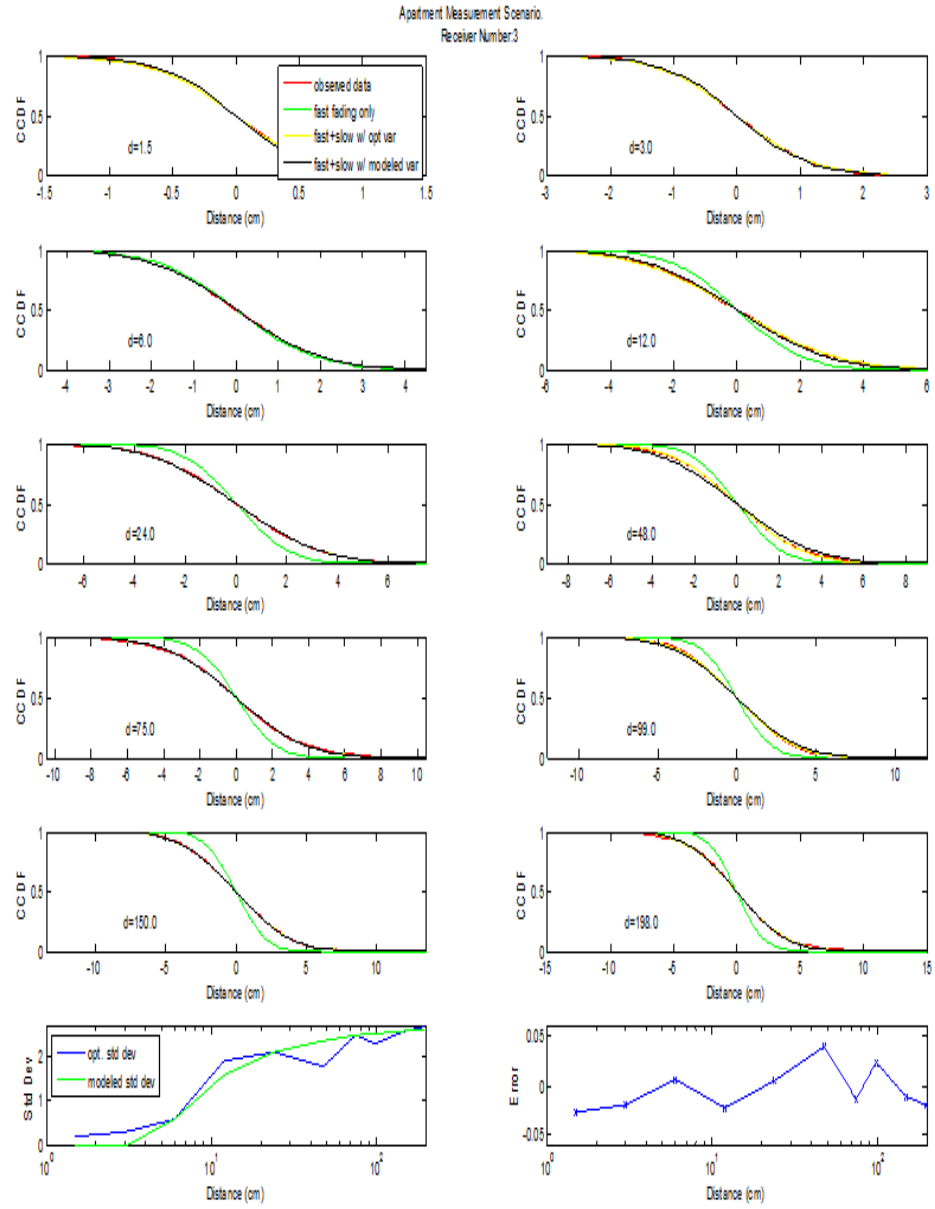


Figure 4.14: The quality of fit for the model Apartment Receiver 3

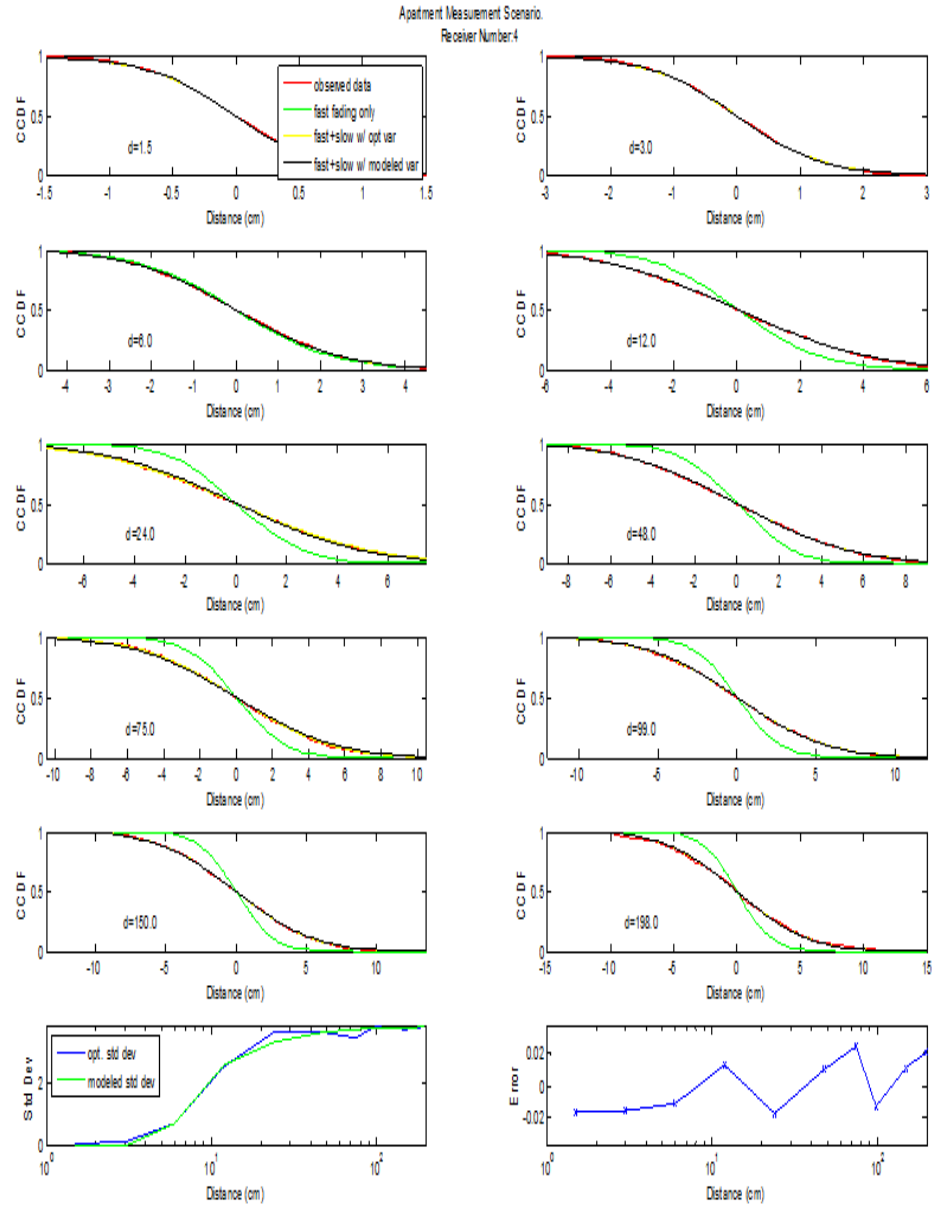


Figure 4.15: The quality of fit for the model Apartment Receiver 4

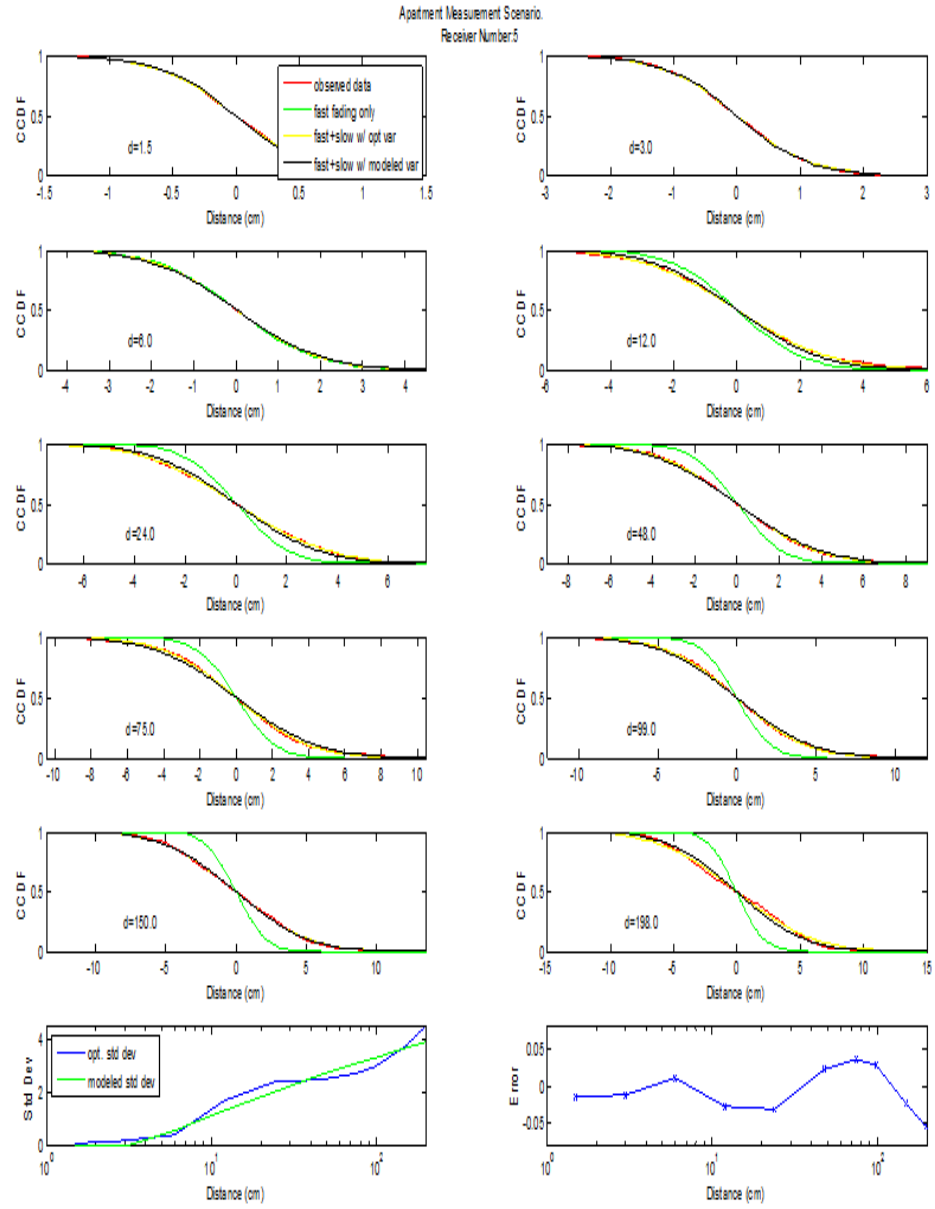


Figure 4.16: The quality of fit for the model Apartment Receiver 5

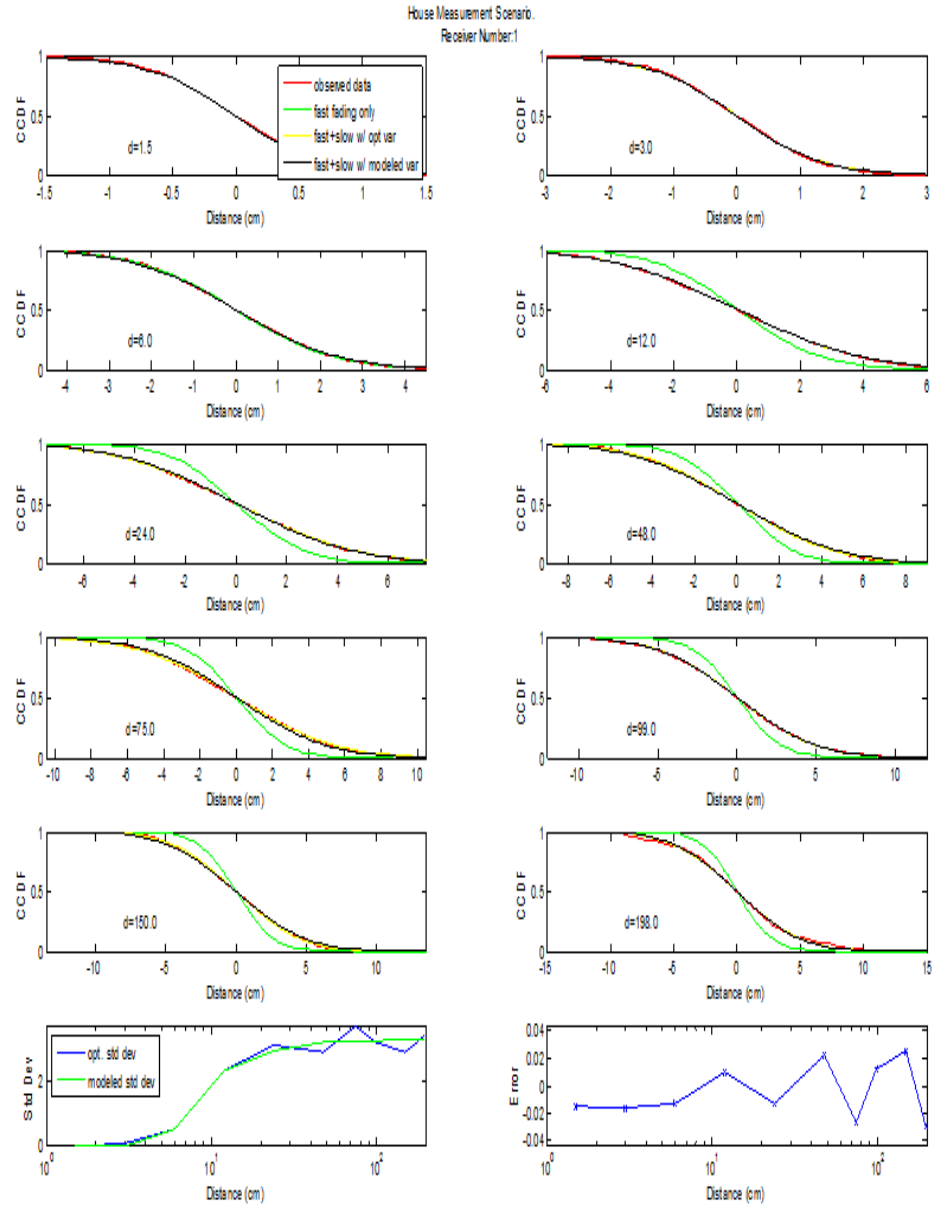


Figure 4.17: The quality of fit for the model House Receiver 1

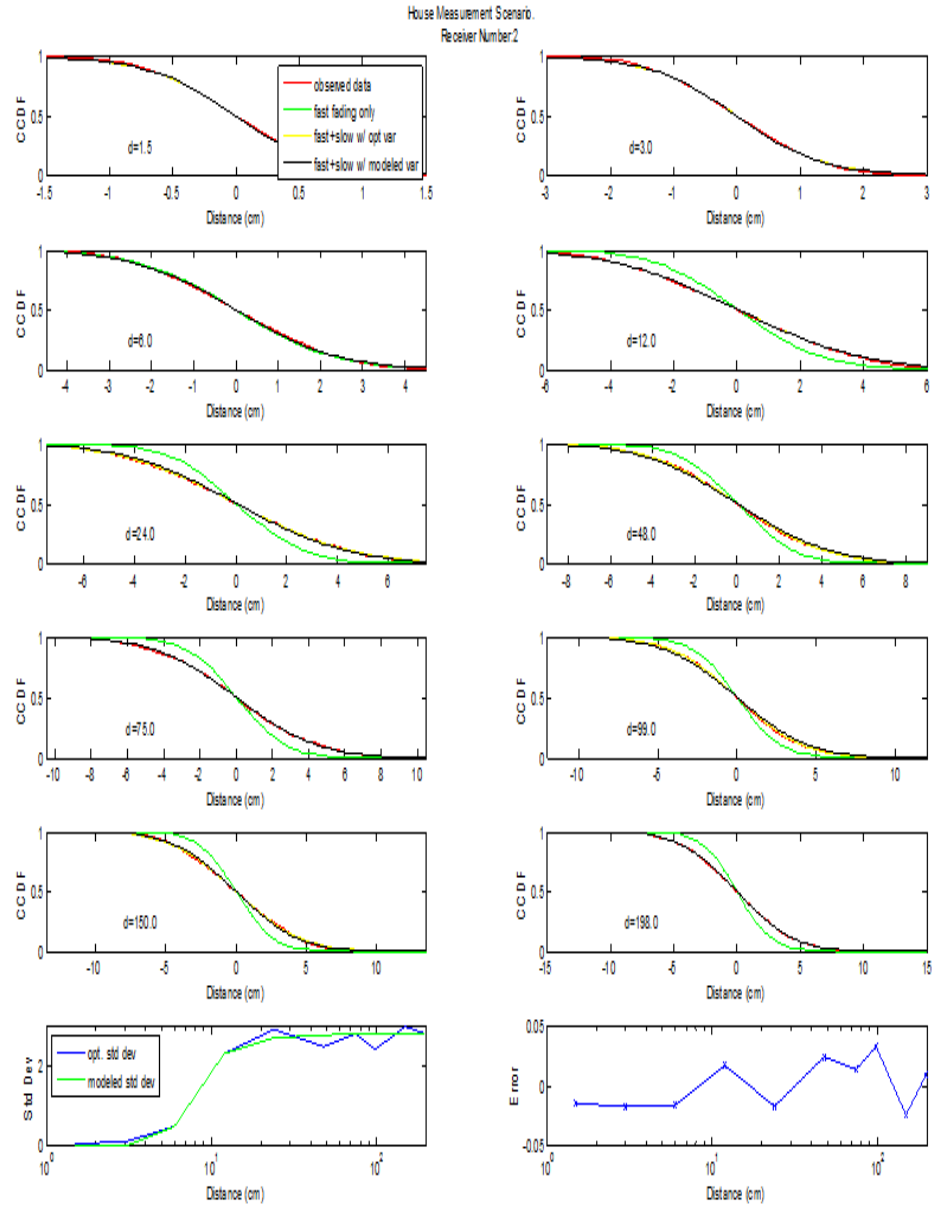


Figure 4.18: The quality of fit for the model House Receiver 2

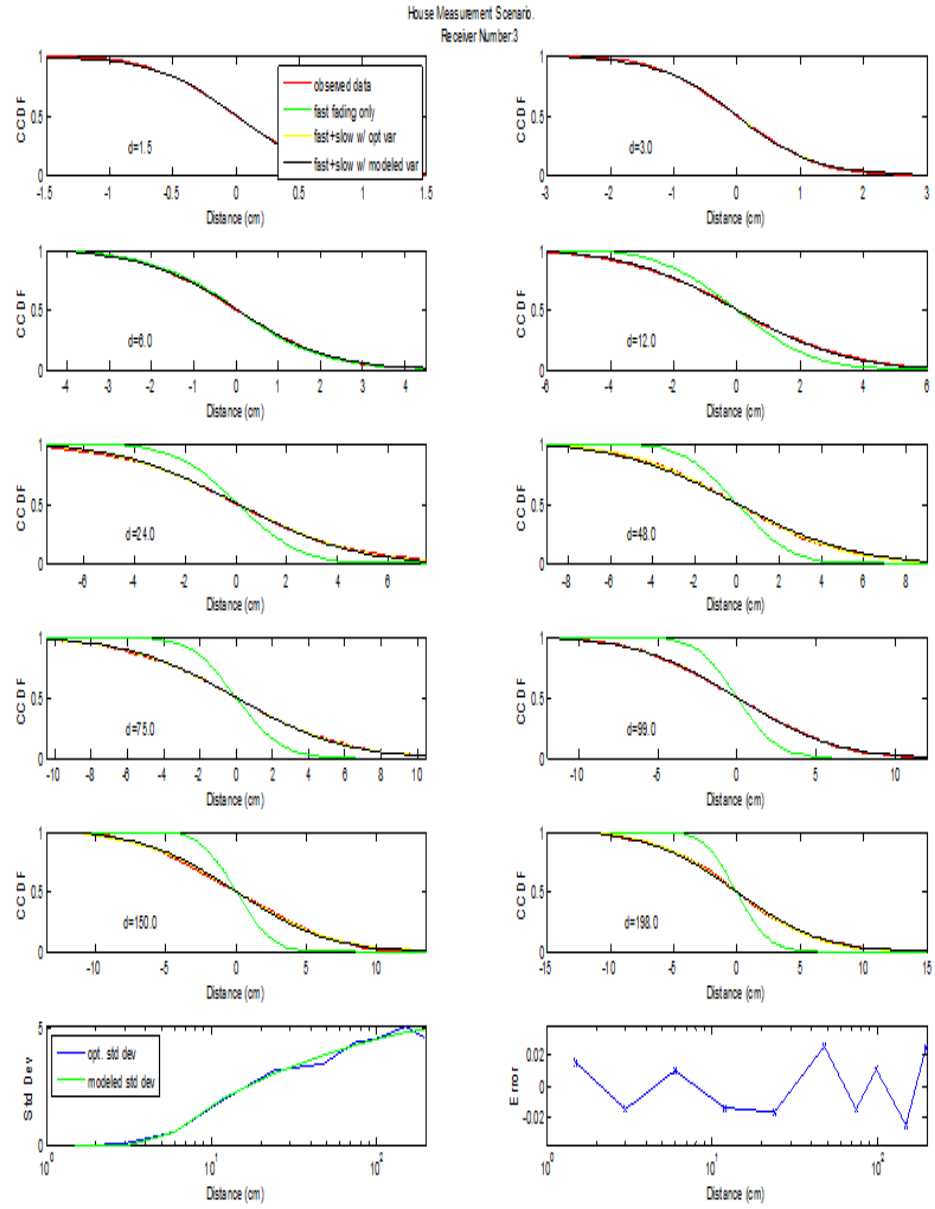


Figure 4.19: The quality of fit for the model House Receiver 3

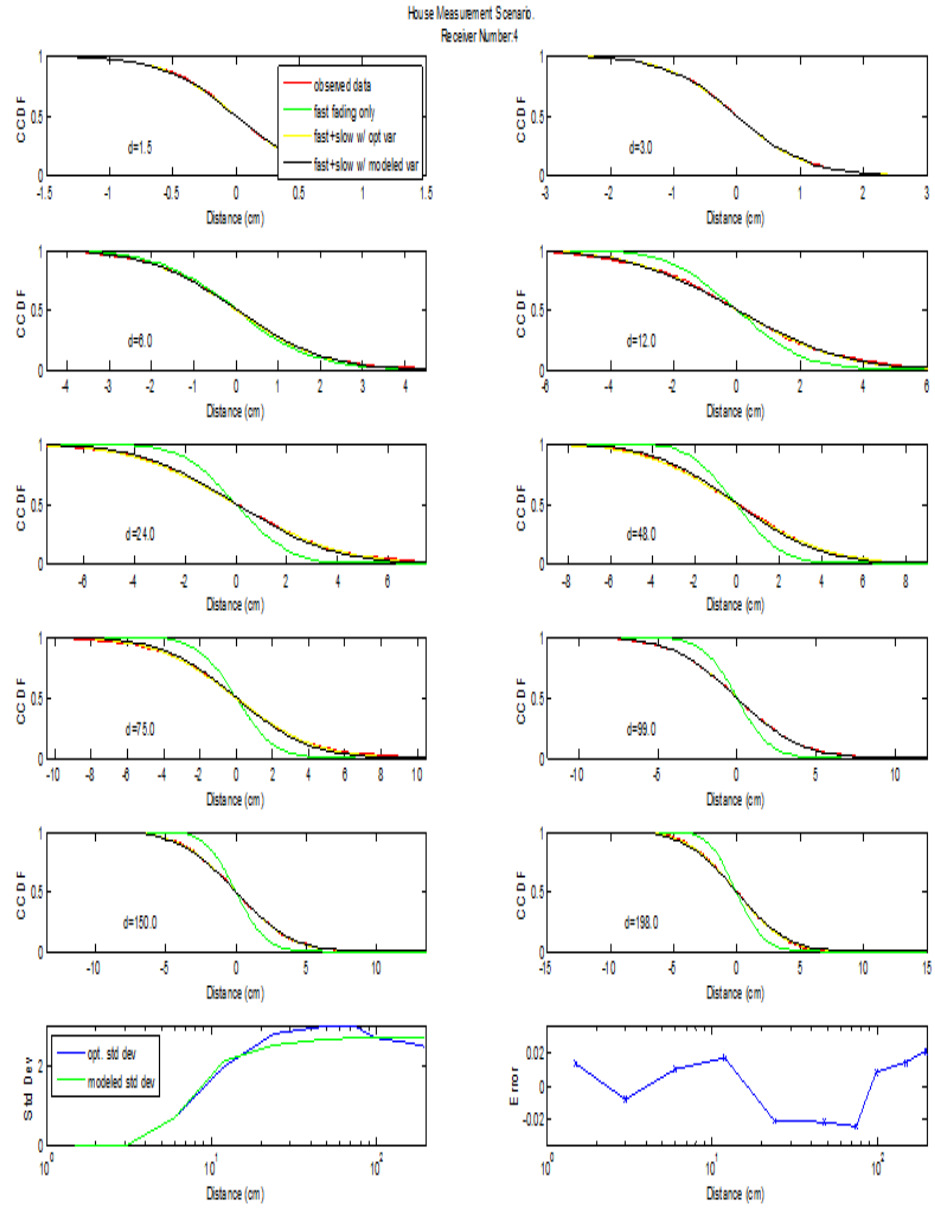


Figure 4.20: The quality of fit for the model House Receiver 4

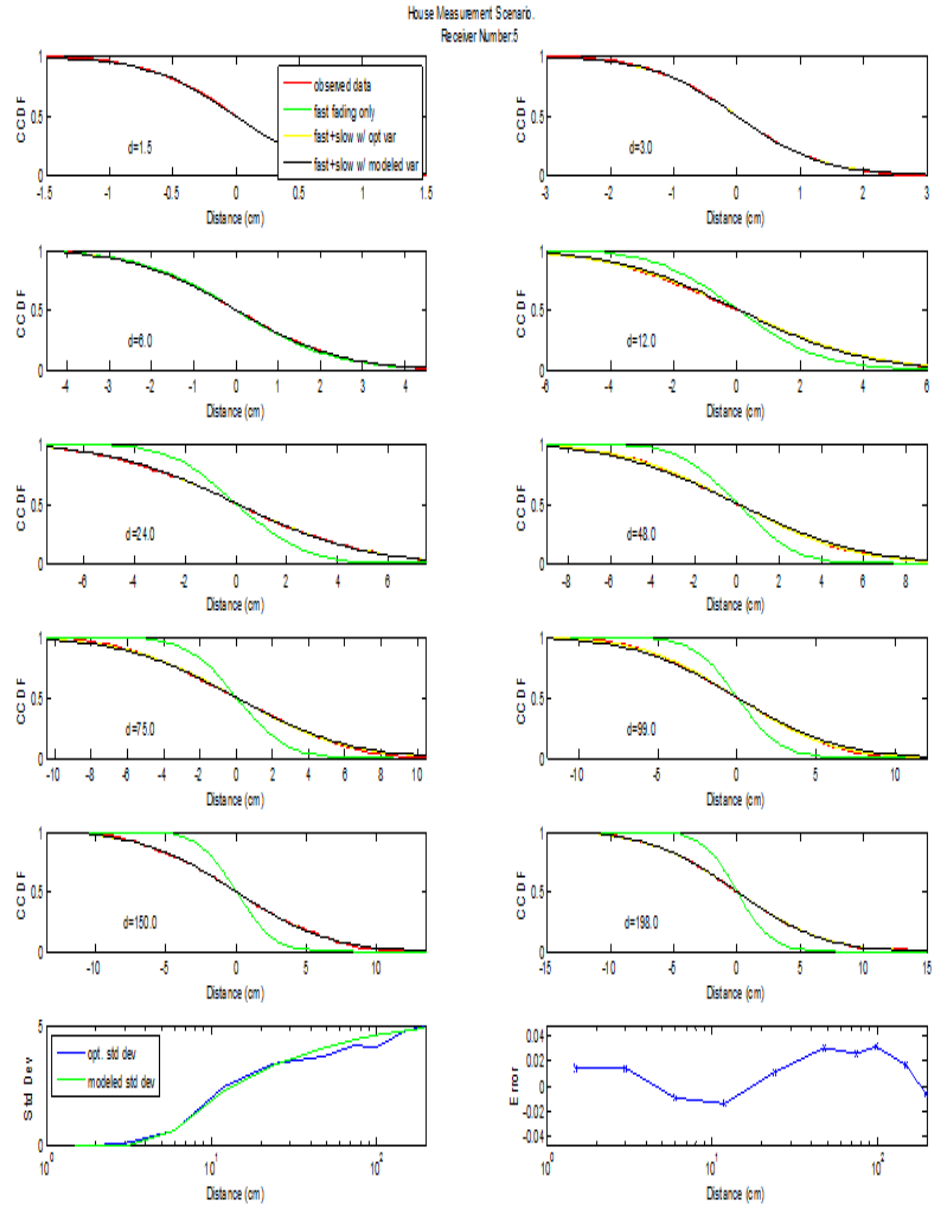


Figure 4.21: The quality of fit for the model House Receiver 5

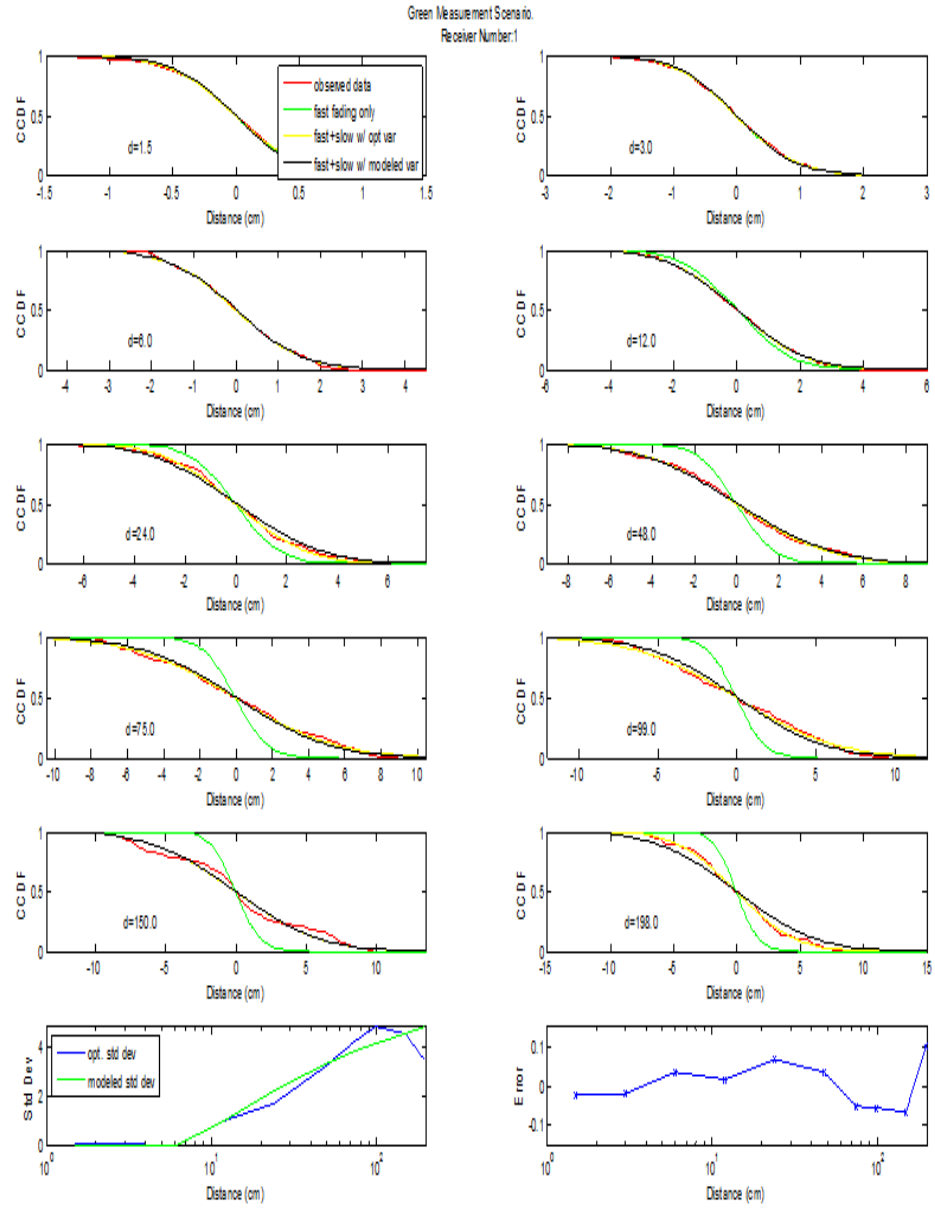


Figure 4.22: The quality of fit for the model Green Receiver 1

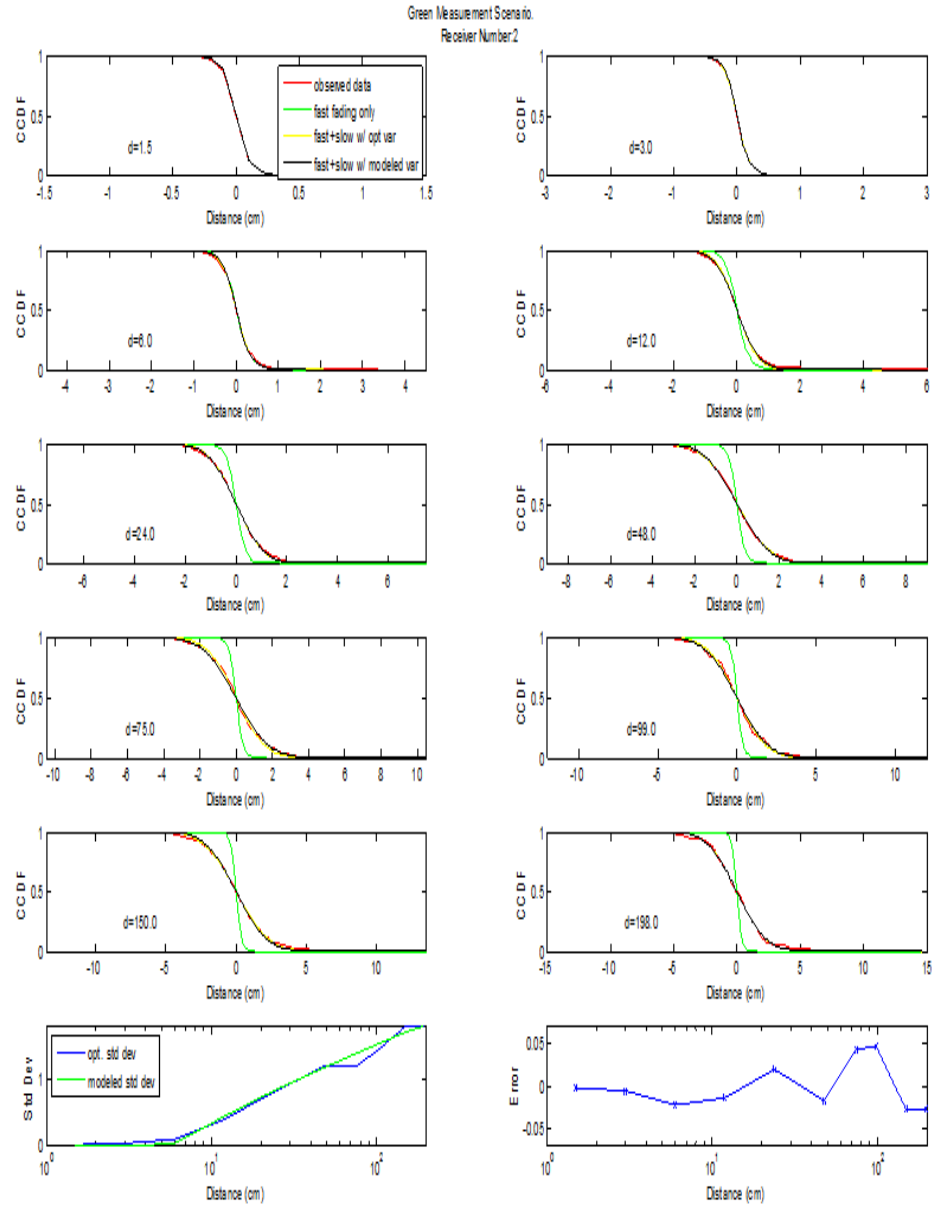


Figure 4.23: The quality of fit for the model Green Receiver 2

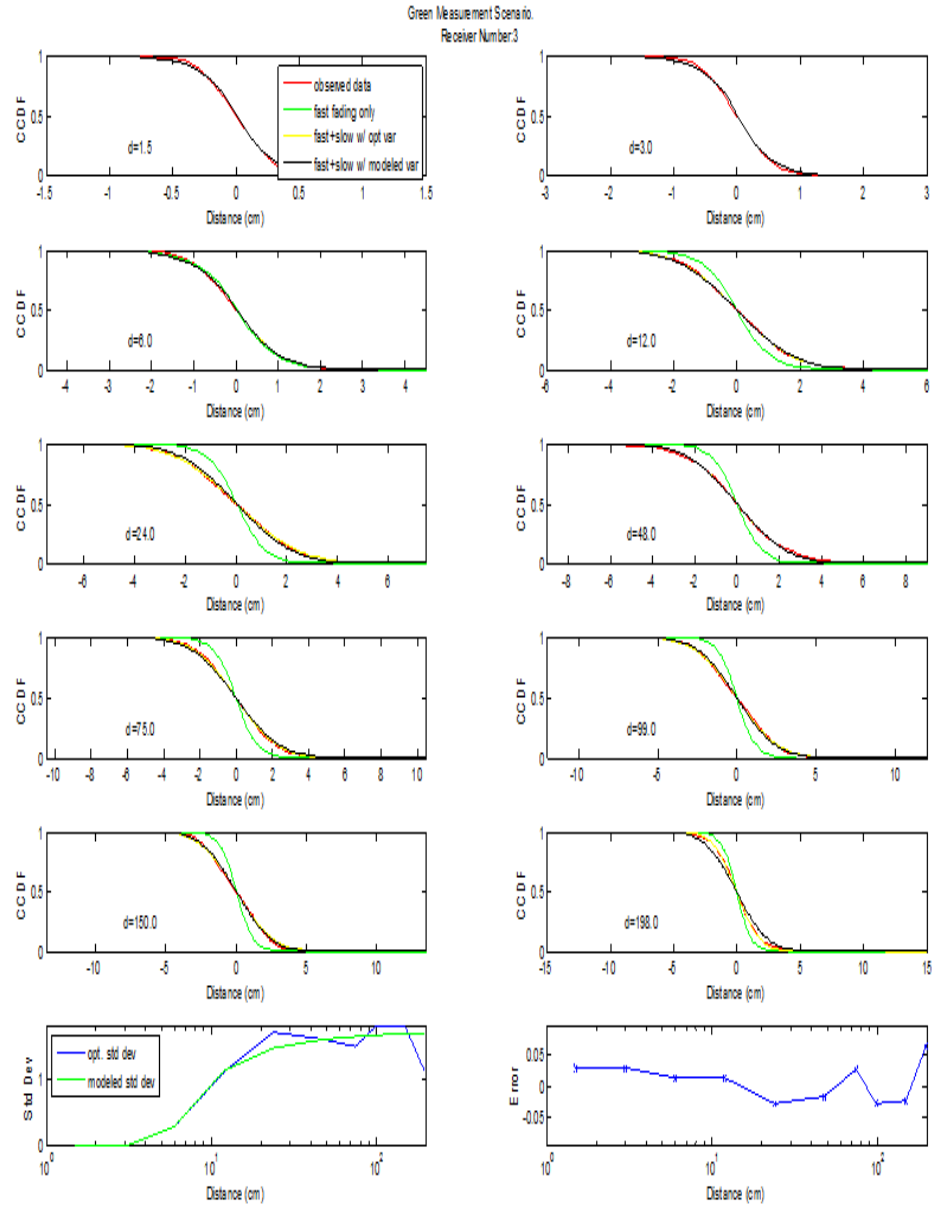


Figure 4.24: The quality of fit for the model Green Receiver 3

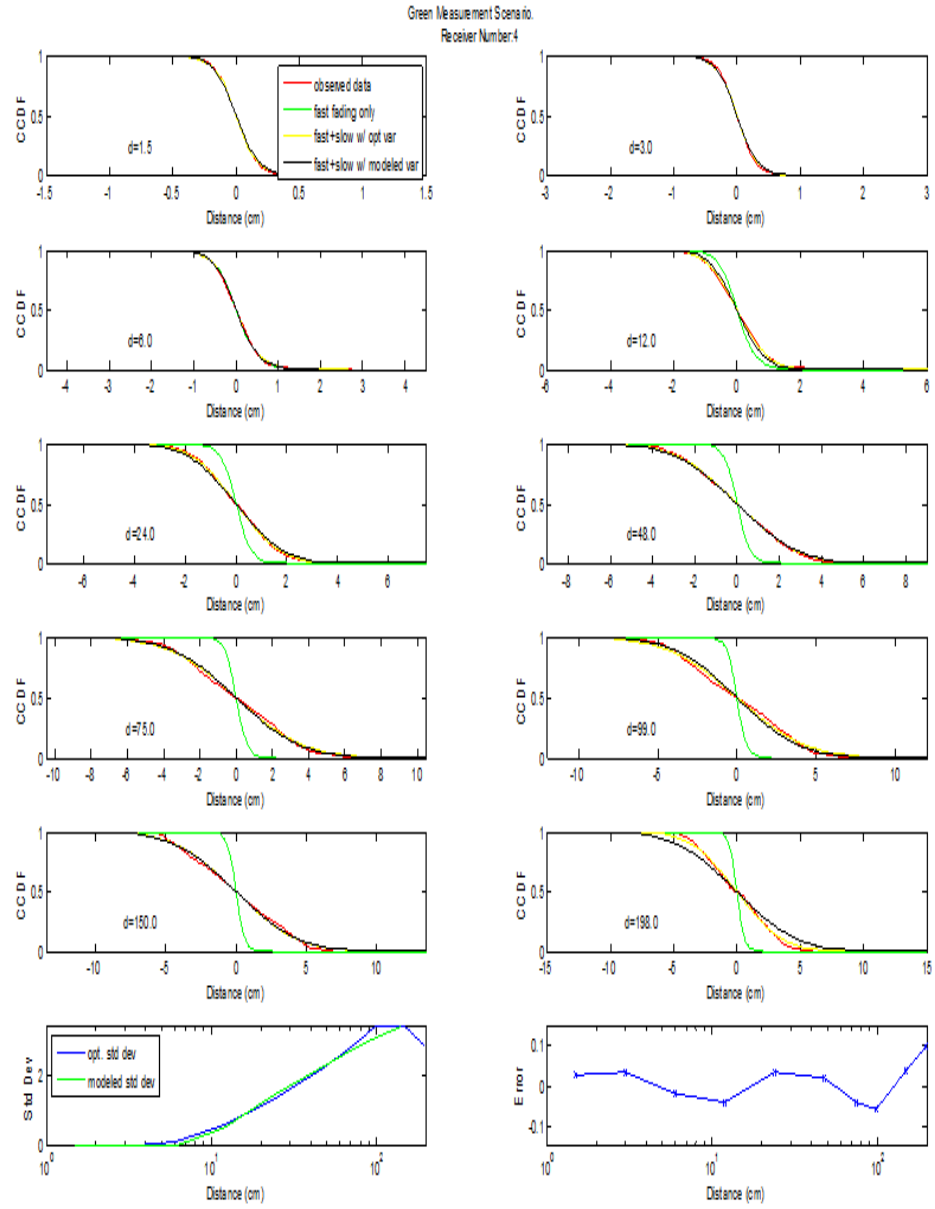


Figure 4.25: The quality of fit for the model Green Receiver 4

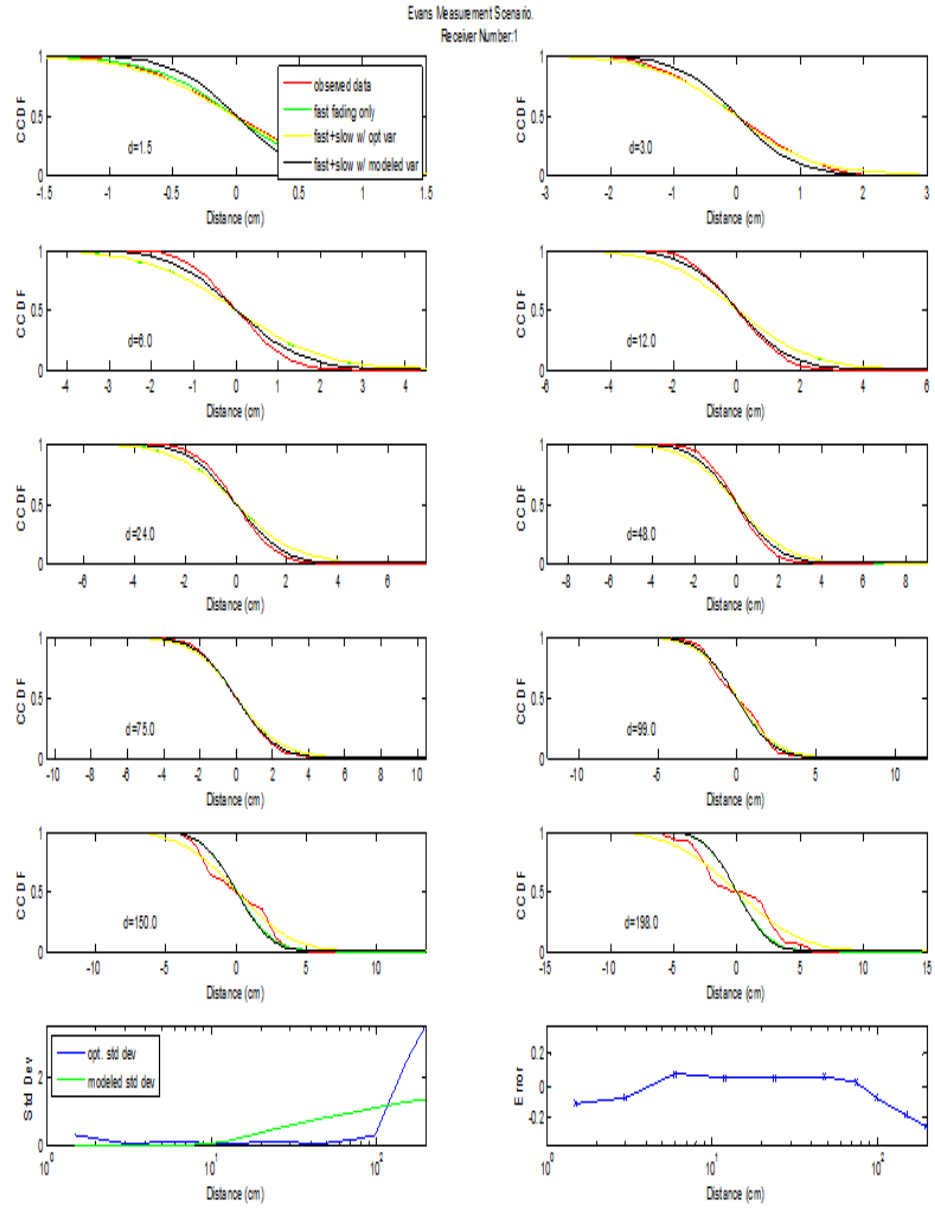


Figure 4.26: The quality of fit for the model Evans Receiver 1

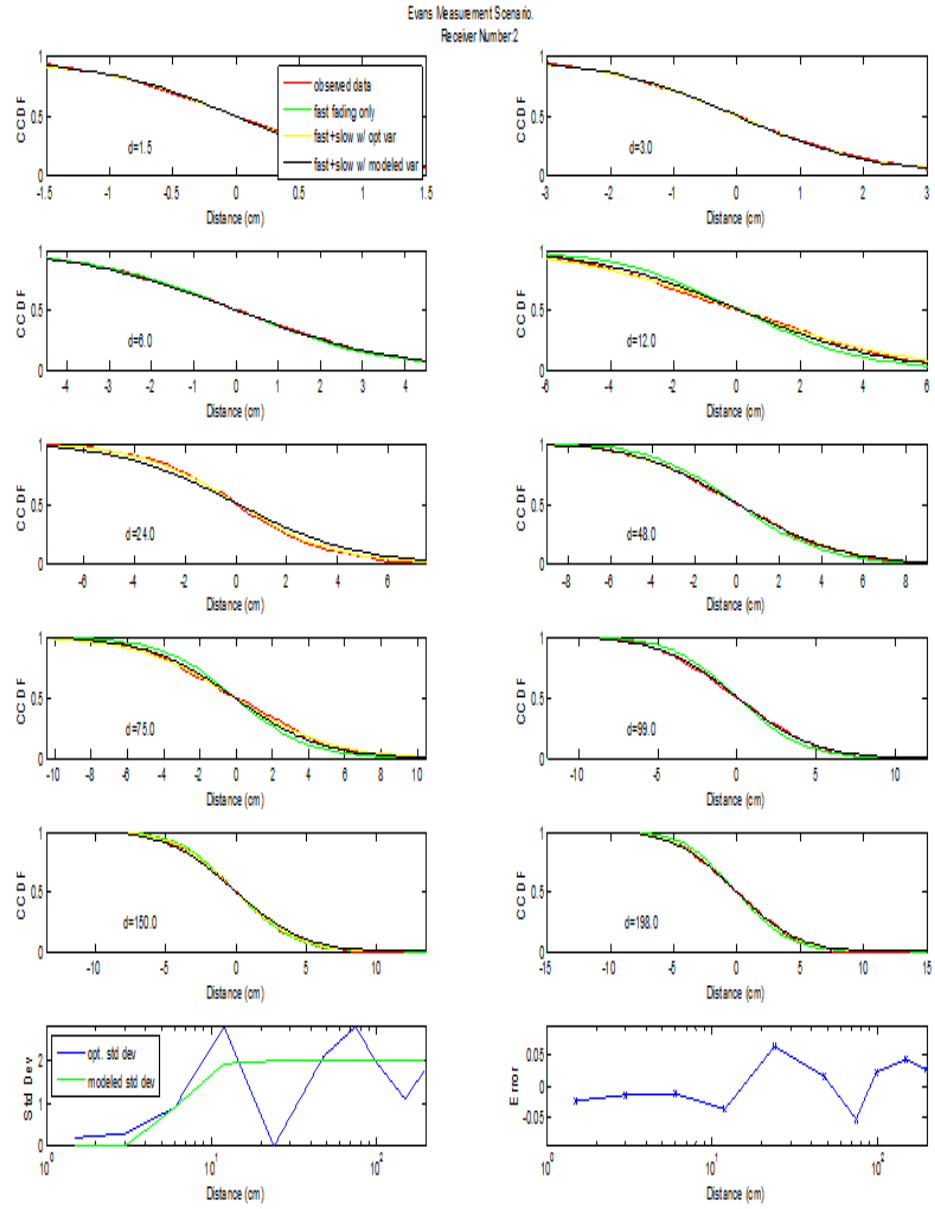


Figure 4.27: The quality of fit for the model Evans Receiver 2

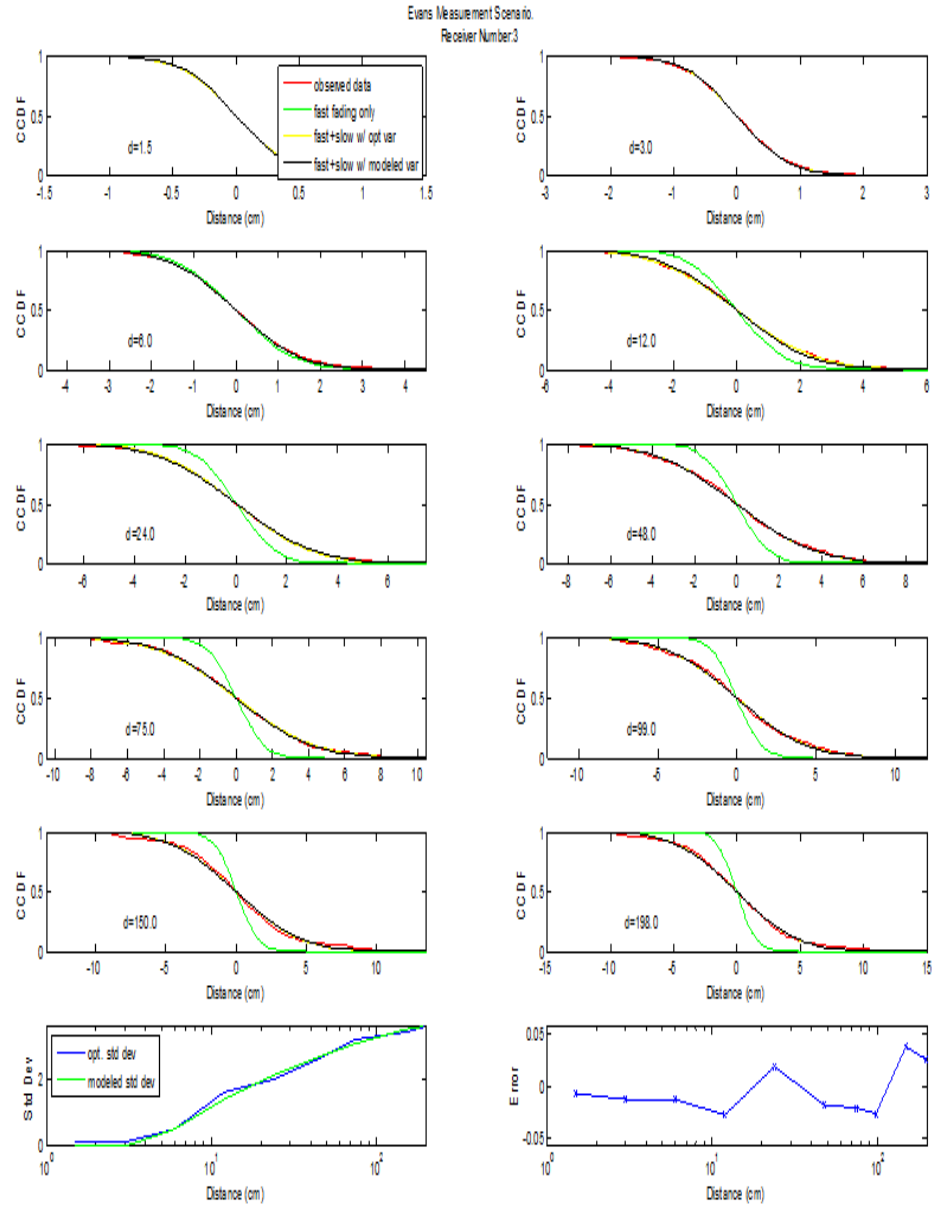


Figure 4.28: The quality of fit for the model Evans Receiver 3

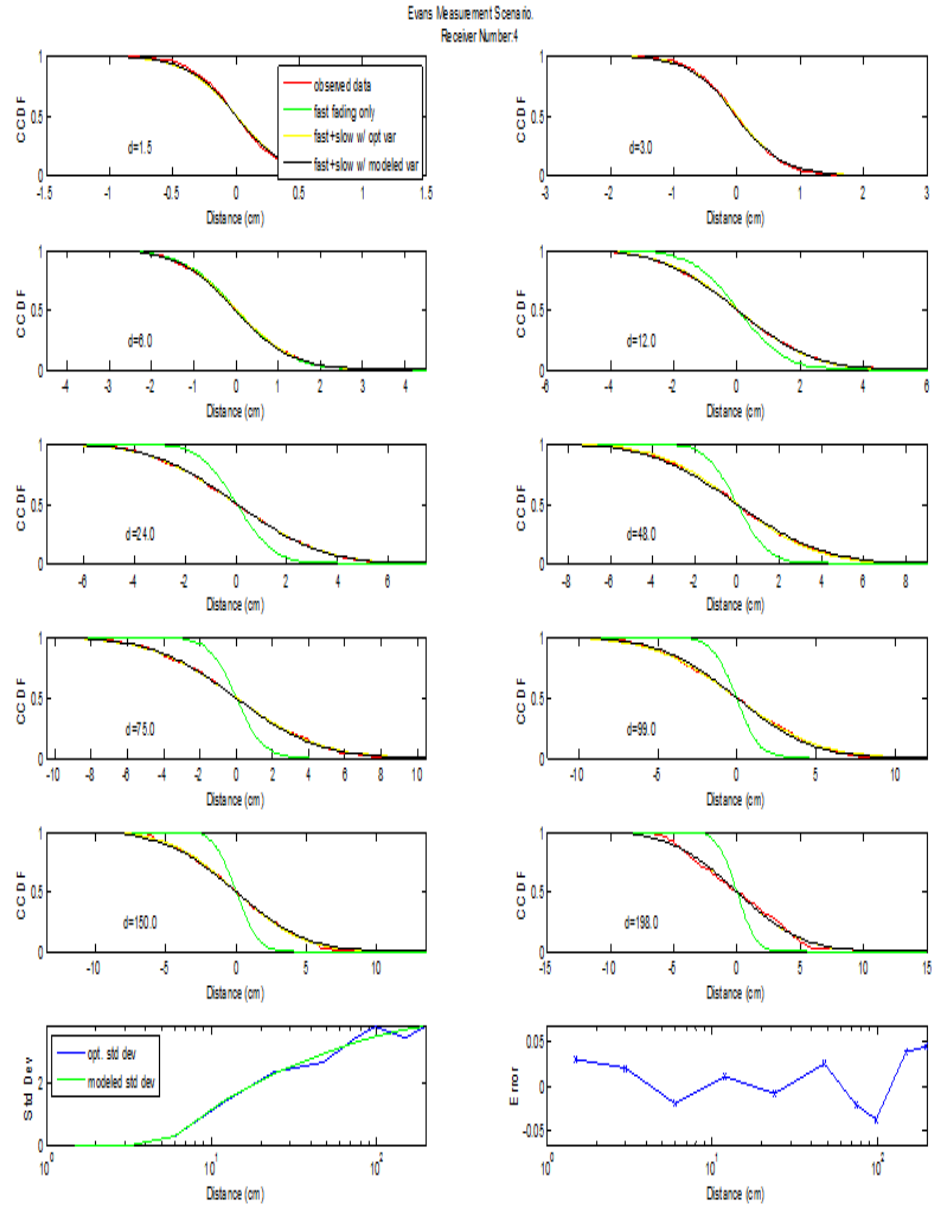


Figure 4.29: The quality of fit for the model Evans Receiver 4

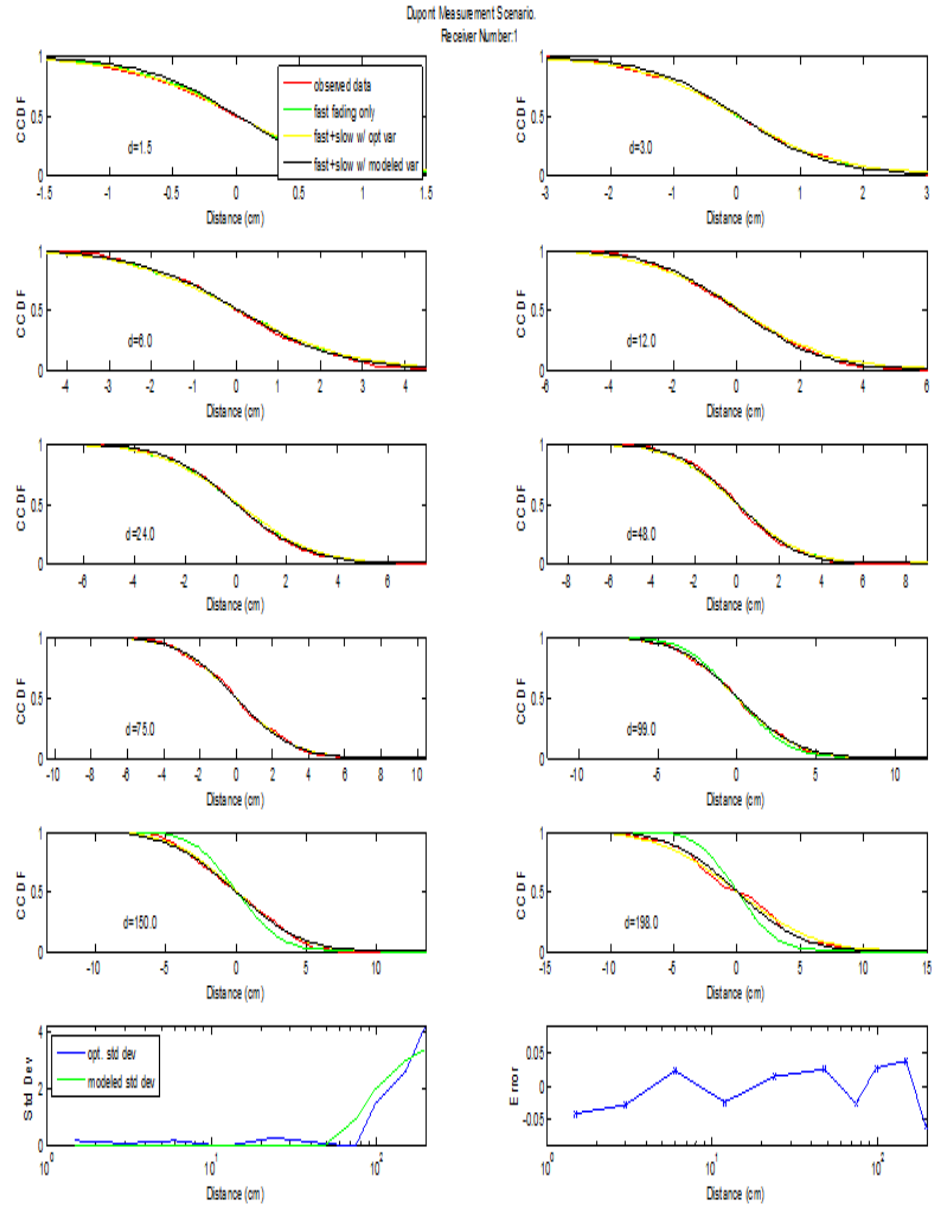


Figure 4.30: The quality of fit for the model Dupont Receiver 1

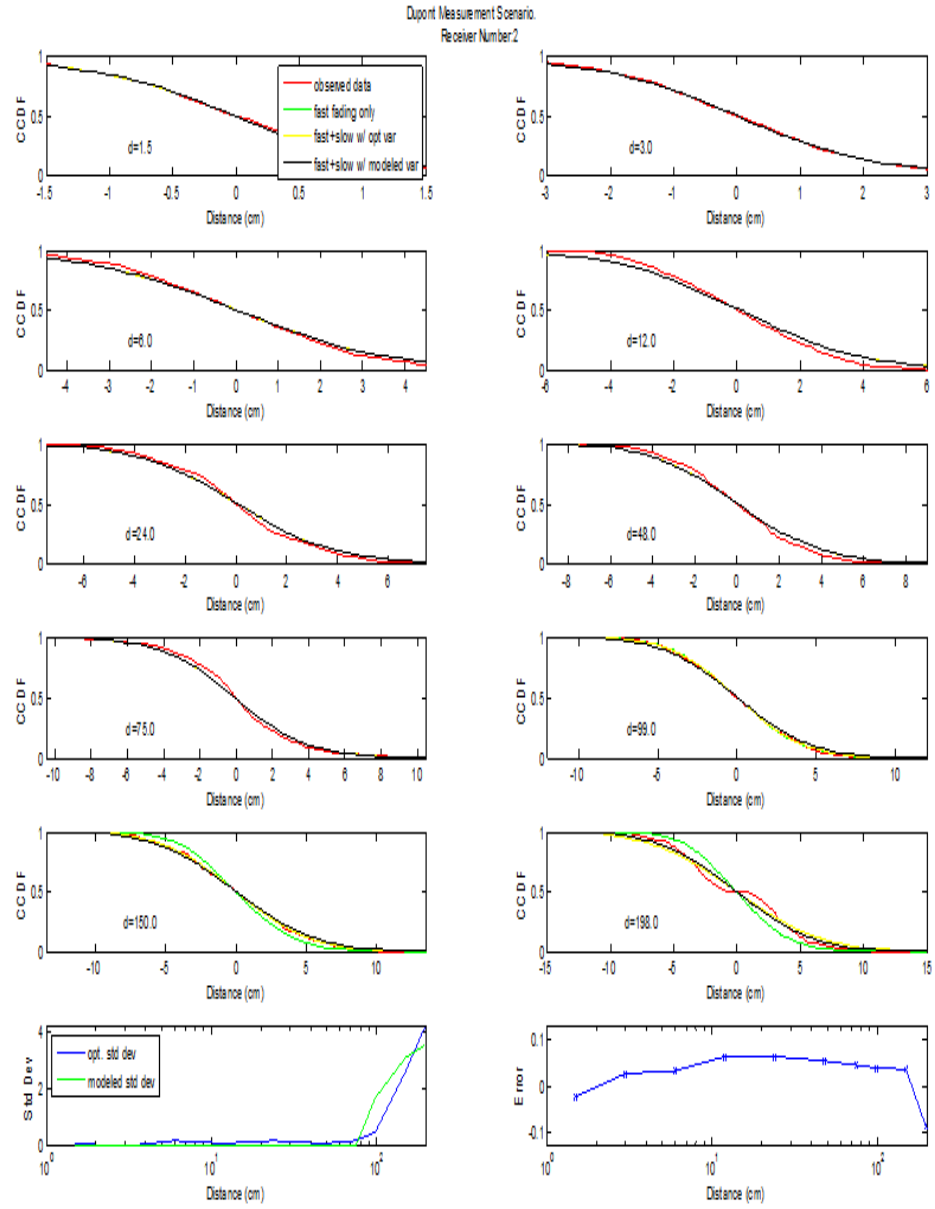


Figure 4.31: The quality of fit for the model Dupont Receiver 2

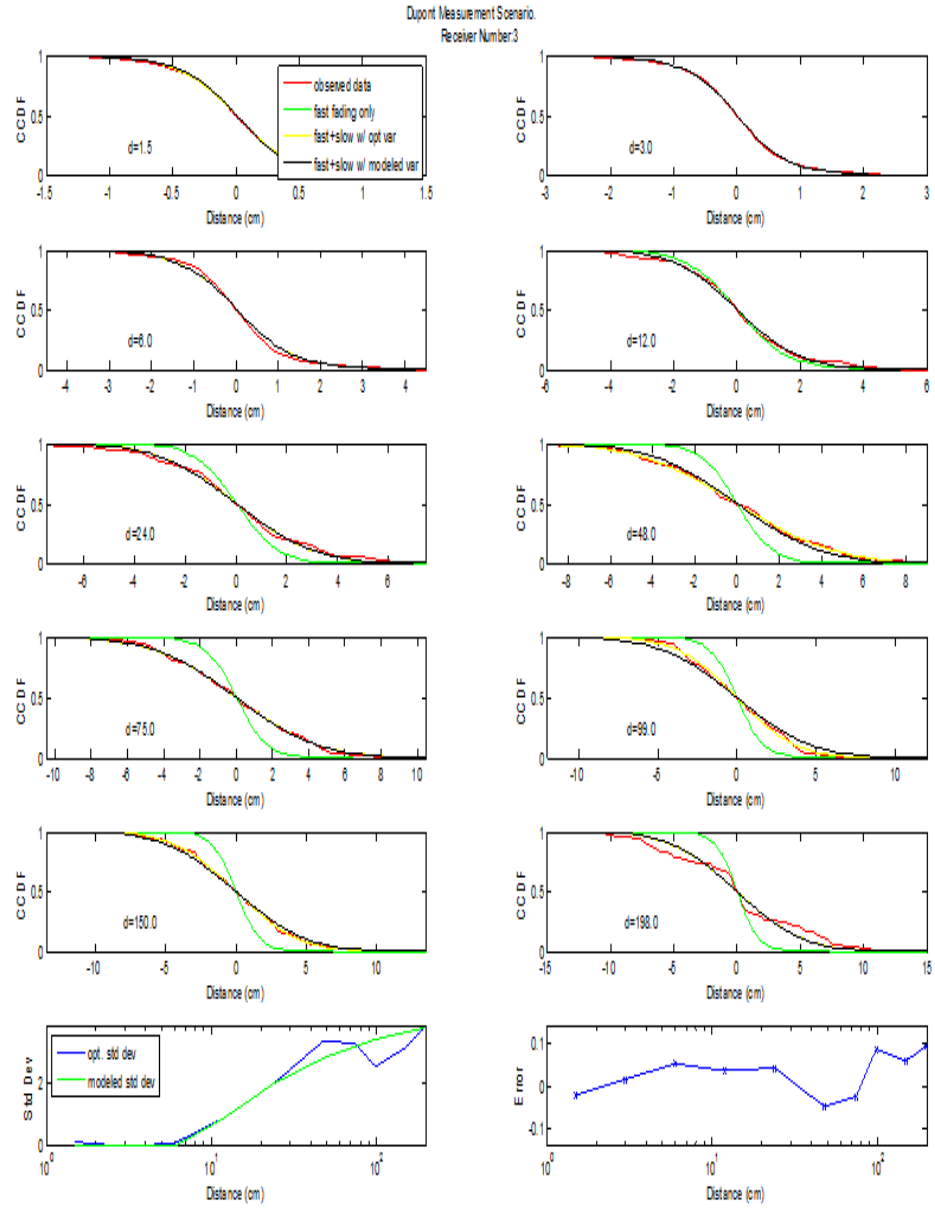


Figure 4.32: The quality of fit for the model Dupont Receiver 3

Figures 4.8 to 4.32 show the quality of fit for the model presented above. Each figure contains 12 frames. The upper ten frames show the CCDF of the change in the signal strength for the ten different distances considered. These frames include 4 curves. One curve represents the observed change in signal strength. The frames also show the change in signal strength if only the fast fading is considered. Note that the fast fading only model provides a good fit at small distances, but fails to provide a good fit for larger distances. Hence, the fast fading model alone cannot explain the variability in the signal strength. Thus, the model includes a lognormal component. Each figure shows two CCDFs of the change in the signal strength for the model with lognormal shadowing. In one model, the standard deviation is optimized for each distance. In the second curve, the parameters σ , α , and h_o are determined to minimize (4.2).

Besides the CCDFs, Figures 4.8 to 4.32 include two lower frames. The frame on the lower left shows the standard deviation of the lognormal fading component as given by the model (4.1) and for the standard deviation that is optimize for each distance. As can be observed, in most cases, the model provides a very good fit. The quality of fit can also be observed by examining the upper ten frames of each figure and observing that the complete model with the modeled standard deviation and the complete model with optimize standard deviation provide nearly the same quality of fit.

Finally, the frame on the lower right shows the modeling error. Specifically, the figures show

$$g(h) = \begin{cases} \max_{c>0} |P(\Delta H_M(h) < c) - P(\Delta H(h) < c)| \\ \quad \text{if } \max_{c>0} |P(\Delta H_M(h) < c) - P(\Delta H(h) < c)| \\ \quad > \min_{c>0} |P(\Delta H_M(h) < c) - P(\Delta H(h) < c)| \\ \min_{c>0} |P(\Delta H_M(h) < c) - P(\Delta H(h) < c)| & \text{otherwise} \end{cases}$$

Thus, if $g(h) > 0$, then the model over estimates the channel variability and if $g(h) < 0$, then the model under estimates the modeling error. As can be observed, the modeling error is quite small.

Figure 4.33 shows the median and 75th percentile of the modeling error for the complete model with the modeled standard deviation and the complete model with optimizes standard deviation. Note that the model error is typically quite small, but does tend to grow for large distances. If the optimized standard deviation is used, the modeling error is only slightly reduced, indicating the quality of the standard deviation model (4.1). However, the modeling error at a displacement of 198 cm for the optimized standard deviation case does not increase as much as the model standard deviation. This indicates the possibility that a different model for the standard deviation should be used for large distances. On the other hand, since the transmitter only moved a total of 3 m, there was limited data to estimate the 2 m displacement case. Hence, this large error at 2 m, could be from statistic variation.

Figure 4.34 shows the values of the delay spread, R , found by minimizing (4.2). Note that in most cases, the delay spread is larger outside than inside. However, the "Dupont" scenario and one of the channels in "Evans" had low delay spread. The other parameters, σ , d_o and α are shown in figures 4.35, 4.36, and 4.37 respectively.

See Chapter 1 for an interpretation of the channel model results.

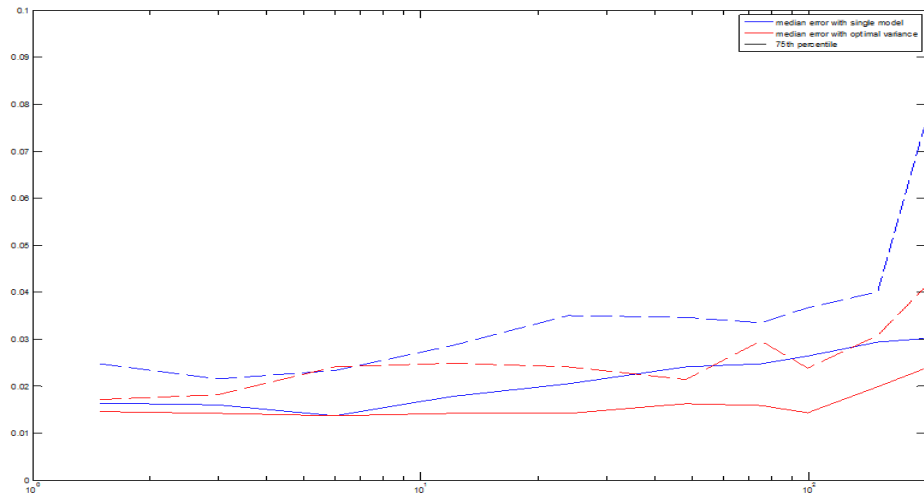


Figure 4.33: The median and 75th percentile of the modeling error for the complete model with the modeled standard deviation and the complete model with optimizes standard deviation.

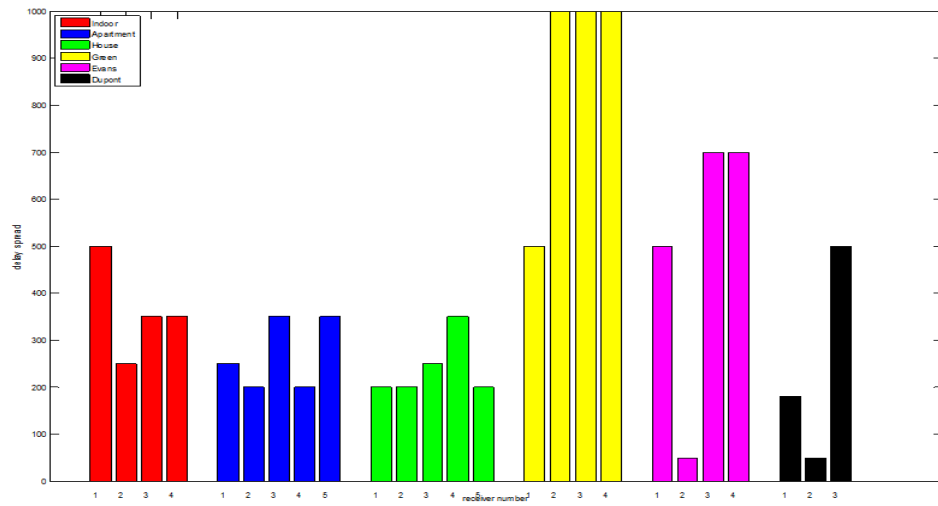


Figure 4.34: The Values of the Delay Spread, R

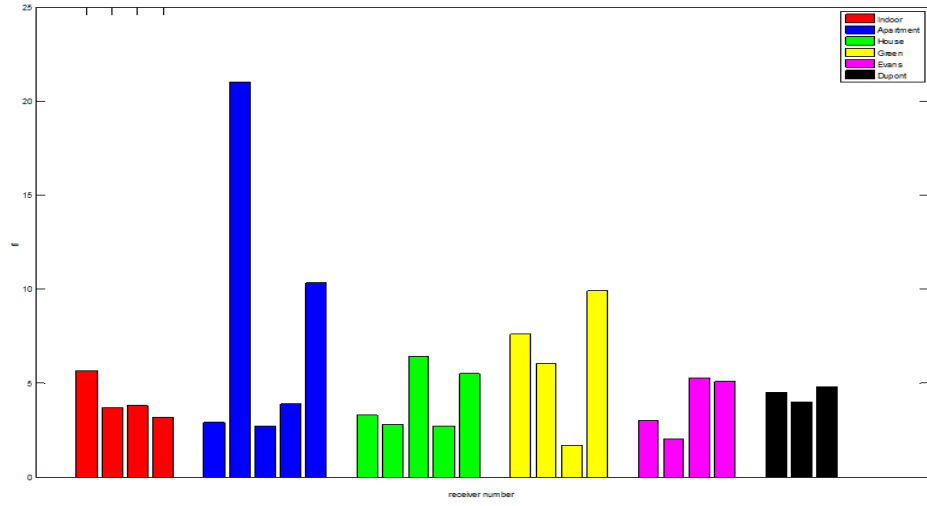


Figure 4.35: The Maximum Standard Deviation of the Lognormal Fading, σ

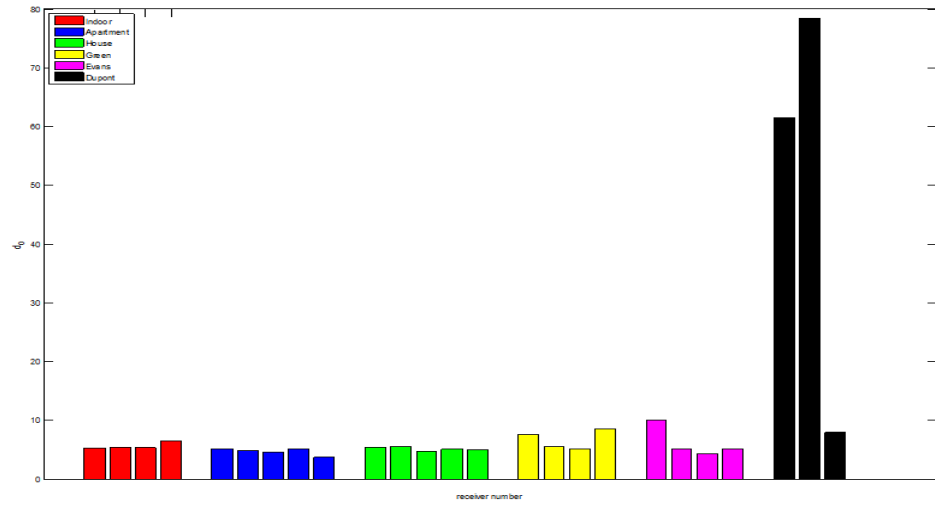


Figure 4.36: The Distance where the Cross-correlation Changes from Zero to Non-zero, d_o

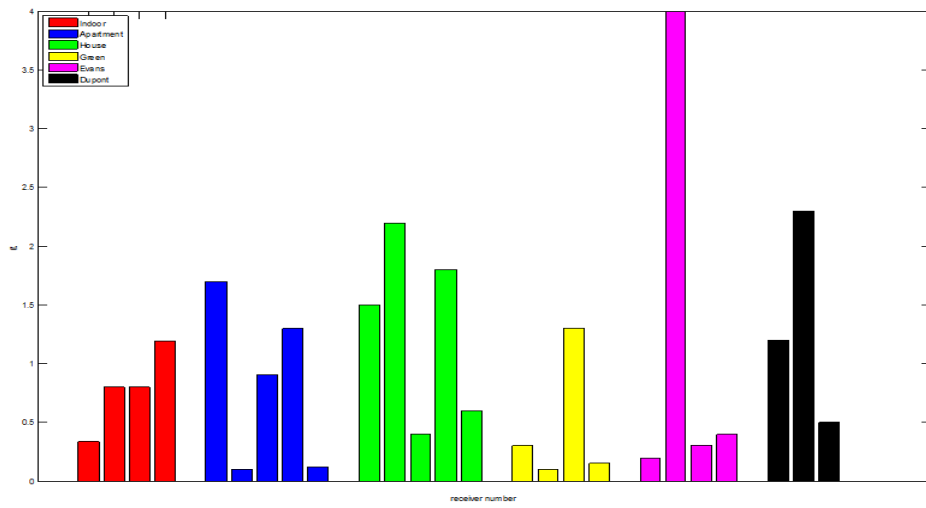


Figure 4.37: The Polynomial Exponent for the Decay of the Cross-correlation, α

Chapter 5

CONCLUSION

This thesis examined the channel variation over moderate displacements of the receiver or transmitter. By moderate, we mean less than 2 meters. Previous studies have focused on channel variation over very short distances (i.e., on the order of a wave length) or very large distances (e.g., tens of meters or more). A large measurement campaign was performed where 25 data sets were collected. A precise measurement system was used that included a robotic linear actuator. This allows precise control of the displacement of the transmitter. Moreover, at each location, a large number of measurements were made, resulting in a precise estimate of the signal strength.

These measurements were used to develop models for the variation of the signal strength. We found that the signal strength is well modeled by standard models that include fast fading and lognormal fading. However, unlike previous work, we found that the lognormal fading is less spatially correlated than other studies had found. Specifically, previous work had found that the lognormal component of the channel is highly correlated until the transmitter is moved tens of meters. However, this study found that the lognormal component is uncorrelated after a meter. Thus, the channel is considerably more variable than previously thought. This finding helps resolve some confusion as to where the 802.11 b/g channel is subject to fast fading. Roughly speaking, 802.11 b/g channel is only moderately subject to fast fading, however, the slow fading cause large channel variations even at moderate displacements of the antenna. This behavior closely resembles the behavior of

fast fading. However, upon careful examination, at antenna displacements on the order of a wavelength, the channel is considerably less variable than a narrow bandwidth channel, hence, fast fading does not have a significant impact on the channel variability, but lognormal fading has a more significant impact than previously known.

Chapter 6

APPENDIX

6.1 Experiment Program

6.1.1 Receiver Controller

This program is working on Receiver laptops to gather transmitted wireless signal.

```
// ReadKernelMessage.c : Receiver program
#include <stdio.h>
#include <string.h>
#include <sys/time.h>
#include <unistd.h>
#include <signal.h>
#include <stdlib.h>
#include <pcap.h>

#define MAX_STRING_LENGTH 2048
typedef void (*sighandler_t)(int);
FILE *ifp;
FILE *ofp;
int ReadMsgs = 0;
float avgRSSI = 0;
float avgSize = 0;
float avgErr = 0;
```

```

float avgRetry = 0;
int FirstSeqNo = 0;
int LastSeqNo = 0;
int nonErrors = 0;
int PreambleLockErrors = 0;
int PLCP_Errors = 0;
int CRC_Errors = 0;
pcap_t *handle;
char errbuf[PCAP_ERRBUF_SIZE];
sighandler_t HandleCtrlC(void) // print result on monitor and save results
in output file when this program is ended with encounter
{
fprintf(stdout, "Encountered Ctrl+c\n");
fprintf(stdout, "Read %d Messages ... RSSI = %f SIZE = %f ERROR = %f
RETRY = %f\n", ReadMsgs, avgRSSI, avgSize, avgErr, avgRetry);
fprintf(stdout, "FirstSeqNo = %d ... LastSeqNo = %d ... NonErrors =
%d\n", FirstSeqNo, LastSeqNo, nonErrors);
PreambleLockErrors = (LastSeqNo - FirstSeqNo) - nonErrors - CRC_Errors
- PLCP_Errors;
fprintf(stdout, "NumPackets = %d NonErrors = %d CRC_Errors = %d
PLCP_Errors = %d PreambleLockErrors = %d\n",
(LastSeqNo - FirstSeqNo), nonErrors, CRC_Errors, PLCP_Errors,
PreambleLockErrors);
fprintf(stdout, "Throughput = %.2f %% CRC_Errors = %.2f %%
PLCP_Errors = %.2f %% PreambleLockErrors = %.2f\n", (1.0*nonErrors)
/ (LastSeqNo-FirstSeqNo), (1.0*CRC_Errors) / (LastSeqNo - FirstSeqNo),
(1.0*PLCP_Errors) / (LastSeqNo - FirstSeqNo), (1.0*PreambleLockErrors)

```

```

/ (LastSeqNo-FirstSeqNo));
fclose(ifp);
fclose(ofp);
exit(0);
}
int main(int argc, char **argv)
{
int NumMsgs = 0;
char IPFileName[MAX_STRING_LENGTH]; //InPut file
char OPFileName[MAX_STRING_LENGTH]; //OutPut file
char DataRate[4];
char line[MAX_STRING_LENGTH];
char dummyString[100];
char dummyInt;
int rssi = 0;
int noise = 0;
int pktSize = 0;
int error = 0;
int retry = 0;
int numErrors = 0;
int errorOcurrred = 0;
int retryOcurrred = 0;
int udpSeqNo = 0;
int macSeqNo = 0;
int FilterRate = 0;
int channel =0;
if(argc < 5)

```

```

{
// ReadKernelMessages ath0 Result.txt -999 XX
fprintf(stderr, "Usage: ReadKernelMessages [Device] [Output-File]
[NumMessages] [DataRate XM] \n");
return -1;
}
char *dev = argv[1];
sprintf(OPFileName, "%s", argv[2]);
NumMsgs = atoi(argv[3]);
sprintf(DataRate, "%s", argv[4]);
handle = pcap_open_live(dev, BUFSIZ, 1, 1, errbuf);
if(handle == NULL)
{
fprintf(stderr, "Could not open device %s\n", dev);
return -1;
}
fprintf(stdout, "Successfully set device %s in promiscuous mode\n", dev);
fprintf(stdout, "Set to read %d messages ... outputfile - %s DataRate - %s\n",
NumMsgs, OPFileName, DataRate);
ifp = fopen("/proc/kmsg", "r"); //open kernel message
if(ifp == NULL)
{
fprintf(stderr, "Could not open the input file /proc/kmsg\n");
return -1;
}
ofp = fopen(OPFileName, "w");
if(ofp == NULL)

```

```

{
    fprintf(stderr, "Could not open the output file %s\n", OPFileName);
    return -1;
}
if(strcmp("XX", DataRate) == 0) // XX -> all DataRate possible
{
    FilterRate = 0;
}
else
{
    FilterRate = 1;
}
signal(SIGINT, (sighandler_t)(HandleCtrlC));
FirstSeqNo = -999;
LastSeqNo = -999;
while(ReadMsgs != NumMsgs)
{
    fgets(line, MAX_STRING_LENGTH, ifp); //Read message from kernel
    if(strlen(line)>0)
    {
        if(strstr(line, DataRate) != NULL || FilterRate == 0)
        {
            fprintf(stdout, "%s", line);
            fprintf(ofp, "%s", line);
            ReadMsgs++;
            //Read DATA packet
            if(strstr(line, "DATA") != NULL)

```

```

{
    sscanf(line, "%s %d %s %s %s %s %s %d %d %d %d %d %d %d %d
%d %d %d\n", dummyString, &dummyInt, dummyString, dummyString,
dummyString, dummyString, dummyString, &rssi, &noise, &pktSize,
&udpSeqNo, &macSeqNo, &error, &retry, &dummyInt, &dummyInt,
&dummyInt, &dummyInt, &channel);
}

```

// Read BEACON or OTHER packet.

In my Madwifi driver, it doesn't save these packet.

```

else if((strstr(line, "BEACON") != NULL) || (strstr(line, "OTHER") !=
NULL))

```

```

{
    sscanf(line, "%s %d %s %s %s %s %s %d %d %d %d %d %d\n",
dummyString, &dummyInt, dummyString, dummyString, dummyString,
dummyString, dummyString, &rssi, &noise, &pktSize, &error, &retry,
&channel);
}

```

else

```

{
}

```

// This error determining code is needed for Throughput calculation.

```

if(error > 0)
{
    errorOcurrred = 1;
    if(error == 2) //CRC error happen
    {
        CRC_Errors++;
    }
}

```



```

    }
    if(error > 2) //Other errors except CRC error are counted as PLCP
    {
        PLCP_Errors++;
    }
}
else
{
    errorOcurrred = 0;
    nonErrors++;
}
if(retry > 0)
{
    retryOcurrred = 1;
}
else
{
    retryOcurrred = 0;
}
avgRSSI = (avgRSSI*(ReadMsgs-1)+rssi)/(ReadMsgs);
avgSize = (avgSize*(ReadMsgs-1)+pktSize)/(ReadMsgs);
avgErr = (avgErr*(ReadMsgs-1)+errorOcurrred)/(ReadMsgs);
avgRetry = (avgRetry*(ReadMsgs-1)+retryOcurrred)/(ReadMsgs);
if(FirstSeqNo == -999 && errorOcurrred == 0)
{
    FirstSeqNo = udpSeqNo;
}

```

```

    if(errorOcurrred == 0)
    {
        LastSeqNo = udpSeqNo;
    }
}
else
{
}
}
else
{
}
}
if((ReadMsgs % 100) == 0 && (ReadMsgs != 0))
{
    //print receiving status on Monitor
    fprintf(stdout, "Read %d Messages ... RSSI = %f SIZE = %f ERROR = %f RETRY = %f\n", ReadMsgs, avgRSSI, avgSize, avgErr, avgRetry);
}
}
fclose(ifp);
fclose(ofp);
//print the result on Monitor
fprintf(stdout, "Read %d Messages ... RSSI = %f SIZE = %f ERROR = %f RETRY = %f\n", ReadMsgs, avgRSSI, avgSize, avgErr, avgRetry);
return 0;
}

```

6.1.2 Transmitter Controller

This program is working on Sender Computer to send data and control Linear Actuator.

```
// ActuatorCtrl.cpp
and control Linear Actuator
#include "stdafx.h"
#include "ActuatorCtrl.h"
#include "Winsock2.h"
#include "signal.h"
#include <stdlib.h>
#include <stdio.h>
#include <time.h>
#ifdef _DEBUG
#define new DEBUG_NEW
#endif

//No. of position (In : 200, Out : 1000)
int TotalPosCount = 1000;    //200
// distance of moving (In : 42500, Out : 8500)
int MoveInterval = 8500;    //42500
int pos = 0;
int Channel[11] = {1,2,3,4,5,6,7,8,9,10,11}; // channels
char s[37];
// The one and only application object
CWinApp theApp;
using namespace std;
//using namespace System::Net::Sockets
#define MAX_BUFFER_SIZE 2048
```

```

struct TxPacket // Packet structure
{
int SeqNumber;
int PacketSize;
int Position;
int Channel;
int dummy1;
char buffer[MAX_BUFFER_SIZE];
};
HANDLE m_hCom;
CString m_sComPort;
// handling when program is ended with encounter
void SignalHandler(int signal)
{
fprintf(stdout, "Closing COM port: %s\n", m_sComPort);
CloseHandle(m_hCom);
exit(0);
}
int _tmain(int argc, TCHAR* argv[], TCHAR* envp[])
{
time_t start, end1, end2; // to see the total time taken during measurment
double dif1, dif2;
time (&start);
int nRetCode = 0;
BOOL m_bPortReady;
DCB m_dcb;
COMMTIMEOUTS m_CommTimeouts;

```

```

BOOL bWriteRC;
DWORD iBytesWritten;
DWORD dwError;
char comport[20];
struct sockaddr_in to;
struct hostent *he;
SOCKET UDPSock = 0;
char broadcast = 1;
char DestIPAddress[20];
int UDPPort;
int TimeInterval;
int PacketSize;
int NumPackets;
int SentPackets = 0;
FILE *fp = NULL;
char line[MAX_BUFFER_SIZE];
char SerialCommand[1024];
typedef void (*SignalHandlerPointer)(int);
SignalHandlerPointer previousHandler;
previousHandler = signal(SIGINT, SignalHandler);
// terminal handler for Linear Actuator
if (!AfxWinInit(::GetModuleHandle(NULL), NULL, ::GetCommandLine(),
0))
{
    _tprintf(_T("Fatal Error: MFC initialization failed\n"));
    nRetCode = 1;
}

```

```

else
{
// reserved for communication with Linear Actuator
m_sComPort = "COM4";
fprintf(stdout, "Setting the total position move count: %d\n",
TotalPosCount);
fp = fopen("CtrlParams.conf", "r"); //Reading Measurement Parameter
if(fp == NULL)
{
fprintf(stderr, "Could not open configuration file CtrlParams.conf\n");
return -1;
}
while(!feof(fp))
{
memset(line, 0, MAX_BUFFER_SIZE);
fgets(line, MAX_BUFFER_SIZE, fp);
if(strlen(line)>=1)
{
if(line[0] == '#')
{
//comment
}
else
{
if(strstr(line, "DEST_IP")!=NULL)
{
sscanf(line, "DEST_IP: %s", DestIPAddress);

```

```

}
else if(strstr(line, "DEST_PORT")!=NULL)
{
    sscanf(line, "DEST_PORT: %d", &UDPPort);
}
else if(strstr(line, "NUM_PACKETS")!=NULL)
{
    sscanf(line, "NUM_PACKETS: %u", &NumPackets);
}
else if(strstr(line, "TIME_INTERVAL")!=NULL)
{
    sscanf(line, "TIME_INTERVAL: %u", &TimeInterval);
}
else if(strstr(line, "PACKET_SIZE")!=NULL)
{
    sscanf(line, "PACKET_SIZE: %u", &PacketSize);
}
else if(strstr(line, "COM_PORT")!=NULL)
{
    sscanf(line, "COM_PORT: %s", comport);
}
else
{
    fprintf(stderr, "%s\n", line);
    fprintf(stderr, "Invalid line in configuration file\n");
}
}

```

```

    }
    else
    {
        //invalid line
    }
}

// Setup Terminal communication for Linear Actuator
m_sComPort = CString(comport);
m_bPortReady = TRUE;
m_hCom = CreateFile(CString(m_sComPort), GENERIC_READ |
GENERIC_WRITE, 0, NULL, OPEN_EXISTING, 0, NULL);
if (m_hCom == INVALID_HANDLE_VALUE)
{
    m_bPortReady = FALSE;
    dwError = GetLastError();
    fprintf(stderr, "COM open failed: Port=%s Error=%d\n",
m_sComPort, dwError);
    return -1;
}
m_bPortReady = SetupComm(m_hCom, 128, 128);
if(m_bPortReady == FALSE)
{
    dwError = GetLastError();
    fprintf(stderr, "COM port setup failed: Port=%s Error=%d\n",
m_sComPort, dwError);
    return -1;
}

```



```

m_bPortReady = GetCommState(m_hCom, &m_dcb);
if(m_bPortReady == FALSE)
{
    dwError = GetLastError();
    fprintf(stderr, "Getting COM port status failed: Port=%s Error=%d\n",
m_sComPort, dwError);
    return -1;
}
m_dcb.BaudRate = 9600;
m_dcb.ByteSize = 8;
m_dcb.Parity = NOPARITY;
m_dcb.StopBits = ONESTOPBIT;
m_dcb.fAbortOnError = TRUE;
m_bPortReady = SetCommState(m_hCom, &m_dcb);
if(m_bPortReady == FALSE)
{
    dwError = GetLastError();
    fprintf(stderr, "Setting COM port status failed: Port=%s Error=%d\n",
m_sComPort, dwError);
    return -1;
}
m_bPortReady = GetCommTimeouts (m_hCom, &m_CommTimeouts);
if(m_bPortReady == FALSE)
{
    dwError = GetLastError();
    fprintf(stderr, "Setting COM port timeouts failed: Port=%s Error=%d\n",
m_sComPort, dwError);

```

```

return -1;
}
m_CommTimeouts.ReadIntervalTimeout = 50;
m_CommTimeouts.ReadTotalTimeoutConstant = 50;
m_CommTimeouts.ReadTotalTimeoutMultiplier = 10;
m_CommTimeouts.WriteTotalTimeoutConstant = 50;
m_CommTimeouts.WriteTotalTimeoutMultiplier = 10;
m_bPortReady = SetCommTimeouts (m_hCom, &m_CommTimeouts);
if(m_bPortReady == FALSE)
{
    dwError = GetLastError();
    fprintf(stderr, "Setting COM port status failed: Port=%s Error=%d\n",
m_sComPort, dwError);
    return -1;
}
bWriteRC = WriteFile(m_hCom, "fd\r",5,&iBytesWritten,NULL);
if(m_bPortReady == FALSE)
{
    dwError = GetLastError();
    fprintf(stderr, "Writing to COM port failed: Port=%s Error=%d\n",
m_sComPort, dwError);
    return -1;
}
fprintf(stdout, "Network initialization ...\n");
WSADATA wsaData;                //Window Socket programming
if (WSAStartup(MAKEWORD(1, 1), &wsaData) != 0) {
    fprintf(stderr, "WSAStartup failed.\n");
}

```

```

    exit(1);
}
if((he=gethostbyname(DestIPAddress))==NULL)
{
    fprintf(stderr, "error in gethostbyname\n");
    return -1;
}
if((UDPSock = socket(AF_INET, SOCK_DGRAM, 0)) >= 0)
{
    fprintf(stdout, "UDP socket created successfully\n", UDPPort);
}
else
{
    fprintf(stderr, "Socket creation failed\n");
    return -1;
}
if(setsockopt(UDPSock, SOL_SOCKET, SO_BROADCAST,
&broadcast, sizeof(broadcast) == -1))
{
    fprintf(stderr, "Error in setting broadcast option\n");
    return -1;
}
else
{
    fprintf(stdout, "Broadcast option successfully set\n");
}
//Setup channel to Channel 1

```

```

sprintf(s,"perl c:\\SetCiscoChannel.pl %d",Channel[0]);
fprintf(stdout, "Channel is %d\\n",Channel[0]);
system(s);
//wait channel changed and receivers notice channel info. from beacons.
Sleep(60000);
int i = 0;
for ( i=0; i<(sizeof(Channel)/sizeof(int)); i++)
{
    to.sin_family = AF_INET;
    to.sin_port = htons(UDPPort);
    to.sin_addr = *((struct in_addr *)he->h_addr);
    memset(&(to.sin_zero), '\\0', 8);
    struct TxPacket txPkt;
    txPkt.SeqNumber = 0;
    txPkt.PacketSize = PacketSize;
    txPkt.Position = -999;
    txPkt.Channel = -999;
    txPkt.dummy1 = 0;
    int forward = 1;
    pos = 0;

    bWriteRC = WriteFile(m_hCom, "fd\\r",12,&iBytesWritten,NULL);
    int abs_posi =0;
    while(pos <= TotalPosCount-1)
    {
        fprintf(stdout, "Moving 1.5cm ... Total = %d\\n", pos);
        for (int j=0; j<4; j++){ //moving 4 times

```

```

if(forward == 1){
    abs_posi = abs_posi+MoveInterval;
    sprintf( SerialCommand,"ma %d\r",abs_posi);
    // moving Linear Actuator
    bWriteRC = WriteFile(m_hCom, SerialCommand,12,&iBytesWritten,
        NULL);
    Sleep(500); //waiting moving Linear Actuator
}
if(bWriteRC <= 0)
{
    dwError = GetLastError();
    fprintf(stderr, "Writing to COM port failed: Port=%s Error=%d\n",
m_sComPort, dwError);
    return -1;
}
}
if(forward == 1){
    SentPackets = 0;
    Sleep(1000);
    while(SentPackets != NumPackets) // Broadcasting Packets
    {
        txPkt.PacketSize = PacketSize;
        txPkt.Position = pos;
        txPkt.SeqNumber = SentPackets;
        txPkt.Channel = Channel[i];
        int a = sendto(UDPSock, (char *)&txPkt, PacketSize, 0,
(struct sockaddr *)&to, sizeof(struct sockaddr));

```

```

    if(a>=0)
    {
        fprintf(stdout, "Channel : %d At Position:%d Sent Packet %d\n",
Channel[i], pos, SentPackets);
    }
    else
    {
        fprintf(stderr, "Channel : %d At position:%d Send failed for %d\n",
Channel[i], pos, SentPackets);
        return -1;
    }
    Sleep(TimeInterval);
    SentPackets++;
}
}
pos++;
Sleep(500);
}
forward =0;
pos =0;
// after one measure finish, change channl to next.
if( i != (sizeof(Channel)/sizeof(int))-1){
    sprintf(s,"perl c:\\SetCiscoChannel.pl %d",Channel[i+1]);
    fprintf(stdout, "Channel is %d\n",Channel[i+1]);
    system(s);
}
time(&end1); // recording one measurement time

```

```

// Linear Actuator moves back to original position
while(pos <= TotalPosCount-1)
{
    fprintf(stdout, "Channel : %d Moving back 1.5cm ... Total = %d\n",
Channel[i], pos);
    for(int j=0; j<4; j++){
        if(forward == 0){
            abs_posi = abs_posi-MoveInterval;
            sprintf( SerialCommand,"ma %d\r",abs_posi);
            bWriteRC = WriteFile(m_hCom, SerialCommand,12,&iBytesWritten,
                NULL);
            Sleep(500);
        }
        if(bWriteRC <= 0)
        {
            dwError = GetLastError();
            fprintf(stderr, "Writing to COM port failed: Port=%s Error=%d\n",
m_sComPort, dwError);
            return -1;
        }
    }
    pos++;
}
}
fprintf(stdout, "Closing COM port: %s\n", m_sComPort);
CloseHandle(m_hCom);
}

```

```

time(&end2); // recording one measurement time + moving back time
dif1 = difftime(end1, start);
dif2 = difftime(end2, start);
printf("Foward used time :%.21f\n",dif1);
printf("Total used time :%.21f\n",dif2);
return nRetCode;
}

```

6.1.3 Cisco AP Channel Control

This perl script is using in Sender Laptop to control Cisco ap channel.

```

#!/ SetCiscoChannel.pl // changing Cisco ap channel
#!/usr/bin/perl -w
use Net::Telnet ();
$numArgs = $#ARGV + 1;
if($numArgs < 1)
{
    print "Usage: SetCiscoChannel.pl [Channel Number [1..11]]\n";
    print "$numArgs";
    exit;
}
$Channel = $ARGV[0];
if($Channel < 1 || $Channel > 11)
{
    print "Usage: SetCiscoChannel.pl [Channel Number [1..11]]\n";
    print "Channel - $Channel\n";
    exit;
}
// terminal communication

```



```

$telnet = new Net::Telnet (Timeout=>10, Prompt => '/bash\$ $/');
$telnet->open('192.168.4.100');
$telnet->waitfor('/Username: $/i');
$telnet->print('Cisco');
$telnet->waitfor('/Password: $/i');
$telnet->print('Cisco');
$telnet->waitfor('/CISCO309_ROBOT>$/i');
$telnet->print('enable');
$telnet->waitfor('/Password: $/i');
$telnet->print('Cisco');
$telnet->waitfor('/CISCO309_ROBOT#$/i');
$telnet->print('config terminal');
$telnet->waitfor('/CISCO309_ROBOT\ (config\)#$/i');
$telnet->print('interface dot11radio 0');
$telnet->waitfor('/CISCO309_ROBOT\ (config-if\)#$/i');
print "setting the channel to $Channel\n";
$command = "channel ".$Channel";
$telnet->print($command);
$telnet->waitfor('/CISCO309_ROBOT\ (config-if\)#$/i');
$telnet->print('end');
$telnet->waitfor('/CISCO309_ROBOT#$/i');
$telnet->print('copy running-config startup-config');
$telnet->print("");
$telnet->waitfor('/CISCO309_ROBOT#$/i');
$telnet->print('exit');
$telnet->print("");
$telnet->print('q');

```

BIBLIOGRAPHY

- [1] City and County of San Francisco, “Request for proposals 2005-19-TechConnect : Community wireless broadband network,” 2005, http://www.sfgov.org/site/tech_connect_index.asp.
- [2] Philadelphia Mayor’s Office, “Government leaders teleconference - wireless: The 21st century technology,” 2004, http://media.centerdigitalgov.com/teleconference_URLs/Wireless_Philadelphia.ppt.
- [3] Taipei Times, “Ma says taipei to be wireless in two days,” December 19 2005, <http://www.taipeitimes.com/News/biz/archives/2005/12/19/2003285096>.
- [4] “UDelModels - models for realistic simulation of urban mesh networks,” <http://udelmodels.eecis.udel.edu>.
- [5] T. Rappaport, *Wireless Communications - Principles and Practice*. Prentice Hall, 2002.
- [6] R. Vijayan and J. M. Holtzman, “Foundations for level crossing analysis of handoff algorithms,” in *ICC*, 1993.
- [7] F. Graziosi and F. Santucci, “A General Correlation Model for Shadow Fading in Mobile Radio Systems,” *IEEE Communication Letters*, vol. 3, pp. 102–104, 2002.
- [8] Nook Industries, “Modular Linear Actuator EGT/EGK 30, 40, 60, 80,” http://www.nookindustries.com/pdf/NookActuatorEGT_EGK.pdf.
- [9] IMS Intelligent Motion Systems, “MDrive23Plus Motion Control,” http://imshome.com/products/mdrive23plus_mdi.html.
- [10] Cisco Systems, “Aironet 1240AG series 802.11A/B/G access point,” <http://www.cisco.com/en/US/products/ps6521/products-data-sheet0900aecd8031c844.html>.
- [11] Proxim Wireless, “ORiNOCO 11b/G card,” <http://www.proxim.com/products/cp/pc.html>.

- [12] A. Communications, “AR5212,” <http://www.atheros.com/pt/AR5002GBulletin.htm>.
- [13] MADWiFi, “Multiband atheros driver for wifi,” <http://madwifi.org>.
- [14] IMS Intelligent Motion Systems, “MD-CC4400-000 USB to RS-422 communication converter cable,” http://imshome.com/downloads/datasheets/discontinued_prod/md_cc400_-000.pdf.
- [15] Nook Industries, “Nook product temperatures and materials,” <http://www.nookindustries.com/Engineering/MaterialTemperatures.cfm>.
- [16] Vivek Shrivastava and Dheeraj Agarwal and Arunesh Mishra and Suman Banerjee and Tamer Nadeem , “ On the (In)Feasibility of Fine Grained Transmit Power Control,” in *Proceedings of the Twelfth Annual International Conference on Mobile Computing and Networking (MobiComm)*. New York: ACM Press, 2006.
- [17] Wikipedia, “Gamma distribution,” http://en.wikipedia.org/wiki/Gamma_distribution.
- [18] “Gamma distribution,” http://www.ds.unifi.it/VL/VL_EN/special/special3.html.